DEVELOPMENT OF FLUORESCENT REPORTERS FOR MONITORING FE-S CLUSTER TRANSFER REACTIONS AND DISCERNING THE ROLE OF GLUTAREDOXIN PROTEINS IN FE-S CLUSTER ASSEMBLY

A Dissertation

by

JAMES NICHOLAS VRANISH

Submitted to the Office of Graduate and Professional Studies of
Texas A&M University
in partial fulfillment of the requirements for the degree of

DOCTOR OF PHILOSOPHY

Chair of Committee,	Ryland Young
Co-Chair of Committee,	David Barondeau
Committee Members,	Gregory Reinhart
	Frank Raushel
Head of Department,	Gregory Reinhart

May 2015

Major Subject: Biochemistry and Biophysics

ABSTRACT

Iron-sulfur clusters are critical cofactors in living organisms. They are synthesized using complex biosynthetic machinery that has evolved to control the reactivity of iron and sulfide and to appropriately target clusters to apo-proteins. In some bacteria and in the mitochondria of eukaryotes, iron-sulfur clusters are synthesized by the ISC machinery, consisting of a core complex of IscS (a cysteine desulfurase that produces persulfides) and IscU (a scaffold protein that assembles iron and persulfides to form clusters). The *in vitro* study of cluster transfer has been hampered by the lack of sufficient methods to investigate the kinetics of these processes. We have developed fluorescently labeled iron-sulfur cluster binding proteins that are sensitive to bound iron-sulfur clusters. The ability of these probes to sense only bound cluster in complex mixtures with multiple proteins was demonstrated by monitoring the DTT-dependent cluster exchange between identical ferredoxin proteins.

We then applied this methodology to try to understand the role of the monothiol glutaredoxins in Fe-S cluster transfer. The monothiol glutaredoxins are thought to function as intermediate cluster carriers, carrying clusters from IscU to apo-target proteins in the cell. We demonstrate IscS:IscU dependent cluster transfer to the *E. coli* monothiol glutaredoxin, Grx4 and then demonstrate the ability of holo-Grx4 to transfer clusters to different [2Fe-2S] containing proteins. Finally, we use kinetic modeling to demonstrate the ability of Grx4 to function as an intermediate carrier to terminal target

proteins.

Finally, we use the fluorescent labeling method to study the function of the dithiol glutaredoxins (Grx1 and Grx3) from *E. coli*. These proteins are less well understood, appearing to promote cell survival to toxins, although some studies suggest that they may function in Fe-S cluster transfer as well. We demonstrate that cluster transfer to Grx1 and Grx3 is highly sensitive to glutathione concentration and may function upstream of Grx4 under certain conditions. We also demonstrate that although Grx3 can transfer clusters to apo-target proteins, these terminal target proteins outcompete Grx3 for IscU bound cluster in combined reaction mixtures. Altogether, these studies demonstrate the utility of the newly developed fluorescent assays to address questions in Fe-S cluster trafficking.

DEDICATION

I would like to dedicate my dissertation to my wonderful wife Colleen, and my two boys Joseph and Patrick. They have stuck by me through the long hours and late nights and I can never thank them enough for their love and support.

ACKNOWLEDGEMENTS

I'd like to thank my collaborators, Dr. William Russell and Dr. David Russell for their help with my mass spectrometry experiments. Additionally, Dr. Tadhg Begley deserves thanks for his assistance and advice concerning fluorescent labeling of proteins using intein chemistry. I'd also like to thank two fabulous undergraduates, Lusa Yu and Rachael Cox, who helped out with production of proteins and experiments contained in Chapter 2. My advisor, Dr. David Barondeau, has provided invaluable advice and guidance throughout my studies and has been instrumental in helping me complete my studies. My fellow lab members (Dr. Chi-Lin Tsai, Dr. Michaella Levy, Dr. Jennifer Bridwell-Rabb, Dr. Nicholas Fox, D.J. Martin, Melissa Thorstad, Shachin Patra, Deepika Das, Robert Hoyuela, Trang Nguyen, Hyeran Choi, and Seth Cory) have provided assistance and advice over the years, challenging my interpretation of data and forcing me to fully support my conclusions. Additionally, my committee members (Dr. Ryland Young, Dr. Gregory Reinhart, and Dr. Frank Raushel) deserve thanks for their advice and direction over the years. JMJ.

TABLE OF CONTENTS

Page

ABSTRACT ii

DEDICATION iv

ACKNOWLEDGEMENTS v

TABLE OF CONTENTS vi

LIST OF FIGURES viii

LIST OF TABLES xi

CHAPTER I INTRODUCTION 1

- Iron-sulfur clusters 1
- Types of iron-sulfur clusters 4
- Cluster biosynthesis 7
- ISC system components 10
- Cluster transfer 19

CHAPTER II FLUORESCENT PROBES FOR TRACKING THE TRANSFER OF IRON-SULFUR CLUSTER AND OTHER METAL COFACTORS IN BIOSYNTHETIC REACTION PATHWAYS 25

- Introduction 25
- Results 28
- Discussion 44
- Materials and methods 50

CHAPTER III INVESTIGATING THE ROLE OF THE MONOTHIOL GLUTAREDOXINS WITH FLUORESCENT PROBES 58

- Introduction 58
- Results 62
- Discussion 79
- Materials and methods 84

CHAPTER IV INVESTIGATING THE ROLE OF THE DITHIOL GLUTAREDOXINS IN FE-S CLUSTER TRANSFER USING FLUORESCENT PROBES 88

Introduction 88
Results 92
Discussion 101
Materials and methods 104

CHAPTER V CONCLUSIONS 107

REFERENCES 112

LIST OF FIGURES

Page

Figure 1-1 Iron-sulfur clusters in nature 2

Figure 1-2 Operon structure of Fe-S biosynthetic systems 9

Figure 1-3 Model for ISC iron-sulfur cluster biosynthesis and transfer 11

Figure 1-4 Sulfur utilization by IscS 13

Figure 1-5 Structures of monothiol and dithiol glutaredoxins 17

Figure 2-1 Overlap of fluorescent emission spectra for BFP and rhodamine with absorbance spectrum of [2Fe-2S] cluster from Fdx 27

Figure 2-2 Production of rhodamine labeled proteins 29

Figure 2-3 Fluorescence quenching reports Fe-S cluster binding to labeled proteins 31

Figure 2-4 Fdx_{Rho} fluorescence is reversibly quenched by [2Fe-2S] binding 31

Figure 2-5 CD spectra of reconstituted [2Fe-2S]-Fdx_{Rho} and as-isolated Fdx 32

Figure 2-6 Substrates and byproducts for Fe-S assembly reactions do not quench fluorescence 33

Figure 2-7 Factors affecting Fdx_{Rho} fluorescence 34

Figure 2-8 Metal dependent quenching of Fdx_{Rho} 36

Figure 2-9 DTT accelerates cluster transfer from [2Fe-2S]-Fdx to apo-Fdx_{Rho} 37

Figure 2-10 Comparison of DTT and GSH catalysis of Fdx cluster exchange 38

Figure 2-11 Extent of fluorescence quenching depends on the ratio of [2Fe-2S]-Fdx and apo-Fdx_{Rho} 39

Figure 2-12 Fluorescence quenching and mass spectrometry analysis of Fdx-Fdx_{Rho} cluster exchange experiment 40

Figure 2-13 Mass spectrometry reveals DTT dependent cluster exchange between [2Fe-2S]-Fdx and apo-Fdx_{Rho} 41

Figure 2-14 Fe-S cluster transfer reactions are unaffected by DTT pretreatment ... 43

Figure 2-15 Fdx cluster exchange is slowed by reduction 44

Figure 2-16 Model of DTT dependent cluster transfer reaction 48

Figure 2-17 Data processing flow chart 53

Figure 3-1 DTT accelerates the cluster transfer from holo-Grx4 to apo-Fdx 61

Figure 3-2 Cluster assembly on $IscU_{Rho}$ in the presence or absence of apo-acceptors 62

Figure 3-3 $Grx4_{Rho}$ quenching reports on cluster transfer and effect on rate with varying acceptor and GSH concentrations 65

Figure 3-4 Effect of DTT on cluster transfer to $Grx4_{Rho}$ 66

Figure 3-5 Effect of IscU on cluster transfer to $Grx4_{Rho}$ 67

Figure 3-6 Size exclusion chromatography of $Grx4_{Rho}$ before and after cluster transfer 68

Figure 3-7 Fluorescence of Grx4Rho is sensitive to cluster and not dimerization 69

Figure 3-8 Quenching of $Grx4_{Rho}$ as a function of $Grx4_{Rho}$ concentration 70

Figure 3-9 Cluster transfer from Grx4 to apo-acceptors is direct and not mediated by GSH 71

Figure 3-10 Global fit analysis of $Grx4_{Rho}$ cluster transfer to apo-Fdx and apo-HcaC 73

Figure 3-11 Cluster transfer to $Grx4_{Rho}$ in the presence of apo-acceptor proteins 74

Figure 3-12 Reaction scheme for kinetic modeling 75

Figure 3-13 Global fit analysis of IscS:IscU cluster transfer to $Grx4_{Rho}$ in the presence of apo-Fdx or HcaC 76

Figure 3-14 Time course of cluster transfer from cluster transfer from holo-IscU to apo-Fdx via Grx4 78

Figure 3-15 Time course of cluster transfer from holo-IscU to apo-Fdx in absence of Grx4 79

Figure 3-16 Fitting of kinetic traces for cluster transfer to apo-Fdx monitored via CD 80

Figure 4-1 GSH dependence of cluster transfer to monothiol and dithiol glutaredoxins 91

Figure 4-2 Competition between $Grx3_{Rho}$ and Grx4 for newly synthesized Fe-S cluster 93

Figure 4-3 Rescue of fluorescence quenching of dithiol glutaredoxins by Fdx and HcaC 95

Figure 4-4 Competition between $Grx3_{Rho}$ and Fdx for IscU bound cluster 96

Figure 4-5 Competition between $Grx3_{Rho}$ and HcaC for IscU bound cluster 97

Figure 4-6 Kinetic scheme for cluster transfer with dithiol Grx and Fdx/HcaC 98

Figure 4-7 Global fit of Fdx:$Grx3_{Rho}$ competition data 100

LIST OF TABLES

Page

Table 2-1 Iron, sulfide, and Rhodamine B quantitation for reconstituted proteins....30

Table 3-1 Kinetic analysis of cluster transfer from [2Fe-2S]-Grx4Rho to apo-acceptors....72

Table 3-2 Global fit parameters for $Grx4_{Rho}$:Apo-Acceptor cluster transfer reactions....77

Table 4-1 Fitting kinetic traces for Grx3Rho competition experiments with Fdx/HcaC....99

CHAPTER I

INTRODUCTION

Iron-sulfur clusters are very important biological cofactors that play a wide variety of functional roles throughout biology (1). They are believed to be among the earliest cofactors used in evolutionary history, evolving well before the great oxidation event (2). The prevalence of iron and sulfur on earth suggests that iron-sulfur minerals may have been present in abundance. Thus it is not too surprising that early proteins may have evolved to bind and utilize these early materials.

Today iron-sulfur clusters can be found in nearly every organism on earth. Unlike in early evolutionary history, soluble iron is not readily available to organisms due to the lack of solubility of Fe^{3+}. Sulfur is now primarily found as oxidized species as well and additionally must be tightly controlled due to the role of sulfide in cell signaling and its toxic effects at high concentrations (3). In order to accommodate these limitations, at least four distinct systems of complex biosynthetic machinery have evolved to create iron-sulfur clusters and insert them into their correct target proteins (4-10). Despite considerable study of these systems, many questions remain regarding the mechanism of cluster biosynthesis and transfer.

Iron-sulfur clusters

Iron-sulfur clusters are composed of alternating ferric or ferrous ions and sulfide ions. They can occur in a variety of different forms, each of which has different properties and functions (Figure 1-1). The most common forms are the [2Fe-2S] cluster

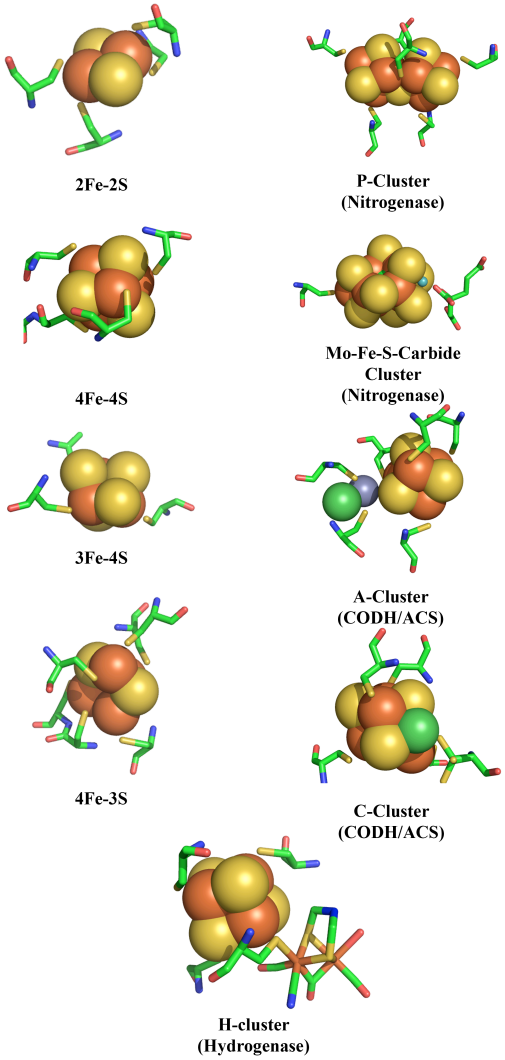

Figure 1-1. Iron-sulfur clusters in nature. Orange spheres represent iron ions and yellow are sulfides. The small blue sphere in the Mo-Fe-S-Carbide is a molybdenum ion and the green center ion is a carbide. The green spheres in the CODH/ACS structures are nickel ions and the grey sphere is a zinc. Coordinating cysteine ligands are shown.

and the [4Fe-4S] cluster, although several other types of clusters with varied numbers of iron and sulfide, alternate geometries, and different metals are well known and characterized (1). These clusters are typically bound to the protein via the iron atoms with cysteine ligands, although other residues are also known to ligate clusters in specific instances (11).

Iron-sulfur clusters play numerous roles in biology. Perhaps their most well known function is serving as electron carrier cofactors in proteins. For instance, the mitochondrial electron transport chain utilizes several iron-sulfur clusters to transport electrons from NADH to the oxygen reductase complex (12-14). Many other redox enzymes are known to pair with a ferredoxin, an iron sulfur cluster-containing protein, whose sole role is to provide a route for electrons to enter the enzyme, thereby providing reducing equivalents for chemical reactions (15).

In other cases iron-sulfur clusters are more intimately involved in chemical reactions. [4Fe-4S] clusters are well established to function with S-adenosylmethionine to catalyze a plethora of reactions throughout the radical SAM superfamily (16). In other cases, such as in aconitase and L-serine dehydratase, clusters simply ligate substrates and serve as a component of the enzyme binding site (17, 18). In more complex enzymes, modified iron-sulfur clusters are essential cofactors for the reduction of protons to form hydrogen gas in hydrogenases (19, 20), serve as crucial cofactors for the reduction of dinitrogen to ammonia in nitrogenase (20, 21), and allow for the assimilation of carbon monoxide into metabolism in carbon monoxide dehydrogenase (22, 23).

Iron-sulfur clusters can play non-catalytic roles as well. Several regulatory proteins such as IscR, SoxR, Aft1, and Fnr bind an iron-sulfur cluster that they use to regulate DNA binding and transcriptional responses (24, 25). These proteins are used to regulate iron-sulfur cluster biosynthesis, general iron metabolism, and cellular respornses to oxidative stress. Intruigingly, these regulators can be bi-functional (as is the case with IscR), allowing for the repression of cluster biosynthesis when clusters are present in abundance, and the induction of stress response genes under conditions of oxidative stress (26). Additionally, proteins involved in DNA repair, such as XPD helicase, have been shown to contain iron-sulfur clusters, and there is considerable evidence that these proteins utilize their clusters to sense DNA damage from considerable distances by utilizing the ability of undamaged DNA to conduct electricity(27, 28). Still other proteins are known to bind clusters with as of yet unknown function. For instance, it has recently been shown that some DNA polymerases contains an iron-sulfur cluster, and some RNA polymerases have been shown to bind clusters as well(29, 30). It's possible that these clusters play purely structural roles in these proteins, but perhaps unanticipated functions will be elucidated for these clusters in years to come.

Types of iron-sulfur clusters

The simplest type of iron-sulfur cluster is the [2Fe-2S] cluster. This type of cluster, though much simpler than other clusters, is present in relatively low abundance in cells(31). [2Fe-2S] clusters function almost exclusively in electron transfer, with two different ligation environments being commonly found. In most cases, [2Fe-2S] clusters

exist in two oxidation states, +2 and +1 (counting the charges of the iron and sulfide atoms alone, ignoring charge from coordinating residues), though a 0 charge state has been observed *in vitro* under extreme reducing conditions(32). In [2Fe-2S] cluster ferredoxins, the clusters are ligated to the protein by four cysteine residues. These proteins have a redox potential of -150 to -450 mV (NHE) which makes them perfect electron conduits from NADH to their destination proteins(33).

Another class of common [2Fe-2S] cluster proteins are the Rieske proteins. In these proteins, one of the iron ions is bound to the protein by two cysteine residues and the other is bound by two histidine residues(34, 35). The loss of the negatively charged cysteines and their replacement with neutral histidine residues stabilizes the reduced form of the cluster relative to its oxidized form, resulting in a substantial increase in the redox potential to -100 to +400 mV(33). Additionally, due to the dual histidine ligation, the redox potential of Rieske proteins varies dramatically with pH(36). It has been demonstrated that this is due to protonation of the ligating histidines, and furthermore, it has been suggested that these histidine ligands can function in proton coupled electron transfer processes(11).

The most common type of cluster (at least in yeast) is the [4Fe-4S] cluster(31). These clusters are cuboid in structure, with iron and sulfide ions alternating at the corners. Thus each iron is bound to three sulfide ions in the cluster, with the fourth ligand coming from an amino acid side-chain or a substrate/cofactor. These clusters are much more versatile than [2Fe-2S] clusters. In nature, depending on the ligation environment, a [4Fe-4S] cluster on a given protein can exist in up to three of four

different possible oxidation states (0, +1, +2, and +3). Most [4Fe-4S] clusters only use the +2 and +1 oxidation states, with this redox couple typically having a potential of -150 to -700 mV(33). Specialized clusters called HiPIPs (High potential iron-sulfur proteins) utilize the +3 and +2 oxidation states with a redox potential of +100 to +400 mV(33). In perhaps the most extreme example of a [4Fe-4S] cluster, the iron protein of the nitrogenase complex is able to access the 0, +1, and +2 oxidation states, allowing it to possibly pump two electrons simultaneously into the core of the enzyme(37). Additionally, closely related [3Fe-4S] and [4Fe-3S] clusters have been found in a few proteins(15, 38). These clusters are thought to function primarily in electron transfer reactions.

Much more complex clusters than these are known to exist in nature. In carbon monoxide dehydrogenase, clusters are coupled with nickel ions to produce an electronic system with the remarkable ability to reduce CO to form acetate(39). In another example, iron-iron hydrogenases couple a [4Fe-4S] cluster with two additional irons, a dithiolate bridge, and carbon monoxide and cyanide ligands(20). This cluster converts protons and electrons to hydrogen gas in order to regenerate NAD+ in anaerobic organisms. The true Fe-S cluster royalty resides in the enzyme nitrogenase. The core subunits contain two unique clusters, the P-cluster and the Mo-Fe-S cluster(21). The P-cluster resembles 2-[4Fe-4S] clusters fused together via a common sulfide ion, resulting in an [8Fe-7S] cluster. The Mo-Fe-S cluster contains one Mo ion, seven irons, 9 sulfides, a molecule of homocitrate, and a carbide(21, 40). This super-cluster is believed

to catalyze the cleavage of the triple bond in dinitrogen, an extremely difficult but critical reaction in nature.

Cluster biosynthesis

Iron-sulfur minerals form quite readily from iron and sulfide ions and can take on numerous forms(41). Early in evolution, it is quite possible that some proteins possessed the ability to bind to these minerals or fragments of them(33). Later in evolutionary history, iron became considerably less available due the formation of iron oxides and sulfide would have been oxidized to form sulfates, thus limiting the ability of iron-sulfide to form. Furthermore, as proteins containing clusters began to evolve to serve a necessary functional purpose, a requirement for a specific type of cluster would likely have developed as evidenced by the varied properties of different cluster types.

Inorganic chemistry has provided clues as to how early cluster biosynthesis may have occurred. Using small molecule thiol compounds as ligands, stable [2Fe-2S] clusters can be generated from ferric iron and sulfide(42). Upon the addition of a reducing agent, these clusters can couple to form [4Fe-4S] clusters(43). Additionally, the second sphere of ligands around the cluster plays a key role in stabilizing [4Fe-4S] clusters in aqueous environments (44-46). This type of synthesis, while effective, has certain limitations. It doesn't allow for regulation of cluster biosynthesis, it requires free iron and sulfide (which are both rare and toxic species), it has the potential to produce a variety of alternate cluster/mineral products, and the produced clusters are typically not very stable in aqueous environments. To circumvent these problems, nature has evolved

several different enzymatic approaches to both produce and insert iron-sulfur clusters into target proteins.

At least four distinct systems from cluster biosynthesis have evolved to present day, the NIF, SUF, CIA, and ISC systems. The NIF system is the most specialized, producing iron-sulfur clusters specifically for nitrogenase(47). The SUF system is able to build clusters for more proteins and appears to have to ability to function under conditions of oxidative stress(48). It is found in the chloroplasts of plants and appears to be a secondary system in *E. coli* where it functions under stress conditions(4). The CIA pathway functions in the eukaryotic cytosol(49). It receives an unknown species from the mitochondrial ISC cluster biosynthetic machinery and uses it to produce numerous cytosolic clusters(50). The ISC system, like the SUF system, is able to build clusters for many targets. It is the main cluster biosysnthesis system in *E. coli(26)*. Also, it is the only system present in human mitochondria, where it produces all of the clusters for the mitochondria and the cytosol/nucleus (via the CIA pathway). At their most basic level, the systems are quite similar, containing a cysteine desulfurase enzyme that produces persulfide species from cysteine as well as a scaffold protein that assembles the iron and sulfur ions to form a cluster (Figure 1-2) (51). The balanced equation (shown below) for cluster biosynthesis shows a requirement for cysteine, ferrous iron, and two electrons. The source of the iron and electrons remains controversial.

$$2\ \text{L-Cysteine} + 2\ Fe^{2+} + 2\ e^{-} \rightarrow [2Fe\text{-}2S]^{2+} + 2\ \text{L-Alanine}$$

These biosynthetic systems are essential in their host organisms, reflecting the lack of alternate chemo-synthetic means of building iron-sulfur clusters. Knockouts of

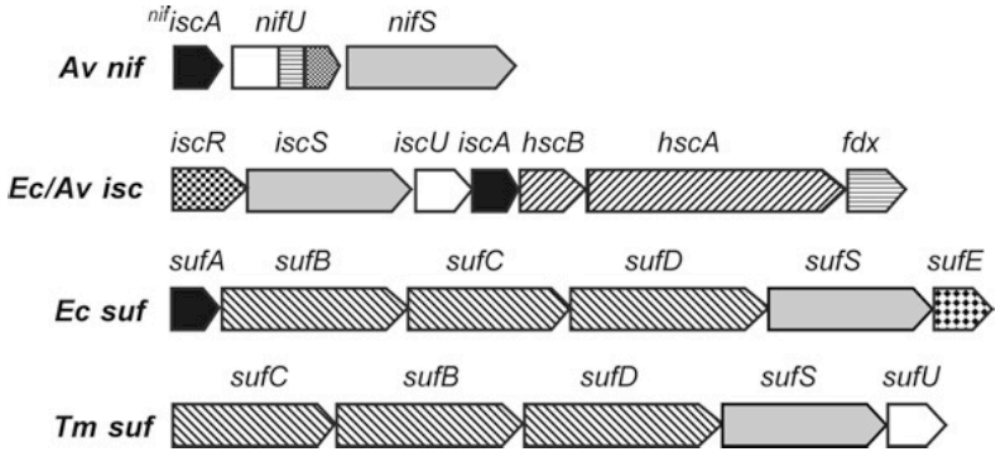

Figure 1-2. Operon structure of Fe-S biosynthetic systems. NIF, ISC, and SUF operons are shown for *Azotobacter vinelandii* (Av), *Escherichia coli* (Ec), and *Thermotoga maritima* (Tm). Cysteine desulfurases are indicated by solid gray genes. U-type scaffold proteins/domains are indicated by white genes. Reproduced with permission from Bandyopadhyay S, Chandramouli K, Johnson MK. 2008. *Biochem. Soc. Trans.* 36 (Pt 6), 1112-9. © The Biochemical Society.

the core genes in cluster biosynthesis are usually lethal to the organism, except in cases where there are multiple cluster biosynthetic systems present (ex. *E. coli* has both the ISC and SUF systems; knockouts in one system are not lethal)(52-55). These core genes include the cysteine desulfurase and the scaffold protein as well as certain other genes that are specific for the three different systems. Additionally, defects in several other genes that are involved in cluster biosynthesis and transfer are associated with diseases in humans(49, 56, 57). These diseases often have deleterious affects on neuromuscular function, consistent with defects in the electron transport chain in the mitochondria

(which contains numerous iron-sulfur clusters). It is quite clear that these biosynthetic systems are essential for proper growth of organisms.

ISC system components

The ISC cluster biosynthetic system has received the most attention due to its primary role in *E. coli* as well as its importance in humans. In *E. coli*, most of the required genes occur in a single operon(6). The operon contains genes for IscS, IscU, HscA, HscB, IscA, Fdx, IscR, and IscX (Figure 1-2). The operon was originally discovered in *Azotobacter vinelandii* when it was revealed that the organism still retained cysteine desulfurase activity even with a knockout of the known NIF cysteine desulfurase, NifS(6). Purification and sequence analysis of the alternate cysteine desulfurase enzyme followed by DNA hybridization analysis against a genomic library from *A. vinelandii* revealed the ISC operon. The IscS gene name was assigned to the cysteine desulfurase (Figure 1-3). HscA and HscB constitute a chaperone/co-chaperone pair(58). IscU has been shown to function as a scaffold protein(59). IscA has been proposed to function as an iron-donor, a transfer protein, or as an alternate scaffold(60-63). Fdx is a [2Fe-2S] ferredoxin and is believed to function as an electron donor for cluster assembly(64). IscR regulates transcription of the ISC operon and related operons by binding an Fe-S cluster, thereby sensing cellular iron-sulfur cluster availability as well as oxidative stress(26). Finally, IscX is a mysterious protein that has been suggested to function as an iron-donor or regulatory protein(65, 66). Later it was revealed that other components were necessary for iron-sulfur cluster biosynthesis. Monothiol glutaredoxins and NfuA are thought to function in cluster transfer to apo-

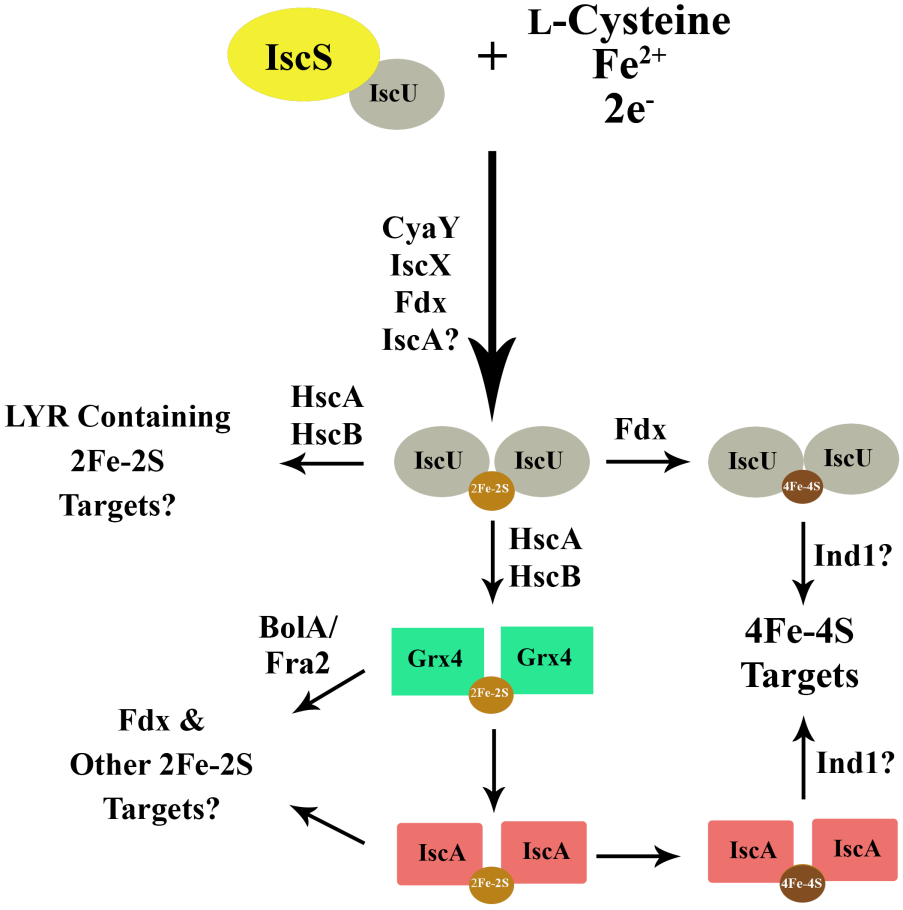

Figure 1-3. Model for ISC iron-sulfur cluster biosynthesis and transfer. A [2Fe-2S] cluster is synthesized on a dimer of IscU by a complex of IscS and IscU using cysteine, ferrous iron, and reducing equivalents. A variety of proposed pathways lead to the formation and transfer of [4Fe-4S] clusters. [2Fe-2S] clusters may be transferred to apo-target proteins by a number of intermediate carriers, some of which are believed to impart specificity to the transfer process.

target proteins(67, 68). Frataxin is another protein that is crucial for cluster biosynthesis, with gene knockouts resulting in embryonic lethality in mice and plants (69, 70). It has

been shown to be required for cluster biosynthesis, and has been proposed to function as an iron donor or regulatory protein(71-73).

The cysteine desulfurase enzyme in the ISC system is IscS. It is a pyridoxal-5-phosphate-dependent enzyme that catalyzes the conversion of cysteine to alanine, forming a persulfide species on a cysteine residue that is on a mobile loop near the active site(74). IscS functions as a dimer and has been shown to bind to numerous components (IscU, frataxin, Fdx, HscB, and IscX) of the ISC system, forming a large complex that assembles iron-sulfur clusters(64, 66, 75-77). The persulfide that is generated on IscS can be transferred to a variety of proteins in the cell, or in *in vitro* assays, can be cleaved by reductants such as DTT(74, 78, 79). This competition between productive sulfur transfer and persulfide cleavage is a major problem plaguing the *in vitro* study of this system (Figure 1-4).

IscU is the scaffold protein for the ISC system. It has been shown to bind to IscS in the vicinity of the mobile loop cysteine that carries the persulfide species(80-82). IscU was originally shown to accelerate cluster formation on ferredoxin in a chemical reconstituion reaction, using iron and sulfide as substrates(83). The protein contains four promixal conserved cysteine residues, three of which are on the surface and are known to be involved in cluster binding(84-86). The fourth cysteine has been demonstrated to be required for cluster formation as well and is the site of persulfide transfer from IscS to IscU(84, 85). The identity of the fourth ligand to the cluster remains debatable with proposals including a neighboring histidine or aspartate residue on IscU or a cysteine from IscS(80, 87). IscU is also known to bind metals, including

iron, with micromolar affinity(88). A complex between the cysteine desulfurase of humans and IscU was recently shown to bind one iron in a stable complex(89). This question of whether the iron or the sulfur is first transferred to IscU for cluster synthesis remains a matter of debate in the field. Additionally, IscU complexed with IscS can build iron-sulfur clusters on itself in the presence of iron and cysteine, and a crystal structure of this holo-IscS/IscU complex has been obtained (80). Furthermore, IscU-bound clusters can be transferred to apo-target proteins (85, 90-92). Taken together these data suggest that IscU functions as the primary scaffold protein for the ISC assembly system.

The chaperone protein HscA and its cochaperone HscB are essential genes for cluster biosynthesis(55). HscA has ATPase activity that it presumably uses to help

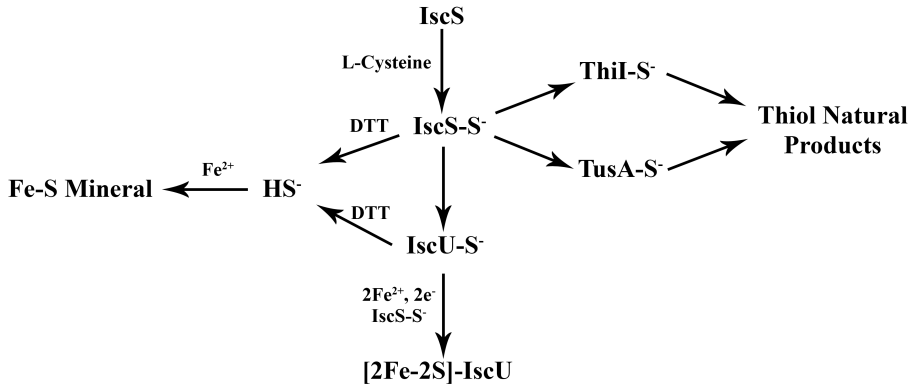

Figure 1-4. Sulfur utilization by IscS. IscS reacts with cysteine to produce a persulfide species that can be transferred to several proteins. DTT is capable of cleaving persulfides, resulting in the formation of bisulfide. In the presence of iron, this material can form iron-sulfur mineral species.

proteins accept iron-sulfur clusters(58). HscB is known to associate with both HscA and IscU. HscA and IscU also have the ability to interact independent of HscB(93, 94). Additionally, interactions between IscS and HscB as well as IscA and HscA are known (77, 95). Curiously, IscS binding HscB appears to prevent IscU binding to IscS, suggesting that the complex likely undergoes changes in quarternary structure during catalysis(77). The purpose of these numerous interactions and the function of their dynamics during catalysis remains unclear. There is considerable evidence that these proteins function during cluster transfer, though the mechanistic details of their role remain mysterious.

Another important protein for cluster biosynthesis is a [2Fe-2S] ferredoxin (Fdx) that is located within the ISC operon. This protein is capable of carrying out one-electron redox processes. Fdx is an essential component of the ISC system and has long been presumed to be involved in catalysis since the balanced chemical reaction for cluster biosynthesis requires two electrons to generate a single [2Fe-2S] cluster(55). Utilizing Fdx in this process seems to be ideal since its inclusion would eliminate the need for a thiol reductant to cleave persulfide intermediates, which might allow for sulfide to escape the assembly complex. If ferredoxin functions as an electron donor for cluster biosynthesis, the mechanism would have to invoke simultaneous electron transfer from ferrous iron and ferredoxin to cleave the persulfide intermediates or alternatively persulfide radical intermediates. Evidence for its role in cluster biosynthesis has been provided by an experiment that demonstrated oxidation of reduced ferredoxin in the

presence of IscS and cysteine(64). This led the authors to favor a model in which a persulfide radical formed, since the reaction did not include exogenous iron.

The association of ferredoxin with other proteins has been quite controversial. Both ferredoxin and IscU have been shown to independently bind to IscS(64, 75, 96, 97). Recent NMR data shows that the conformation of IscU was perturbed when ferredoxin was added to a solution of IscS-complexed IscU(64). This perturbation was consistent with IscU dissociating from the IscS assembly complex. However, this data could also be interpreted as an Fdx induced conformational change in IscU upon formation of a ternary complex. Furthermore, competition between ferredoxin and IscU appears to be inconsistent with the role of ferredoxin in cluster biosynthesis.

Still other components of the ISC cluster biosynthetic pathway are known. Among the most prevalent in the literature is frataxin (bacterial homolog is CyaY). In humans, defects in frataxin are the cause of the neurodegenerative disease Freidreich's ataxia(98). This disease is associated with defects in cluster biosynthesis and formation of iron aggregates in the mitochondria(99). In bacteria, CyaY has been shown to bind IscS, although the cyaY gene is not encoded in the ISC operon (75, 100). Additionally, it has modest μM iron binding affinity, and has been proposed to be an iron donor for cluster biosynthesis(72, 101). Seemingly conflicting studies suggest that frataxin functions as an allosteric activator in eukaryotes and as an inhibitor in prokaryotes, though this difference was later shown to be due to differences in the eukaryotic and prokaryotic cysteine desulfurases(100). Recent studies suggest that these observations of activation and inhibition may require reinterpretation, since the measured iron-sulfur

cluster assembly assays likely included non-productive Fe-S solution chemistry in addition to cluster biosynthesis, greatly complicating data analysis(102). Additionally, the interaction of CyaY with various components of cluster biosynthesis has been controversial. Kinetic and Biolayer interferometry binding experiments suggest that CyaY binding to IscS is enhanced by the presence of IscU, indicating a larger ternary complex(75, 103). Recent NMR studies, on the other hand, suggest that IscU and CyaY compete for binding based on changes in the IscU conformation upon CyaY addition(64). Another puzzling binding observation is that CyaY and Fdx appear to compete for binding to IscS(64, 104). This observation greatly complicates our mechanistic understanding of cluster biosynthesis since both CyaY and Fdx appear to be critical components for cluster biosynthesis. Finally, there is some evidence that frataxin is involved in cluster transfer since HscA and frataxin appear to be evolutionarily linked(105).

IscX is a mysterious protein encoded in the ISC operon of *E. coli*, but it is not well conserved, even within prokaryotes. Studies have shown that IscX can bind iron and that it binds to IscS with weak affinity(65, 66). Recent studies have shown that IscX regulates cluster biosynthesis, appearing to function as an inhibitor, seemingly in conflict with its proposed role as an iron donor(65).

Another important group of proteins are the glutaredoxins (Grx's). These proteins have been shown to function in two-electron transfer processes, having the ability to activate enzymes such as ribonucleotide reductase or glutithionylated proteins(67). Interestingly, they also have the ability to bind clusters (primarily [2Fe-

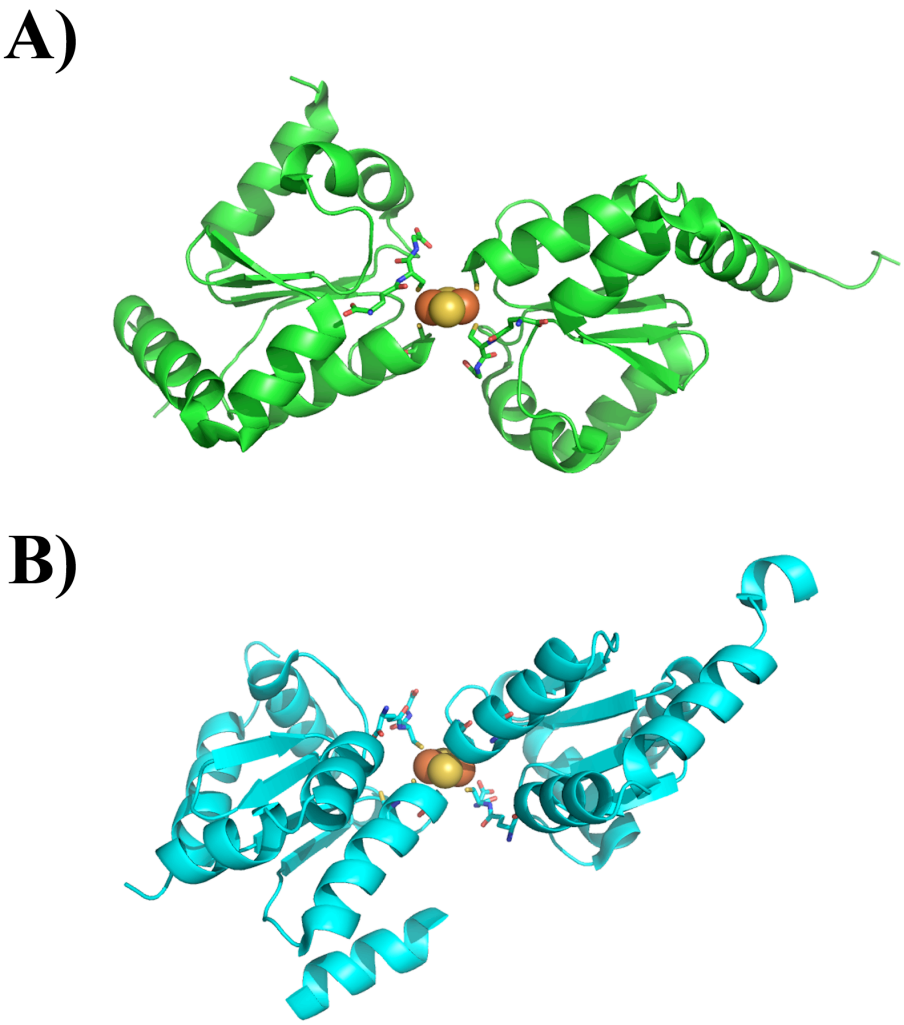

Figure 1-5. Structures of monothiol and dithiol glutaredoxins. (A) E. coli monothiol glutaredoxin Grx4. (B) Human dithiol glutaredoxin, Grx2. The structures are oriented so that their [2Fe-2S] clusters are similarly aligned. GSH ligands and active site cysteine residues are shown.

2S]) , in a process that conflicts with their electron transfer role(106). In the holo-form of these proteins, the [2Fe-2S] cluster is bound to two monomers of glutaredoxin(107).

Each monomer provides one cysteine ligand to opposite Fe atoms (the same cysteine that is involved in thiol reduction). The other two ligands are 2 molecules of glutathione (GSH) that are non-covalently bound to the complex. Two varieties of Grx's are known, the monothiol Grx's and the dithiol Grx's(67). These names refer to the number of cysteine residues found at the GSSG reduction site/cluster binding site. Both classes are capable of binding clusters, albeit with different dimerization geometries (Figure 1-5) (108). Additionally, the classes appear to have different functions, with the monothiol Grx's functioning in cluster transfer and the dithiol Grx's perhaps functioning in sensing or resistance to oxidative stress(67, 92, 106).

Two other proteins have been proposed to function specifically in the formation of [4Fe-4S] clusters. While IscU has been shown to be able to form [4Fe-4S] clusters *in vitro*, knockout studies have implicated IscA and NfuA as being important for [4Fe-4S] cluster formation *in vivo*(109-111). Additionally, these proteins have been shown to bind to [2Fe-2S] clusters and [4Fe-4S] clusters(68, 111, 112). In addition, the ability of IscA to bind iron appears to be critical for its function, indicating that it may bind mononuclear iron and function in repair of [4Fe-4S] clusters or iron donation to a preformed [2Fe-4S] cluster intermediate(62, 113, 114). Furthermore, both IscA and NfuA have been shown to be able to transfer their clusters to apo target proteins(68, 112). Importantly, despite the ability of IscA to form a cluster in the presence of IscS, iron, and cysteine, there is no evidence for an interaction between IscA and IscS, suggesting that IscA is not a scaffold and is likely involved in downstream cluster transfer processes(60, 95).

Cluster transfer

Iron-sulfur cluster transfer presents a unique challenge in biology. Iron-sulfur cluster proteins can have widely varied protein folds and ligating residues that often resemble the binding sites for other physiological metals. The same could be said for other metallocofactors such as zinc and copper as well. However, iron-sulfur clusters are unique because they cannot exist as free species and the fact that organisms can rely on a single system to insert clusters into multiple types of cellular targets(42, 52, 54, 55). The ability of this machinery to do its job given these strict requirements is truly remarkable.

The mysteries of cluster transfer begin at the very beginning (Figure 1-3). The nature of the initial cluster source is still controversial. IscU appears to be the primary scaffold protein that assembles the initial cluster, based on its ability to catalyze cluster formation of apo-proteins, its ability to form a cluster on itself from IscS/cysteine/Fe, and the observation that it binds IscS near the mobile loop cysteine(59, 83). Different groups disagree about whether the synthesis of the cluster occurs in complex with IscS or as a ping-pong type reaction with alternating Fdx and IscU binding(64, 104). Most groups then agree that IscU must dissociate from IscS in order to carry out transfer, based on data that suggests that the chaperones are unable to bind IscU when it is complexed with IscS(77). In vitro studies have suggested that [2Fe-2S] IscU dimerizes with another monomer of IscU(59). This species can then accept a second [2Fe-2S] cluster as well(59). IscU has been shown to interact with the chaperone proteins HscA

and HscB, with the ternary complex stimulating the ATPase activity of HscA dramatically(115). Holo-[2Fe-2S]-IscU has been shown to be able to transfer its cluster to both Fdx and a monothiol glutaredoxin(90, 92). In the presence of HscA, HscB, and ATP these transfer rates increase by 10-1000 fold, suggesting that this holo-IscU species is physiologically relevant(90, 92). Seemingly in conflict with this observation, a recent paper suggests that *in vivo* HscB is only required for transfer of clusters to proteins containing a semi-conserved LYR motif(116). However, neither glutaredoxin nor Fdx (the proteins that have shown chaperone enhancement in *in vitro* cluster transfer assays) contain a LYR motif. Recent studies by our group question this model by showing that IscS complexed IscU can transfer clusters to ferredoxin faster than uncomplexed [2Fe-2S]-IscU(102). This suggests that holo-IscU apart from the complex may not be the actual cluster donor. Furthermore, a recent crystal structure showing a complex between holo-IscU and IscS was determined, showing that a cysteine on IscS can serve as a cluster ligand(80). This adds additional support for an IscS/IscU/[2Fe-2S] complex being the biologically relevant transfer species.

Adding another layer of complication is the observation that *in vitro* IscU can reductively couple two [2Fe-2S] clusters to form a [4Fe-4S] cluster(91). This species forms most readily with non-physiological reductants such as dithionite, although it can be formed in lower yields with the aid of electrons from a reduced ferredoxin. Furthermore, it has been shown that the [4Fe-4S] cluster on IscU can transfer rapidly to apo-aconitase in a chaperone independent fashion(117). This rapid transfer suggests that IscU may be capable of forming [4Fe-4S] clusters for proteins *in vivo*.

Monothiol glutaredoxins have been implicated in cluster transfer processes downstream of IscU. [2Fe-2S] clusters from IscU can be transferred to glutaredoxin in a chaperone dependent process(92). In addition, a [2Fe-2S] cluster on glutaredoxin can be transferred to ferredoxin in the presence of DTT, in a chaperone independent process(92). The overall rate of chaperone assisted cluster transfer to ferredoxin passing through glutaredoxin appears to be faster than transfer to ferredoxin alone(92). It is worth noting that these studies use DTT in two out of the three kinetic reactions and that they utilize [2Fe-2S] IscU as a cluster source. Furthermore, no transfer reaction has ever been carried out in the presence of both glutaredoxin and ferredoxin, and their concentrations were never varied in the available kinetic studies. As a result, their ability to compete for the cluster remains entirely unknown. Additionally, the dithiol glutaredoxins have been shown to be capable of transferring their clusters to ferredoxin in the presence of DTT(118). Transfer of clusters from either monothiol or dithiol glutaredoxins appears to be inhibited by GSH (in the presence of DTT), suggesting that GSH may compete with DTT for the cluster(118). *In vivo* data suggests that the dithiol glutaredoxins are not as important for cluster biosynthesis, despite their known cluster binding and transfer ability(67, 119). Instead they appear to affect cellular sensitivity to oxidative stress with little data supporting specific effects on Fe-S cluster metabolism (67).

Additionally, monothiol glutaredoxins are known to form cluster heterodimers with other proteins such as BolA/Fra2(120, 121). The role of these heterodimeric cluster species is still mysterious although *in vivo* data suggests that these heterocomplexes do

form and are important for cellular regulation of iron metabolism(25, 122). BolA-Grx cluster complexes have different ligands, spectroscopic characteristics, and cluster stabilities relative to Grx-Grx complexes (123-125). BolA has been shown to impact cellular redox potential, and together with Grx may function as a regulatory protein(122). Additionally, when glutaredoxin complexes with Fra2, the complex is able to transfer clusters to Aft1/2, a regulatory protein that controls eukaryotic iron metabolism(25). Whether glutaredoxins function in regulation, transfer, or both remains to be determined.

Another putative intermediate carrier encompasses a family of proteins known as the A-type proteins. Among them are IscA, NfuA, and SufA. These proteins have been shown to accept [2Fe-2S] clusters from IscU, either directly or indirectly (via Grx or NfuA), in a DTT dependent fashion(68, 112, 125). IscA can reductively couple two [2Fe-2S] clusters to form a [4Fe-4S] cluster(112). Knockout studies of IscA demonstrate that [4Fe-4S] cluster containing proteins are impaired relative to [2Fe-2S] cluster proteins (109, 110). This suggests that IscA is involved in maturation of [4Fe-4S] clusters. Puzzling though, are *in vitro* data that demonstrate the ability of IscA to transfer either a [2Fe-2S] cluster or a [4Fe-4S] cluster to the appropriate target proteins(61, 83, 112). This at the surface seems to conflict with a model whereby the [2Fe-2S] clusters are stored to synthesize a [4Fe-4S] cluster. Importantly, both of these types of transfer reactions were carried out in the presence of DTT.

Additional factors are required for certain cluster types. A protein, Ind1 was recently shown to be required for cluster biosynthesis specifically in complex I of the

electron transport chain(126). Atm1 is an ATP dependent transporter found in the mitochondrial membrane that is required to export clusters or cluster precursors to the cytosol, thereby linking the ISC and CIA biosynthetic machinery. Other specific targeting factors are known as well. For instance, Fra2 can form heterodimers with glutaredoxin to target clusters specifically to nuclear regulatory proteins(25). Overall, cluster biosynthesis and transfer is a very complex process with numerous critical components that still have unknown functions.

DTT is found all throughout the *in vitro* study of cluster transfer. This is curious because small molecule thiol ligands are known to bind to iron-sulfur clusters. Additionally, thiol compounds have been shown to destabilize clusters on iron-sulfur proteins in mixed aqueous-organic solutions(127). This leads one to question whether the apparent 'requirement' for DTT is to function as a thiol reductant to maintain the cluster binding site or if it might perhaps act as a cluster chelator. Data from our group has shown that the cluster transfer from IscU to ferredoxin in humans is absolutely dependent on DTT(102). Furthermore, DTT was shown to cause holo-IscU to lose its cluster(102). Thus the function of DTT in cluster transfer warrants further study.

It is also important to note that the *in vitro* cluster transfer studies that have been carried out to date have been limited in their scope. The primary method of studying cluster transfer has been CD spectroscopy(85, 90, 92). Iron-sulfur clusters that are bound to proteins have non-equal Fe-S bonds, so the ligand to metal charge transfer bands in the visible region absorb circularly polarized light. In contrast, clusters bound to small molecule ligands such as GSH and the more symmetrical [4Fe-4S] clusters

typically do not have a strong CD signal(128, 129). This technique has been useful primarily due to the relatively unique signatures that clusters have when bound to different proteins. However, these signals are weak, and assays often require ~10-100μM protein concentrations. Additionally, they have been limited to studies of cluster transfer between only two proteins, due to the difficulties in deconvoluting three or more overlapping spectra at intermediate time points. Other studies in the literature have relied on reconstituting clusters on enzymes such as aconitase or on using separation based techniques such as column chromatography(61, 117, 130). Such assays, while useful, are limited in that they are not easily ammenable to real-time kinetic analysis and only allow for cluster transfer to a certain subset of cluster binding proteins. In order to fully study cluster transfer *in vitro*, new methodology is required. This methodology would ideally have the ability to measure real time cluster transfer kinetics and report on the cluster content of a single protein in a complex reaction mixture. Additionally, the method should work at a variety of protein concentrations, allow for use of the IscS-IscU assembly complex, and allow for rapid high-throughput analysis of many samples.

CHAPTER II

FLUORESCENT PROBES FOR TRACKING THE TRANSFER OF IRON-SULFUR CLUSTER AND OTHER METAL COFACTORS IN BIOSYNTHETIC REACTION PATHWAYS[*]

Introduction

Enzymes require small organic molecules or metal ion cofactors to expand the limited chemical reactivity of amino acids and achieve biological functions. For metal ion cofactors, elaborate biosynthetic and delivery systems have evolved to provide specificity and control indiscriminate reactivity(131). Delivery systems for some metal cofactors, such as copper and iron-sulfur (Fe-S) clusters, appear to function as a bucket brigade, passing the cofactor from protein to protein until incorporation into the final target(132, 133). Major challenges for deconvoluting these pathways revolve around establishing which species are kinetically competent intermediates, defining the sequence of transfer reactions, and understanding target specificity. Kinetic experiments are critical to establish if a transfer reaction is fast enough to be physiologically relevant

---

[*] Reprinted with permission from "Fluorescent Probes for Tracking the Transfer of Iron–Sulfur Cluster and Other Metal Cofactors in Biosynthetic Reaction Pathways" by James N. Vranish, William K. Russell, Lusa E. Yu, et al., 2015. *J. Am. Chem. Soc.,* 137 (1), 390–398, Copyright 2014 by American Chemical Society.

and to determine which factors affect the flux through transfer branch points. These transfer reactions are often difficult to monitor due to similar ligand environments and nearly identical spectroscopic properties of the metal cofactor when bound to donor and acceptor proteins. Compromised metallocofactor biosynthesis and trafficking pathways are directly linked to human disease(56, 57, 134). Thus, the development of strategies to monitor the progress of metal cofactor transfer reactions is highly desirable.

Fe-S clusters are one of the most ubiquitously used and chemically diverse metal cofactors, existing with different ligand environments and stoichiometries, including commonly found [2Fe-2S] and [4Fe-4S] clusters(1). Fe-S clusters are best known for their electron transport roles in the respiratory chain and photosynthetic complexes. However, these cofactors also have key roles in substrate binding and activation, initiation of radical chemistry, and in sensing small molecules or environmental conditions(1, 135). These clusters are synthesized and delivered by the bacterial NIF, ISC, and SUF systems, and by eukaryotic ISC (in mitochondria), SUF (in chloroplasts), and CIA (in the cytosol) systems(5, 6, 49, 136). The synthesis and delivery of Fe-S clusters is a complex process that appears to involve branched pathways(59-61, 68, 110), utilize chaperone proteins for some cluster transfer reactions but not others(85, 90, 116), require additional protein factors to convert from [2Fe-2S] clusters to [4Fe-4S] clusters(60, 109, 110, 137), and necessitate intermediate carrier proteins that provide specificity for selected Fe-S targets(68, 92, 125, 126, 137-139).

Current methodology for monitoring Fe-S cluster assembly and transfer reactions has focused largely on absorption and circular dichroism (CD) spectroscopies(85, 90,

92). Absorption spectroscopy is non-ideal due to its inability to distinguish between solution mineralization chemistry and clusters bound to proteins. CD spectroscopy also has serious limitations including a requirement for very high protein concentrations(90, 92, 140), difficulty in detecting [4Fe-4S] clusters(129), interference due to other cofactors (such as the PLP in cysteine desulfurase enzymes)(141), and poor signal-to-noise for multicomponent analysis and time resolved experiments (142). Other studies utilize enzyme assays or separation-based techniques that do not allow for facile kinetic analysis and often report solely on the thermodynamics of cluster transfer reactions(61, 117, 130).

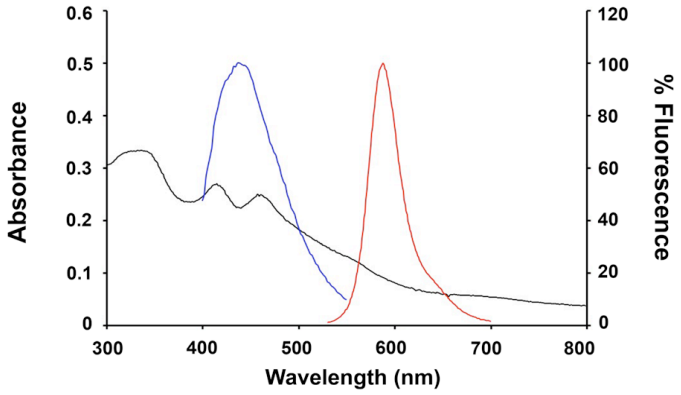

Figure 2-1. Overlap of fluorescent emission spectra for BFP and rhodamine with absorbance spectrum of [2Fe-2S] cluster from Fdx. Absorbance spectrum of 190 μM [2Fe-2S]-Fdx (black) was recorded with a 0.2 cm pathlength cuvette. The fluorescent emission spectra of apo-BFP-LAM (blue) and apo-$Grx4_{Rho}$ (red) were recorded with excitation wavelengths of 360 nm and 520 nm, respectively.

Fluorescence spectroscopy has the potential to overcome many of these limitations. Pioneering work using GFP variants, fluorescence resonance energy transfer (FRET), and fusion protein technology led to the development of *in vivo* metal ion sensors(143). Similarly, a homo-FRET mechanism has been used to monitor the [2Fe-2S] cluster induced dimerization of glutaredoxin molecules that are fused to GFP variants(142). Fluorophores associated with small molecules(144), DNA(145), or proteins(146) have also been used to report metal ion content or proximity of the metal to the fluorophore. Based on these studies, we recognized the potential for a fluorescent labeling approach that would be general for reporting the binding and transfer of Fe-S clusters, and would not be limited to Fe-S proteins that oligomerize. Here we show that Fe-S cluster binding can be detected by fluorescence quenching for multiple Fe-S proteins and that this labeling strategy can be used to detect the binding of other metals. We then use this phenomenon to investigate the surprising [2Fe-2S] cluster exchange reaction between labeled and unlabeled ferredoxin.

Results

Generation of fluorescently labeled Fe-S containing proteins. We hypothesized that placing a fluorophore spatially near an Fe-S cluster would create a reporter for cluster binding. Fe-S proteins were labeled with either a blue fluorescent protein (BFP) tag, which are convenient to generate, or a small molecule fluorophore, which minimizes the size of the label and can potentially bring the fluorophore into closer proximity to the cluster. BFP was selected as the fluorescent protein tag as the

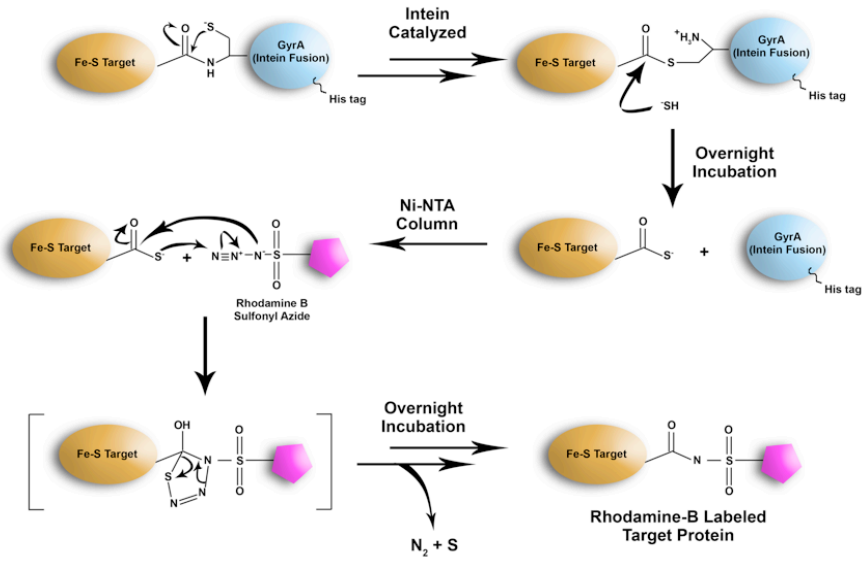

Figure 2-2. Production of rhodamine labeled proteins. Fe-S cluster binding proteins are expressed with a C-terminal GyrA-His fusion. This intein protein catalyzes thioester bond formation on the protein backbone between the two proteins. The thioester is cleaved with sulfide to cleave the protein fusion and generate a C-terminal thiocarboxylate on the Fe-S target. The thiocarboxylate is then reacted with Rhodamine B sulfonyl azide to form a stable sulfonylamide linkage.

emission at ~450 nm had spectral overlap with characteristic absorbance bands (between 400-500 nm) for iron-sulfur clusters (Figure 2-1), thus increasing the likelihood of energy transfer based quenching. Sulforhodamine B was selected as a small molecule fluorophore since it is sufficiently different from BFP that both fluorophores may be detected in a combined reaction mixture. The fluorescence emission for rhodamine has modest spectral overlap with typical Fe-S clusters (Figure 2-1), but has similar properties to Cy3, a fluorophore that has been shown to respond to nearby Fe-S clusters(145). We

adapted a recently developed intein labeling method(147) to specifically label proteins with rhodamine on the C-terminus (Figure 2-2), leaving cysteine residues unmodified.

Two BFP fusion and three intein-labeled Fe-S proteins were constructed. The *Escherichia coli* monothiol glutaredoxin (Grx4), which binds a single [2Fe-2S] cluster at a homodimeric interface using a cysteine residue and glutathione (GSH) molecule from each Grx4 subunit, was labeled with rhodamine ($Grx4_{Rho}$). The *E. coli* ISC ferredoxin, which binds a [2Fe-2S] cluster with 4 cysteine ligands, was labeled with either a N-terminal blue fluorescent protein (BFP-Fdx) or a C-terminal rhodamine (Fdx_{Rho}) fluorophore. The *E. coli* Rieske protein HcaC, which binds a [2Fe-2S] cluster with 2 cysteine and 2 histidine ligands, was labeled with rhodamine ($Rieske_{Rho}$). Finally, the E. coli lysine 2,3-aminomutase, which contains a [4Fe-4S] cluster, was labeled as a BFP fusion (BFP-LAM). Near stoichiometric rhodamine incorporation was achieved for intein labeling of Grx4, Fdx, and Rieske (0.76-1.07 fluorophores per protein; Table 2-1). These proteins were purified and chemically reconstituted with Fe-S clusters. Size exclusion columns were used to isolate the appropriate oligomeric states for the holo-

Table 2-1. Iron, sulfide, and Rhodamine B quantitation for reconstituted proteins.

	$Grx4_{Rho}$	$Rieske_{Rho}$	Fdx_{Rho}	BFP-Fdx	BFP-LAM
Fe / monomer	0.8 ± 0.4	2.1 ± 0.4	2.7 ± 0.5	1.5 ± 0.1	4.4 ± 0.1
S^{2-} / monomer	0.8 ± 0.4	2.0 ± 1.1	1.6 ± 0.2	1.2 ± 0.1	3.7 ± 0.2
Rho / monomer	0.76 ± 0.04	1.00 ± 0.03	1.07 ± 0.03	N/A	N/A

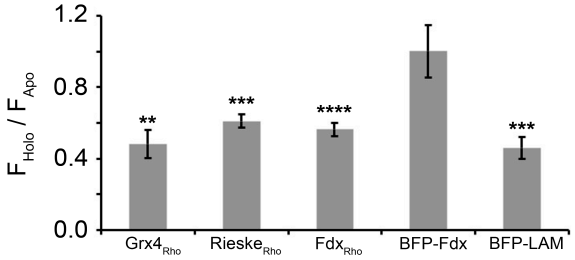

Figure 2-3. Fluorescence quenching reports Fe-S cluster binding to labeled proteins. The fluorescence intensity was measured for chemically reconstituted proteins and divided by that of the apo protein. Error bars (SD) are shown for multiple replicates (n = 3). ** $P < 0.01$, *** $P < 0.001$, **** $P < 0.0001$.

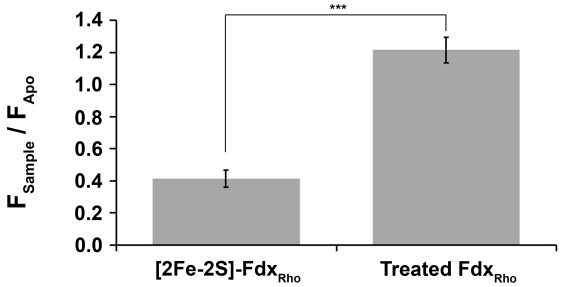

Figure 2-4. Fdx_{Rho} fluorescence is reversibly quenched by [2Fe-2S] binding. The F_{sample}/F_{apo} was determined for the [2Fe-2S]-Fdx sample by measuring the fluorescence intensity of 0.3 μM apo-Fdx_{Rho} before (F_{apo}) and after [2Fe-2S] cluster reconstituted (F_{sample}). Next, the reconstituted [2Fe-2S]-Fdx_{Rho} was treated to remove the cluster (see Methods). The F_{sample}/F_{apo} was determined for treated Fdx_{Rho} by measuring the fluorescence intensity of the cluster removed Fdx_{Rho} (F_{sample}) with the F_{apo} from above. Error bars (SD) represent multiple trials (n=3). *** $P < 0.001$

proteins and remove any aggregated materials or unreacted reagents. Iron and sulfide levels for the proteins (Table 2-1) were consistent with efficient reconstitution of appropriate [2Fe-2S] and [4Fe-4S] clusters with the exception of BFP-Fdx. Multiple attempts at reconstituting BFP-Fdx produced protein with less iron (1.5 per protein) and sulfide (1.2 per protein) than expected for a [2Fe-2S] cluster.

Four of the five constructs exhibited substantial quenching upon Fe-S cluster incorporation. Reconstitution of the [2Fe-2S] cluster on $Grx4_{Rho}$ converted the protein from a monomer to a dimer and decreased the fluorescence intensity to ~48% of apo-$Grx4_{Rho}$ (Figure 2-3). Reconstitution of the iron-sulfur clusters for monomeric Fdx_{Rho}, $Rieske_{Rho}$, and BFP-LAM reduced the fluorescence intensity to 56%, 61%, and 46% of the intensity of the apo proteins, respectively (Figure 2-3). Removing the Fe-S cluster

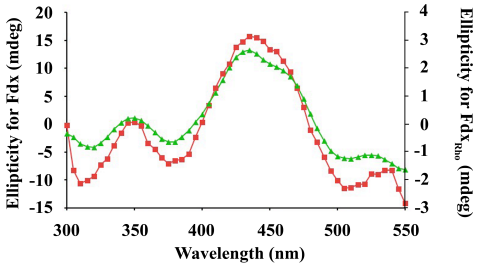

Figure 2-5. CD spectra of reconstituted [2Fe-2S]-Fdx_{Rho} and as-isolated Fdx. CD spectra were recorded using a 1 cm pathlength cuvette for 20 μM [2Fe-2S]-Fdx_{Rho} (red) and 20 μM as-isolated Fdx (green). Fdx_{Rho} was reconstituted in the cuvette by the addition of 9 mM DTT, 0.4 mM $FeCl_3$, and 0.3 mM Na_2S. Spectra were collected, contributions due to fluorophore were subtracted out, and curves were smoothed with a window size of 3.

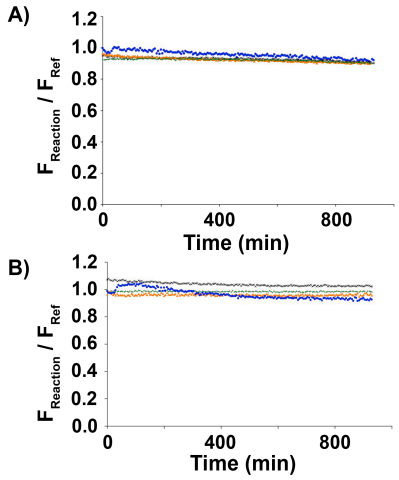

Figure 2-6. Substrates and byproducts for Fe-S assembly reactions do not quench fluorescence. (A) 5 μM of fluorescent apo protein was incubated with 100 μM ferrous ammonium sulfate and 10 mM GSH. Control wells contained GSH and fluorescent apo protein only. The data points correspond to the following apo-proteins: BFP-LAM (dark blue), Fdx_{Rho} (orange), $Grx4_{Rho}$ (green), and $Rieske_{Rho}$ (black). The maximum error (SD) was 0.09 $F_{Reaction}/F_{Ref}$. (B) 5 μM of fluorescent apo protein was incubated with 0.5 μM IscS, 10 mM GSH, and 100 μM L-cysteine. As a control, the reference well contained 5 μM fluorescent apo protein and 10 mM GSH. The fluorescence of the IscS/cysteine wells was divided by the fluorescence of the wells lacking IscS and cysteine. The same color scheme was used in A and B. The data points are the average of three runs for each fluorescent construct, and the maximum observed error (SD) for any data point was 0.06 $F_{Reaction}/F_{Ref}$.

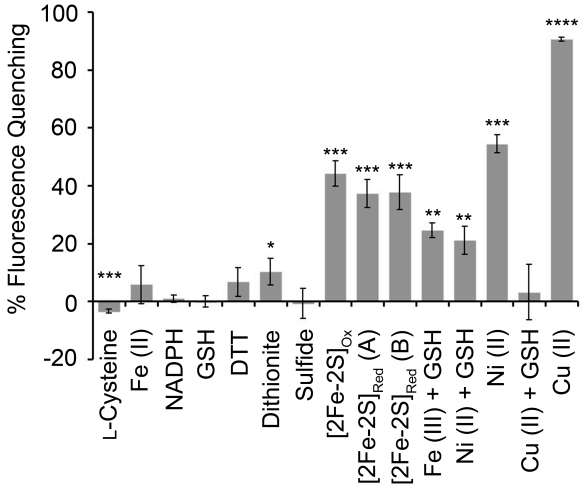

Figure 2-7. Factors affecting Fdx_{Rho} fluorescence. The fluorescence of apo- or [2Fe-2S]-Fdx_{Rho} was measured immediately after the addition of various reagents and plotted relative to a control containing apo-Fdx_{Rho}. [2Fe-2S] clusters were reconstituted and reduced with dithionite (A) or FldR/NADPH (B). Error bars (SD) are shown for multiple replicates (n = 3). * $P< 0.05$, ** $P< 0.01$, *** $P< 0.001$, **** $P< 0.0001$.

from [2Fe-2S]-Fdx_{Rho} recovered the fluorescence intensity (Figure 2-4), establishing a correlation between reversible Fe-S cluster binding and fluorescence quenching. Additionally, reconstituted Fdx_{Rho} has similar CD peak locations to Fdx, implying that the cluster binding site is not substantially perturbed by cluster binding (Figure 2-5). The ability to detect different classes of Fe-S proteins suggests this labeling approach may have broad application in monitoring the cluster content of Fe-S cluster binding proteins.

Next, we evaluated the sensitivity of the fluorescent reporter to reagents used in Fe-S assembly assays and to cluster oxidation states. First, we tested if the apo proteins that exhibited cluster-dependent quenching, $Grx4_{Rho}$, $Rieske_{Rho}$, Fdx_{Rho}, and BFP-LAM,

were also sensitive to substrates used in Fe-S cluster assembly reactions. In E. coli, Fe-S clusters are synthesized by an IscS-IscU complex using L-cysteine, Fe^{2+}, and electrons as substrates(59). Control Fe-S assembly reactions containing apo-fluorescent target proteins and either ferrous iron or IscS and L-cysteine did not exhibit fluorescence quenching for any of the apo labeled proteins (Figure 2-6). We then focused on the sensitivity of Fdx_{Rho} to individual reagents relevant to Fe-S cluster assembly and transfer reactions. The fluorescence of apo-Fdx_{Rho} was unaffected by addition of Fe^{2+}, NADPH, GSH, DTT, or sulfide (Figure 2-7). The addition of dithionite slightly quenched the fluorescence (10%), whereas L-cysteine addition slightly enhanced the fluorescence intensity (3%). However, the magnitudes of these changes were small compared to those generated by cluster binding (Figure 2-7). Moreover, the reporter was sensitive to both oxidized and reduced [2Fe-2S] clusters (Figure 2-7). Reduction of the cluster by either dithionite or NADPH (with the native Fdx reductant flavodoxin reductase (FldR)) resulted in nearly the same amount of fluorescence quenching (37-38%) as the oxidized cluster. These studies indicate the reporter is sensitive to the binding of either oxidized or reduced Fe-S clusters, but largely insensitive to substrates, reagents, and byproducts of Fe-S assembly reactions. Thus, this labeling strategy is a potential new tool for interrogating the kinetics of Fe-S assembly and transfer reactions (see Discussion).

We then tested if the Fdx_{Rho} reporter was sensitive to other metal ion cofactors. Treating apo-Fdx_{Rho} with various metals in the presence of 10 mM GSH revealed significant quenching for Ni^{2+} (21%) and Fe^{3+} (25%) (but not Cu^{2+} (3%)) when compared to apo-Fdx_{Rho} (Figure 2-7). Titration of Ni^{2+} into apo-Fdx_{Rho} exhibited binding

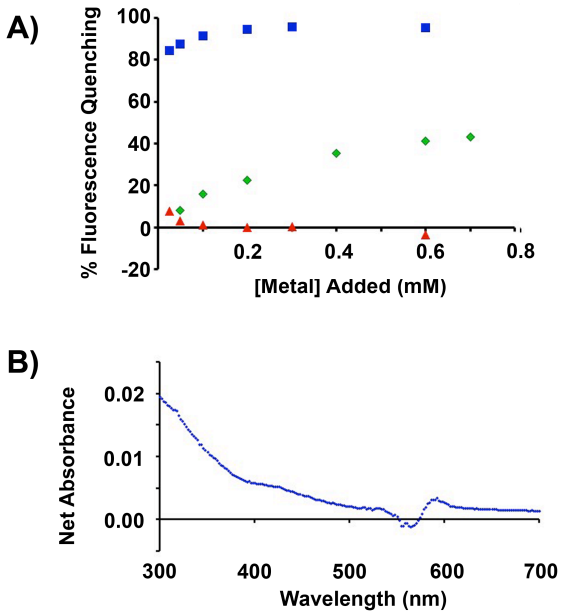

Figure 2-8. Metal dependent quenching of Fdx_{Rho}. (A) Overlay of titrations of 1 µM apo-Fdx_{Rho} with Ni^{2+} (and 10 mM GSH; green) and Cu^{2+} without (dark blue) and with 10 mM GSH (red). (B) Net absorbance of 100 µM Ni^{2+} added to 5 µM apo-Fdx_{Rho} subtracted from the absorbance of 5 µM apo-Fdx_{Rho}.

characteristics (formation of a Ni-Fdx_{Rho} species), an absorbance band at < 300 nm, and fluorescence quenching that plateaued at ~50% of that for apo-Fdx_{Rho} (Figures 2-8A and 2-8B). Interestingly, addition of Cu^{2+} in the absence of GSH eliminated the apo-Fdx_{Rho} fluorescence signal (Figures 2-7 and 2-8A). The signal was recovered by subsequent addition of GSH (Figure 2-8A), consistent with GSH removing copper from a Cu-Fdx_{Rho} species. Together this suggests binding of the metal to Fdx_{Rho} is critical for quenching. Overall, the sensitivity of the fluorescence to binding of other transition metal species

suggests this labeling strategy may also be valuable for investigating additional metal trafficking and biosynthetic pathways.

DTT facilitates [2Fe-2S] cluster self-exchange reactions. This labeling approach has the potential to advance the enzymology of Fe-S cofactor biosynthesis by

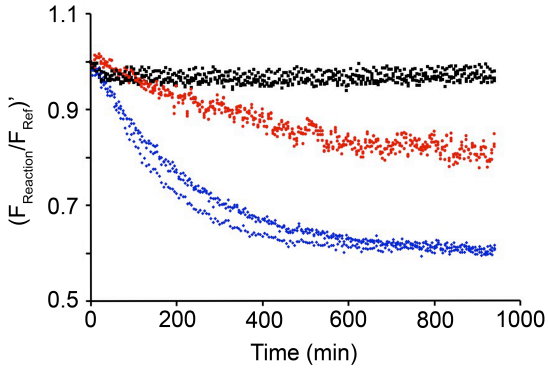

Figure 2-9. DTT accelerates cluster transfer from [2Fe-2S]-Fdx to apo-Fdx_{Rho}. [2Fe-2S]-Fdx (20 μM) was incubated with apo-Fdx_{Rho} (1 μM) and 0 mM (black), 8 mM (red), or 16 mM (blue) DTT. Three repetitions of each DTT concentration are overlaid. Data were fit as pseudo first order reactions in KaleidaGraph (not shown) to determine apparent rates of 0.0013(1) μM cluster min^{-1} (R^2 = 0.955) and 0.00495(4) μM cluster min^{-1} (R^2 = 0.998) for the 8 and 16 mM DTT reactions, respectively. The minimum fluorescence was assumed to correspond to 1 μM of transferred cluster. The relationship between the apparent rate constants and DTT concentration suggests a second order reaction with respect to DTT.

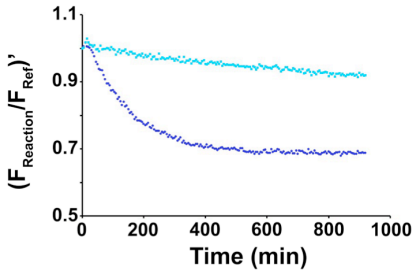

Figure 2-10. Comparison of DTT and GSH catalysis of Fdx cluster exchange. [2Fe-2S]-Fdx (10 μM) and apo-Fdx_{Rho} (0.5 μM) were incubated with 20 mM DTT (dark blue) or 20 mM reduced glutathione (cyan). Each plot is an average of 4 experiments with the maximum error (SD) for any data point being 0.03 $(F_{Reaction}/F_{Ref})$'.

allowing detection of cluster formation on selected proteins in complex reaction mixtures that may contain additional Fe-S proteins and chromophores. The power of this approach is highlighted with an extreme example in which the kinetics of Fe-S cluster transfer reactions are monitored between two Fdx molecules that have identical Fe-S spectroscopic properties. Unlabeled [2Fe-2S]-Fdx and apo-Fdx_{Rho} were reacted in the presence or absence of DTT (Figure 2-9). In the absence of DTT, the addition of [2Fe-2S]-Fdx resulted in no significant changes in fluorescence intensity for Fdx_{Rho}. In contrast, additionof both DTT and [2Fe-2S]-Fdx resulted in time-dependent rhodamine quenching with a final intensity (~60% of initial value) consistent with the formation of a [2Fe-2S]-Fdx_{Rho} species (Figure 2-3). Increasing the DTT concentration increased the rate of quenching, suggesting a role for DTT in the rate-limiting step for the transfer reaction from [2Fe-2S]-Fdx to apo-Fdx_{Rho}. Substitution of GSH for DTT greatly diminished the quenching rate (Figure 2-10). Next, the ratio of [2Fe-2S]-Fdx to apo-

Fdx_{Rho} was varied to determine if the extent of fluorescence quenching was consistent with a thermodynamic cluster redistribution and to evaluate the relative cluster binding constants of labeled and unlabeled Fdx (Figure 2-11). The final fluorescence intensities (65% for 20:1, 70% for 4:1, and 88% for 1:1) are similar to those calculated (58% for 20:1, 65% for 4:1, and 78% for 1:1; assuming 56% intensity for [2Fe-2S]-Fdx_{Rho} (Figure 2-3) and identical Kd values). These results are consistent with the cluster on [2Fe-2S]-Fdx being redistributed in a DTT-dependent process between Fdx and Fdx_{Rho} and indicate that these two proteins have similar cluster binding affinities.

A coupled fluorescence and mass spectrometry experiment was used to further interrogate the Fe-S cluster self-exchange reaction on Fdx. A complete reaction

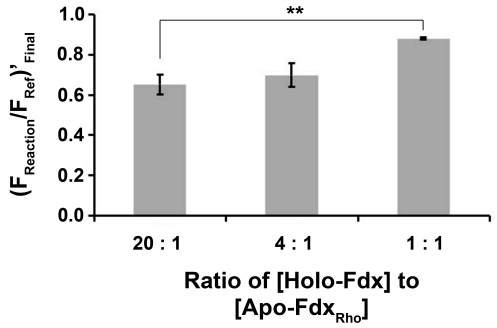

Figure 2-11. Extent of fluorescence quenching depends on the ratio of [2Fe-2S]-Fdx and apo-Fdx_{Rho}. Reactions were carried out with 20 mM DTT, 0.5 μM apo-Fdx_{Rho}, and varying concentrations of [2Fe-2S]-Fdx (10 μM, 2 μM, or 0.5 μM). The $F_{reaction}$ and F_{Ref} are the fluorescence intensity after 19 h for reactions with and without [2Fe-2S]-Fdx. Error bars (SD) are shown for multiple replicates (n = 3). ** $P < 0.01$.

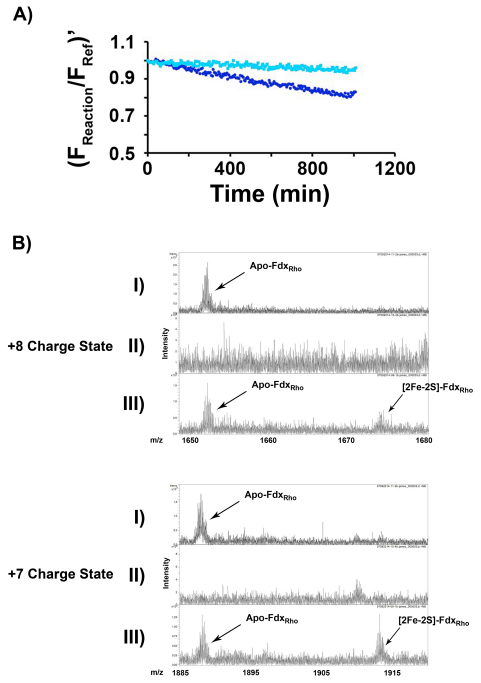

Figure 2-12. Fluorescence quenching and mass spectrometry analysis of Fdx-Fdx$_{Rho}$ cluster exchange experiment. A) Time dependent fluorescence quenching for mass spectrometry samples lacking DTT (cyan) and the complete reaction (blue). Both reactions contained 80 µM [2Fe-2S]-Fdx and 40 µM apo-Fdx$_{Rho}$. B) Spectra are displayed for the +8 and +7 charge states for Fdx$_{Rho}$ in ferredoxin cluster transfer assays. I) 40 µM apo-Fdx$_{Rho}$ was incubated with 80 µM [2Fe-2S]-Fdx. II) 80 µM [2Fe-2S]-Fdx was incubated with 20 mM DTT. III) 40 µM apo-Fdx$_{Rho}$ was incubated with 80 µM [2Fe-2S]-Fdx and 20 mM DTT. The reactions components were incubated for ~16 h, desalted, and analyzed by FT-ICR-MS. Deconvolution of the mass spectra revealed a peak in III) with [M+H] = 13380 Da (± 0.5 Da), consistent with the expected mass of [2Fe-2S]-Fdx$_{Rho}$ (minus the N-terminal methionine) of 13381.0 Da.

containing unlabeled [2Fe-2S]-Fdx, DTT, and apo-Fdx$_{Rho}$ and control reactions lacking either DTT or apo-Fdx$_{Rho}$ were performed. The complete reaction, but not the control lacking DTT, showed time-dependent fluorescence quenching (Figure 2-12A). Next,

mass spectrometry was used to monitor the loss of cluster from unlabeled [2Fe-2S]-Fdx. The control reactions lacking DTT (Figure 2-13A) or apo-Fdx_{Rho} (Figure 2-13B)

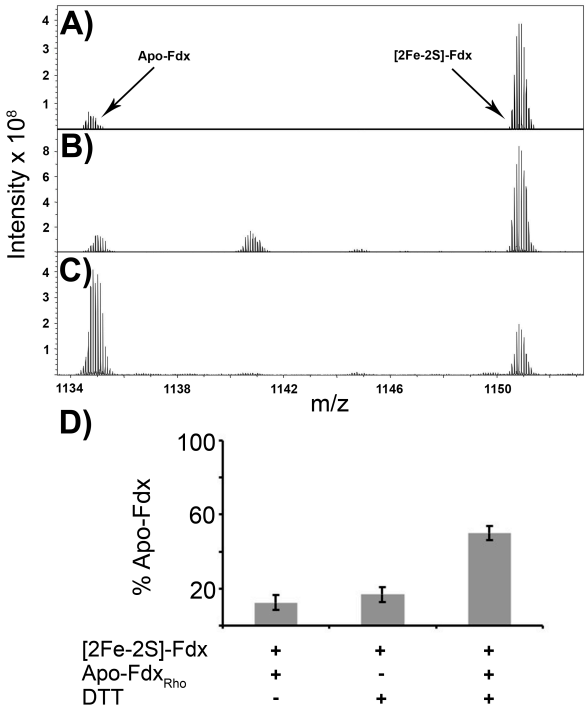

Figure 2-13. Mass spectrometry reveals DTT dependent cluster exchange between [2Fe-2S]-Fdx and apo-Fdx_{Rho}. Mass spectra for the +11 charge species of unlabeled-Fdx at the conclusion of cluster transfer reactions for samples (A) lacking DTT, (B) lacking apo-Fdx_{Rho}, or (C) a complete reaction with [2Fe-2S]-Fdx (80 μM), apo-Fdx_{Rho}(40 μM), and DTT (20 mM). Deconvolution of m/z peaks identified [2Fe-2S]-Fdx ([M+H]=12642.0 Da, expected mass 12643.7 Da) and apo-Fdx ([M+H]=12467.1 Da, expected mass 12467.9 Da) species. An additional peak in sample B is consistent with apo-Fdx plus two sulfur atoms. (D) Peak intensities for [2Fe-2S]-Fdx and apo-Fdx were integrated for all visible charge states and the percentage of apo-Fdx was plotted for the samples from (A), (B), and (C). The 50% apo-Fdx observed in the presence of DTT and apo-Fdx_{Rho} agrees well with the expected 41% (assuming [2Fe-2S]-Fdx is 12% apo to start). Error bars represent a standard error of 4%.

revealed that the majority of the unlabeled ferredoxin contained a [2Fe-2S] cluster. In contrast, the complete reaction resulted in significant cluster loss from the unlabeled Fdx significant cluster loss from the unlabeled Fdx (Figure 2-13C). Integrating the signals for all charge species indicated significantly more apo-Fdx was present in the complete reaction (~50%) than the control reactions (12% and 17%; Figure 2-13D). Moreover, the intensity of a peak assigned to [2Fe-2S]-Fdx_{Rho} increased for the complete reaction compared to the control reactions (Figure 2-12B). These results are consistent with cluster loss from unlabeled [2Fe-2S]-Fdx and DTT-dependent transfer of this species to Fdx_{Rho}. Collectively, fluorescence quenching and mass spectrometry experiments reveal that DTT catalyzes the Fe-S cluster transfer reaction from holo- to apo-Fdx, resulting in the redistribution of [2Fe-2S] clusters. These results also demonstrate that this labeling methodology permits the challenging real time detection of cluster content of a labeled protein in the presence of unlabeled proteins with identical Fe-S spectroscopic properties.

DTT accelerates transfer through ligand exchange reaction. The observation Fdx cluster exchange depends on DTT concentration suggests that DTT may be functioning in a ligand-substitution reaction to generate a DTT-cluster intermediate that can redistribute the cluster between apo-Fdx molecules. However, other possible roles for DTT include: (i) preparing the apo-Fdx_{Rho} for cluster transfer by reducing disulfides or chelating adventitiously bound metal ions; and (ii) reducing the Fe-S cluster (similar to mitoNEET(148)) resulting in a more labile species. To test the first alternative, Fdx_{Rho} was pre-reduced with 20 mM DTT for 4 hours and then diluted into a cluster

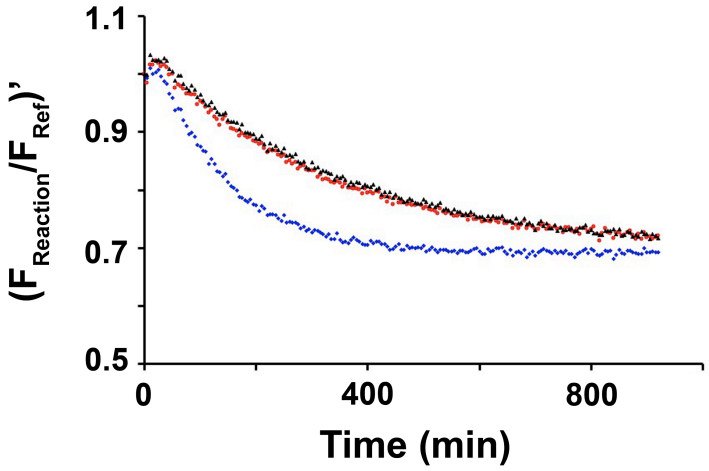

Figure 2-14. Fe-S cluster transfer reactions are unaffected by DTT pretreatment. Reactions contained 10 µM [2Fe-2S]-Fdx with either 20 mM DTT (dark blue) or 8 mM DTT (red and black). In the case of the black triangles, the apo-Fdx_{Rho} was pre-reduced with 20 mM DTT for 4 hours at 16 ºC in an anaerobic glovebox. The displayed data is the average of three runs for each sample with the maximum error (SD) for any data point being 0.04 $(F_{Reaction}/F_{Ref})'$.

transfer reaction containing a final concentration of 8 mM DTT. The additional incubation time with DTT had no effect on the cluster exchange kinetics (Figure 2-14), indicating that DTT is not reducing disulfides on Fdx_{Rho} or chelating bound metals. To test the second alternative, we added reagents known to reduce [2Fe-2S]-Fdx and measured the fluorescence quenching of Fdx_{Rho}. Notably, the oxidized and reduced forms of the Fe-S cluster exhibit similar quenching for [2Fe-2S]-Fdx_{Rho} (Figure 2-7). Substitution of dithionite for DTT resulted in a very slow quenching of fluorescence (Figure 2-15). Adding dithionite to standard exchange reactions along with DTT resulted

in almost identical rates as the dithionite-substituted reaction lacking DTT (Figure 2-15). This indicates that dithionite inhibits DTT-mediated cluster exchange. Substitution of the native ferredoxin electron donation system, FldR and NADPH, for DTT resulted in no cluster exchange (Figure 2-15). Addition of both DTT and FldR/NADPH resulted in exchange rates that were much slower than reactions with just DTT. Combined, these results suggest that DTT mediates the exchange reaction through a ligand substitution process and that reduced iron-sulfur clusters exchange on a much slower time scale than oxidized clusters. These experiments highlight the advantages of this labeling approach for detecting different types of Fe-S clusters and monitoring the transfer kinetics of these clusters under experimental conditions that would be challenging with other methods.

Discussion

A major challenge for understanding metal trafficking and metal cofactor

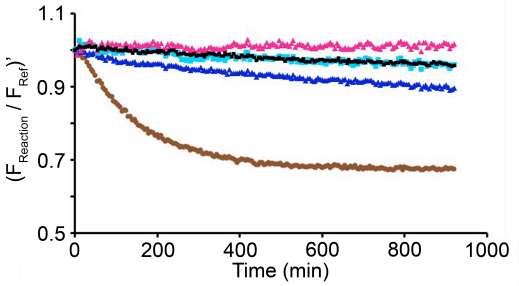

Figure 2-15. Fdx cluster exchange is slowed by reduction. Reactions contained apo-Fdx_{Rho} (0.5 µM), [2Fe-2S]-Fdx (10 µM) plus 20 mM DTT (brown), 1 mM sodium dithionite (cyan), 50 nM FldR and 100 µM NADPH (pink), 20 mM DTT and 1 mM sodium dithionite (black), or 20 mM DTT, 50 nM FldR, and 100 µM NADPH (dark blue). The plotted data is the average of at least three runs for each sample, with the maximum error (SD) for any data point being 0.06 $(F_{Reaction}/F_{Ref})'$.

biosynthesis is the lack of spectroscopic probes for measuring the rates of metal transfer reactions. It is imperative to distinguish between the thermodynamics and kinetics of *in vitro* metal transfer reactions. Thermodynamic studies provide information about whether or not a particular transfer can occur, but provide little information about whether or not that transfer is fast enough to be physiologically relevant. Here two fluorescent labeling strategies were described that successfully report iron-sulfur cluster binding, and are well suited to function as kinetic probes for metal transfer reactions. These fluorophore labeling strategies were demonstrated to be effective in reporting the presence of Fe-S clusters with different stoichiometries ([2Fe-2S] and [4Fe-4S] clusters), ligand sets (Grx4, Fdx, and Rieske [2Fe-2S] clusters), and oxidation states ($[2Fe\text{-}2S]^{2+}$ and $[2Fe\text{-}2S]^{1+}$ clusters). Notably, this is in contrast to the difficulties encountered when monitoring [4Fe-4S] cluster transfer reactions with CD spectroscopy(129), and the dramatic loss in absorbance signals upon cluster reduction. Perhaps the most important advantage of fluorescent labeling over existing methodology is the ability to detect the real-time Fe-S cluster incorporation of a specific labeled protein in the presence of unlabeled Fe-S binding proteins or other chromophores. Additionally, the ability to use different fluorophores with substantially different fluorescent properties permits the simultaneous monitoring of cluster transfer to multiple [2Fe-2S] or [4Fe-4S] binding proteins, and testing different factors as partitioning determinants for target specificity. This methodology can be used to determine kinetic parameters (k_{cat}, K_i and K_m values) for a wide variety of cluster transfer reactions, including experiments that evaluate the ability of multiple proteins to compete for a common cluster source. This method

represents a vast improvement over other techniques in terms of sensitivity, sample requirements, and range of concentrations that can be used in an assay. An additional benefit is the suitability of these fluorescence probes with high-throughput plate reader methodology.

There are multiple strategies to fluorescently label metal binding proteins. The first labeling approach, generation of a fusion protein with BFP, is straightforward in that it does not require any subsequent chemistry after protein isolation to incorporate the fluorophore. Fluorescent protein tags can also be beneficial in the solubilization and purification of proteins. However, we observed mixed results using this approach with no observable quenching for BFP-Fdx, but strong quenching (54%) upon [4Fe-4S] cluster binding to BFP-LAM. The second approach, intein labeling, allows for the site-specific labeling of any protein on its C-terminus. All three proteins labeled using this intein chemistry exhibited strong cluster-dependent quenching (39-52%). In addition, this labeling approach has many attractive qualities including inexpensive reagents, limited reactivity with amino acids side chains, and high yields.

The fluorescent constructs described here use a variety of different quenching mechanisms. The BFP constructs likely depend on FRET quenching with the cluster acting as an acceptor. FRET is a non-radiative process that depends on the donor-acceptor spectral overlap, varies with donor-acceptor orientation, and can occur over distances of up to 100 Å. In the case of BFP-LAM, the spectral overlap between the [4Fe-4S] cluster absorbance (between 400-500 nm) and BFP fluorescent emission (peak at ~450 nm) and the apparent long distance between the [4Fe-4S] cluster and

fluorophore (estimated at > 50 Å)(149) are consistent with FRET and not with quenching mechanisms limited to shorter distances. Thus, the quenching for BFP-LAM but not BFP-Fdx may be explained by the greater absorbance of a [4Fe-4S] cluster, the lower cluster content of BFP-Fdx, and/or differences in BFP-cluster distances or orientations.

Quenching for the rhodamine constructs may be more complex. In the case of $Grx4_{Rho}$, cluster induced dimerization brings the two rhodamine molecules within homoFRET distance (R0 = 55-58 Å)(107, 150). The Fdx_{Rho} and $Rieske_{Rho}$ proteins exhibit similar quenching to $Grx4_{Rho}$ upon [2Fe-2S] cluster binding but do not dimerize, ruling out a homoFRET quenching mechanism. Rather, it is likely that these fluorophores are quenched by a combination of FRET (with the cluster acting as an acceptor) and electron transfer. We estimate the distances between the cluster and fluorophore are between 6 and 36 Å based on the crystal structures of Fdx(151) and Rieske(152). These distances and the spectral overlap between [2Fe-2S] clusters and rhodamine are appropriate for FRET quenching. However, the quenching observed for Ni-Fdx_{Rho}, which has weak spectral overlap between the Ni^{2+} absorbance and rhodamine, suggests a non-FRET mechanism such as electron transfer may also be relevant.

Here we highlight some of the strengths of this labeling methodology by investigating the exchange of [2Fe-2S] clusters between holo-Fdx and apo-Fdx_{Rho}. The [2Fe-2S] clusters on Fdx are resistant to degradation in air and bind with very high affinity(85, 90, 92). Despite this thermodynamic stability, the addition of DTT was

found to mediate the exchange of [2Fe-2S] clusters between Fdx proteins. The rate dependence on DTT suggests a bimolecular reaction in which both DTT and [2Fe-2S]-Fdx participate in the transition state of the slow step in the reaction. These results support a model in which DTT functions in a ligand substitution reaction to form a [2Fe-2S]-DTT species that redistributes the [2Fe-2S] clusters between Fdx and Fdx_{Rho} (Figure 2-16). Interestingly, DTT alone was unable to cause a significant loss of cluster from [2Fe-2S]-Fdx (Figure 2-13). This suggests that while the cluster is labile in the presence of DTT, the equilibrium lies toward cluster binding to Fdx (Figure 2-16). We further demonstrate that cluster reduction decreases the exchange rate. This is a somewhat surprising result as cluster reduction is often thought, based on the reduced

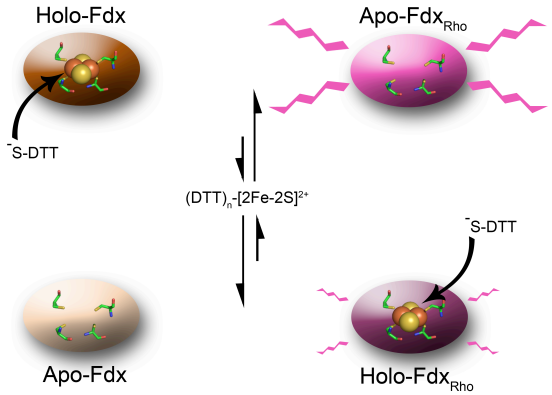

Figure 2-16. Model of DTT dependent cluster transfer reaction. DTT initiates ligand substitution reaction through nucleophilic attack of the $[2Fe\text{-}2S]^{2+}$ cluster on Fdx. This forms a DTT-$[2Fe\text{-}2S]^{2+}$ cluster species that readily transfers the cluster either back to apo-Fdx or to apo-FdxRho, which results in fluorescence quenching.

thermodynamic stability of some reduced Fe-S clusters, to trigger transfer reactions in Fe-S cluster biosynthesis. We postulate that the negatively charged DTT molecule is able to bind an oxidized cluster more readily than a reduced cluster, as would be expected based on electrostatic arguments. This lowers the transition state energy for the oxidized [2Fe-2S] cluster more than the reduced cluster, resulting in the observed differences in cluster transfer rate. These results further emphasize the need to examine the kinetics and not just the thermodynamics of metal transfer reactions.

The DTT-dependent acceleration of cluster exchange reactions raises questions about the physiological role of small molecule thiols in cluster transfer. The ligand substitution process described for DTT may be similar to that occurring for physiological cluster transfer reactions. Thiol-containing small molecule such as GSH(128) or trypanothione(119), which have been proposed to be important species in trafficking Fe-S clusters, may mediate *in vivo* cluster transfer reactions. Alternately, thiol-containing proteins such as monothiol glutaredoxins may mimic DTT and mediate the transfer of Fe-S clusters. It is also possible that the physiological cluster transfer reactions operate through a different mechanism than the ligand substitution exchange reactions mediated by DTT. This is supported by the ability of DTT to greatly enhance Fdx cluster exchange relative to GSH. Since the use of DTT is nearly ubiquitous in previous cluster transfer reactions, the transfer rates and conclusions for many of these studies warrant reinvestigation. DTT is likely even more efficient at catalyzing cluster transfer reactions for Fe-S assembly and transfer proteins, which are designed to transiently bind Fe-S clusters, than for the terminal Fe-S acceptor protein Fdx.

In summary, fluorophore labeling strategies were demonstrated to have general application in reporting Fe-S cluster content. An even more dramatic binding signal may be generated by placing the fluorophore near the metal binding site using artificial amino acid technology(153). The sensitivity of labeled Fe-S acceptor proteins to cluster binding, but insensitivity to Fe^{2+}/sulfide/GSH/NADPH (and low sensitivity to cysteine), along with the ability to monitor a labeled protein in the presence of unlabeled Fe-S proteins will make these probes transformative new tools for investigating *in vitro* Fe-S cluster assembly reactions. Furthermore, the ability to detect other metal ions suggests that this labeling approach may also have applications in the *in vitro* studies of additional metal transfer reactions.

Materials and methods

Protein preparations. BFP (GFP-sol variant(154) with Y66H and H145F substitutions) and a C-terminal tetra-glycine linker were cloned into a pET28a vector after the N-terminal His-tag using the MEGAWHOP(155) protocol. *E. coli* ferredoxin (Fdx) and lysine aminomutase (LAM) were amplified from genomic DNA and cloned into the BFP vector on the C-terminal side of the tetra-glycine linker. In addition, Fdx, Grx4, and Rieske (HcaC subunit of 3-phenylpropionate dioxygenase) were PCR amplified from *E. coli* genomic DNA and cloned into the NdeI and XhoI sites of pTwin1-His (Jena Bioscience). DNA sequences were confirmed by the Texas A&M Gene Technology Lab.

Five vectors (*BFP-Fdx*, *BFP-LAM*, *pTwin1-His-Fdx*, *pTwin1-His-Grx4*, and *pTwin1-His-Rieske*) were separately transformed into Rosetta (DE3) cells and grown in

LB medium (BD Biosciences) at 37 °C until the OD_{600} reached 0.5 -1.0. The temperature was decreased to 25 °C and protein expression was induced with 0.5 mM IPTG for 16 h. The cells were collected by centrifugation and disrupted by sonication in 20 mM Tris, 5 mM imidazole, 500 mM NaCl pH 7.5. The lysate was loaded on a 5 mL Ni-NTA column (GE Life Sciences) and eluted with a gradient to 500 mM imidazole. For the BFP-Fdx and BFP-LAM samples, the proteins were dialyzed and loaded on a 27 mL anion exchange column (POROS HQ 50 mM) with 50 mM Tris pH 7.5 and eluted with a gradient to 1 M NaCl. The BFP-Fdx and BFP-LAM fractions were concentrated, treated with 1-10 mM DTT, and loaded on a 26/60 Sephadex 300 column (GE Life Sciences) equilibrated with 50 mM Tris, 150 mM NaCl pH 7.5 (Buffer A). For the samples from pTwin vectors, the eluate from the Ni column was mixed with an equal volume of 400 mM Na_2S, 800 mM KH_2PO_4 and incubated for 16 h (Safety note: Prepare 400 mM Na_2S, 800 mM KH_2PO_4 in a fume hood by slowly adding 1.6 M KH_2PO_4 to a solution of 800 mM Na_2S). This step resulted in intein cleavage and production of thiocarboxylate species. The samples were dialyzed against 50 mM KPO_4, 100 mM KCl, pH 6.0 buffer (in a fume hood) and reapplied to the Ni column. The cleaved proteins flowed through the column. The samples were concentrated to ~1 mM and treated for 16 h with greater than five equivalents of Lissamine-rhodamine-B sulfonyl azide, which was synthesized from sulforhodamine B acid chloride (Sigma-Aldrich) and sodium azide (Sigma-Aldrich) as previously described[29] and stored at -20 °C in DMSO. The Fdx_{Rho}, $Grx4_{Rho}$, and $Rieske_{Rho}$ samples were separately applied to a 1 mL anion column and washed extensively with 50 mM Tris pH 7.5 buffer. Addition of up to 1 M NaCl eluted the pink

protein samples from the column. Occasionally, on column denaturation with 6 M urea and refolding was used to increase the yield. Analysis of the samples by SDS-PAGE and fluorescent gel imaging showed that the protein samples were successfully labeled and that excess fluorophore had been removed. Protein concentrations were determined using a Bradford assay. Rhodamine B was quantitated using the extinction coefficient(156) at 564 nm of 84000 M^{-1} cm^{-1}. The purified proteins were flash frozen in liquid nitrogen.

Preparation of apo and Fe-S cluster target proteins. Fe-S clusters were removed from Fdx_{Rho}, BFP-Fdx, $Grx4_{Rho}$, and $Rieske_{Rho}$ by acid precipitation with 10% trichloroacetic acid following incubation with 67 mM D,L-DTT, 67 mM NaOH for at least 5 minutes at room temperature. Proteins were pelleted and washed 5 times with 1 mL of metal free water. The proteins were resuspended in Buffer A in an anaerobic glovebox (mBraun, 16 °C, O_2 < 1 ppm). Lysine aminomutase was purified aerobically and did not contain an Fe-S cluster. Thus, the as-isolated protein was treated as apo-protein.

Apo-proteins were mixed with 10 mM BME, DTT, or GSH in a buffered solution (typically pH 7.2 for rhodamine-labeling constructs and pH 9.0 for BFP constructs). Ferric chloride and sodium sulfide or ferrous ammonium sulfate and 1 mM IscS, 5 mM IscU, and 1 mM cysteine were used for the cluster reconstitution. The iron and sulfide concentrations were kept below 1 mM. The cluster reconstitution reactions proceeded for 1 h to overnight depending on the particular protein. The reconstituted proteins were

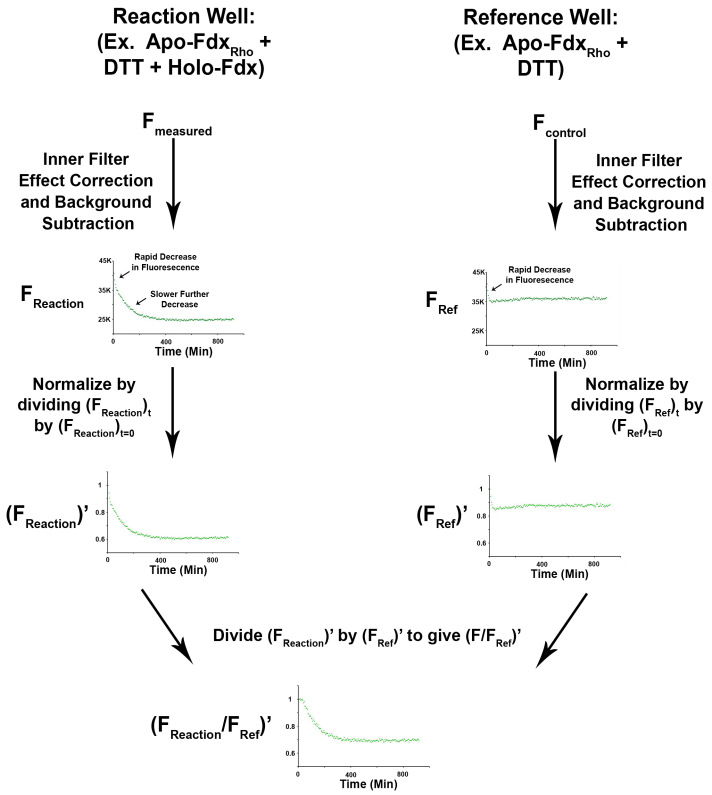

Figure 2-17. Data processing flow chart. A reaction and reference well were used for each experiment. The wells were identical except that the reference well lacks necessary components to initiate the reaction. The fluorescence was measured at each time point for the wells to produce $F_{measured}$ and $F_{control}$. The fluorescence was corrected for the inner filter effect and autofluorescence of the plates ($F_{Reaction}$ and F_{Ref}). Both samples showed rapid decreases in fluorescence that was attributed to photobleaching or protein adhesion. The two wells were normalized to a fluorescence value of 1 by dividing the fluorescence at time t by the fluorescence at time 0. This accounted for small deviations in fluorescence between wells ($(F_{Reaction})'$ and $(F_{Ref})'$). $(F_{Reaction})'$ was divided by $(F_{Ref})'$ to remove fluorescence decreases that were not due to the reaction, generating the final value of $(F_{Reaction} / F_{Ref})'$.

desalted with a 5 mL desalting column and applied to a Superdex 200 10/300 size exclusion column (GE Life Sciences). Only protein eluting at the correct size was used

for experiments (dimer for Grx4, and monomers for Fdx, Rieske, and LAM). In some cases, a 1 mL monoQ column (Pharmacia Biotech) was used to remove additional iron and sulfide. The ferrozine assay (extinction coefficient of 28000 M^{-1} cm^{-1} at 562 nm) was used to quantitate iron(157). For the rhodamine labeled proteins, the absorbance due to rhodamine was subtracted from the total absorbance (rhodamine plus ferrozine complex) prior to iron quantitation. Sulfide was quantified using a methylene blue assay that included pretreatment of the protein with NaOH and zinc acetate(158).

Fluorescence assays. Assays were carried out in a Tecan M200 fluorescent plate reader using top-read fluorescence and bottom-read absorbance measurements. The plate reader is located in an anaerobic glovebox (oxygen < 0.5 ppm). Greiner 96 well plates with black sides, clear flat bottoms, and a non-binding coating were used. Plates were kept in the glovebox overnight before use to allow oxygen dissolved in the plastic to diffuse out. The fluorescence of the BFP proteins was measured with excitation and emission wavelength of 380 nm and 450 nm, respectively. Rhodamine-labeled proteins were monitored with excitation wavelength of 550 nm and emission wavelengths of 600 nm. Assays were typically monitored for 16 hours at 25 °C while covered with low-fluorescent clear tape.

Fluorescence data processing. A data processing flow chart is provided as Figure 2-17. Raw fluorescence data for the reaction ($F_{measured}$) was corrected for the inner filter effect by recording the absorbance of each sample at the excitation (Abs_{ex}) and emission (Abs_{em}) wavelengths and then calculating the corrected fluorescence ($F_{reaction}$)

with the first term of equation (1). For the BFP samples, the plates exhibited significant autofluorescence (F_{auto}) and required subtraction of a second correction term in equation (1).

$$F_{reaction} = F_{measured} \times 10^{\left(\frac{Abs_{ex}+Abs_{em}}{2}\right)} - F_{auto} \times 10^{\left(\frac{Abs_{ex}+Abs_{em}}{2}\right)} \qquad (1)$$

This second term was obtained from the average fluorescent signals from three wells containing buffer (F_{auto}), and was also corrected for the inner filter effect. A reference sample (F_{ref}) was also used to correct for any photobleaching or adhesion to the plate. F_{ref} was calculated using equation (2) using a second control sample ($F_{control}$) that included the fluorescent protein at the same concentration as the reaction, but lacked a reagent that was necessary to initiate the reaction (holo-ferredoxin in this case). Inner-filter effect and autofluorescence corrections were also applied.

$$F_{Ref} = F_{control} \times 10^{\left(\frac{Abs_{ex}+Abs_{em}}{2}\right)} - F_{auto} \times 10^{\left(\frac{Abs_{ex}+Abs_{em}}{2}\right)} \qquad (2)$$

The fluorescence intensity for the reference sample (F_{ref}) was scaled to be 100% throughout the assay. When the fluorescence signals of the sample and reference wells at time 0 were within error of each other, their fluorescent signals were normalized (by dividing the fluorescence at time t by the fluorescence at time 0) in order to allow the fluorescence experiment to start at a value of 1. The normalized fluorescence values of the reaction and reference wells were then divided to generate the final ($F_{reaction}/F_{ref}$)' value in equation (3).

$$\left(\frac{F_{reaction}}{F_{ref}}\right)'_t = \left(\frac{F_{reaction,\ t}}{F_{reaction,\ t=0}}\right) \Big/ \left(\frac{F_{ref,\ t}}{F_{ref,\ t=0}}\right) \qquad (3)$$

Fe-S cluster transfer and control reactions. Control quenching reactions included 0.5-5 μM Fdx_{Rho} (either holo or apo) in 50 mM HEPES, 150 mM KCl pH 7.2 (Buffer A) and were performed at 25 °C. Some reactions included 10 mM GSH at pH 7.2. Reagents tested include L-cysteine (1 mM), ferrous ammonium sulfate (100 μM), NADPH (1 mM), GSH (10 mM), D,L-DTT (20 mM), sodium dithionite (1 mM), sodium sulfide (1 mM), FldR (100 nM) with NADPH (1 mM), ferric chloride (100 μM), nickel (II) chloride (100 μM), or copper (II) sulfate (100 μM). The fluorescence was collected immediately and compared to a sample lacking the additives. In separate kinetic control experiments, 5 μM Fdx_{Rho} was incubated with either ferrous ammonium sulfate (100 μM) and GSH (10 mM) or with IscS (0.5 μM), cysteine (100 μM), and GSH (10 mM) at 25 °C in a solution of Buffer A with 10 mM GSH. The fluorescence was collected upon iron or cysteine addition and compared to a sample that lacked iron or both IscS and cysteine.

For cluster transfer reactions, apo-Fdx_{Rho} was diluted into a solution of Buffer A, typically to a concentration of 0.5 μM. Reducing agents DTT, GSH, sodium dithionite, or FldR/NADPH were added to the reaction. The reaction was initiated by the addition of holo-Fdx. The samples were mixed by pipetting and the plate was covered with low-fluorescent plastic tape. The temperature of the plate reader was maintained at 25 °C throughout the assay. Every five minutes, the fluorescence was measured (excitation:

550nm, emission: 600nm) along with absorbance at the excitation and emission wavelengths, and the sample was shaken further to prevent localized photobleaching. The reaction was typically allowed to proceed for ~16 hrs.

Mass spectrometry. Complete Fdx cluster transfer assays that included 80 μM [2Fe-2S]-Fdx, 40 μM Fdx_{Rho}, and 20 mM D,L-DTT in Buffer A were allowed to proceed overnight. Control reactions lacked Fdx_{Rho} or DTT. 50 μL aliquots from the reactions were desalted into 10 mM ammonium acetate using Bio-Rad Micro-spin 6 columns, diluted 1:10 into 10% acetonitrile, and analyzed by direct infusion into a Bruker 9.4 T FT-ICR-MS. The source voltage was 4000 V and the mass window was 130 – 2700 m/z with a transient length of 1.9 seconds. The data from 40 spectra were averaged. Raw data were deconvoluted using Bruker software.

CHAPTER III

INVESTIGATING THE ROLE OF THE MONOTHIOL GLUTAREDOXINS WITH FLUORESCENT PROBES

Introduction

Iron-sulfur clusters (Fe-S) are found throughout all of the kingdoms of life, where they serve a wide variety of critical functions(1). Fe-S clusters are involved in electron transport(12-15), catalysis of biological reactions(16-18), and regulation of cellular responses to oxidative stress(24, 25). It is not surprising that defects in the biosynthesis and transfer of Fe-S clusters are associated with numerous human diseases(49, 56, 57). Despite the importance of these cofactors, many mysteries remain regarding their biosynthesis and insertion into their target proteins.

In many bacteria and the eukaryotic mitochondria, the ISC biosynthetic machinery is responsible for cluster biosynthesis(6, 159). The ISC pathway utilizes a core complex consisting of a cysteine desulfurase (IscS) and a scaffold protein (IscU) (6, 59). IscS catalyzes the conversion of cysteine to alanine and a persulfide(74). IscU serves as the site for cluster assembly(80, 83). The persulfides that are formed on IscS can be transferred to IscU, where they are combined with ferrous iron and two electrons to form a [2Fe-2S] cluster(84, 85).

The cluster that is formed on IscU must then be transferred to a variety of apo target proteins in the cell. Several proteins have been implicated in the process of transferring clusters, including the chaperone/co-chaperone pair of HscA/HscB(55),

IscA(109-111), and the monothiol glutaredoxins (Grxs) (160, 161). The role of the glutaredoxins has been quite mysterious. Grxs come in two varieties, the monothiol and dithiol glutaredoxins, with their respective names indicating the number of cysteine residues present in the active site of these enzymes. The Grxs are so named due to their ability to catalyze disulfide reduction reactions on molecules such as ribonucleotide reductase in a process that utilizes reduced glutathione (GSH) (162). While similar to thioredoxins, they are uniquely able to reduce S-glutathionylated proteins (163, 164). Interestingly, both classes of Grxs also possess the ability to bind an Fe-S cluster(107, 165-168). Curiously, this binding requires two monomers of Grx that both provide a single cysteine ligand to opposite iron atoms of the cluster with the other two ligands coming from two molecules of non-covalently bound GSH. Even more intriguing is the observation that the ligating cysteine is the residue that is required for Grxs thiol reduction function(169). While crystal structures indicate that monothiol Grxs bind a [2Fe-2S] cluster, other studies have demonstrated the ability of this class of Grxs to bind both linear [3Fe-4S] and traditional [4Fe-4S] clusters(170). The physiological relevance of these cluster forms remains a matter of debate. Interestingly, monothiol Grxs can also bind clusters in heterodimeric complexes with BolA/Fra2, forming complexes with perturbed cluster properties and specific regulatory functions(25, 120, 121, 124, 171).

In Fe-S cluster biosynthesis, glutaredoxins have been proposed to function as intermediate cluster carriers for transfer processes or as cluster storage proteins based on *in vivo* and *in vitro* studies (92, 172). Holo-monothiol and dithiol glutaredoxins have been shown to transfer their clusters to ferredoxin (Fdx), but *in vivo* data more strongly

links the monothiol Grxs to Fe-S cluster biosynthesis (67, 92, 118). Additionally, the monothiol glutaredoxins have been shown to be able to transfer clusters to IscA and to aconitase(125, 170). Clusters bound to monothiol glutaredoxins are generally regarded as more labile than clusters bound to dithiol Grxs(67). Additionally, the monothiol glutaredoxins have also been shown to accept a cluster from holo-IscU, in a chaperone enhanced fashion(92). The independently measured rates of transfer from IscU to monothiol glutaredoxin and then glutaredoxin to ferredoxin was determined to occur faster than the transfer from IscU to ferredoxin alone, providing the first kinetic evidence for the role of glutaredoxin as an intermediate cluster carrier(92). However, it is important to note that several of these transfer steps include DTT, which has been shown to artificially enhance the rates of cluster transfer reactions. Furthermore, these rates were measured without any determination of K_m values and didn't allow for competition between glutaredoxin and ferredoxin for a common cluster source, thus calling into question the relevance of these findings in a biological setting that includes all three proteins at much lower protein concentrations. Additionally, these studies utilized a [2Fe-2S]-IscU dimer species as the cluster source, despite the fact that it has never been established to be a kinetically competent intermediate of the cluster biosynthetic pathway.

In a previous paper, we demonstrated the ability of fluorescent Fe-S cluster binding proteins to report on their cluster content in mixtures containing other chromophores. Here we extend the utility of this assay to investigate proposed transient cluster formation on *E. coli* IscU and monothiol Grx4. We expand the known

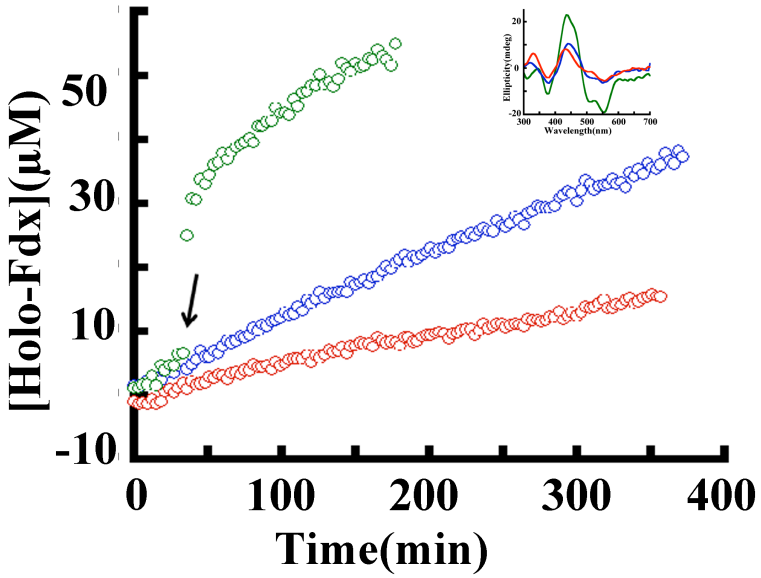

Figure 3-1. DTT accelerates the cluster transfer from holo-Grx4 to apo-Fdx. Reactions contain 10μM IscU, 20μM Grx4, 40μM apo-Fdx, 400μM Fe^{2+} and 100 μM cysteine and 10 mM GSH (Blue). The reaction is spiked with 5mM DTT after 50 min (green). The control lacks Grx4 (Red). Inset: CD spectra for the reactions at the end of 120 minutes.

functionality of Grx4 by demonstrating its ability to function as general intermediate carrier proteins while simultaneously providing insight into the mechanism of the associated cluster transfer events. This study shows the power of this technique to detect pathway intermediates and directly investigate the complex network of cluster transfer reactions.

Results

Cluster transfer between IscU/Grx4 and Fdx is enhanced by DTT. CD spectroscopy has been widely used to monitor Fe-S cluster transfer reactions. Previous results suggest that cluster transfer from IscU to Fdx is greatly enhanced in the presence of both monothiol Grx and chaperones. In the absence of chaperones, Grx appeared to be unable to accelerate cluster transfer from IscU to Fdx. It is worth noting that many of

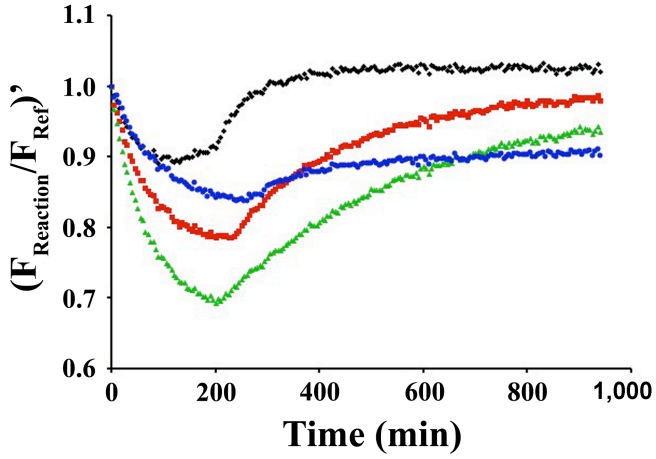

Figure 3-2. Cluster assembly on $IscU_{Rho}$ in the presence or absence of apo-acceptors. Reactions contained 10 mM GSH, 30 µM Fe2+, 0.5 µM IscS, 5 µM $IscU_{Rho}$, 30 µM cysteine (blue). Other reactions also contained apo-target proteins: 40 µM Grx4 (black), 20 µM Fdx (red), or 20 µM HcaC (green).

the reactions that led to these conclusions included DTT, which has been shown to artificially enhance cluster transfer reactions.

In order to test the DTT dependence of glutaredoxin mediated IscU:Fdx transfer, cluster transfer reactions were carried out and monitored with CD spectroscopy (Figure 3-1). In the absence of Grx4 cluster transfer from IscU to Fdx was very slow and does not show a substantial increase even in the presence of DTT (data not shown). Inclusion of Grx4 resulted in greater apparent cluster signal relative to the sample lacking Grx and a greater apparent rate. Spiking the reaction with DTT in the presence of Grx4 resulted in very rapid cluster transfer to Fdx. At the conclusion of the reaction, the CD spectrum of the reaction containing DTT resembles that of holo-Fdx while the DTT-free Grx4 containing sample appears to be a complex mixture of spectra. Due to the difficulty in resolving the individual component CD spectra of the DTT-free Grx4 containing sample at intermediate time points, our recently developed fluorescent cluster transfer assay was employed to determine the function of Grx4.

Direct evidence for transient cluster formation on IscU. To establish the utility of fluorescently labeled proteins for investigating enzymatic cluster transfer reactions, the ability of IscU to function as a scaffold protein in a complete cluster biosynthesis/transfer reaction was first demonstrated. IscU was purified as an intein construct and fluorescently labeled with sulforhodamine B as done previously ($IscU_{Rho}$). When a cluster assembly reaction was carried out with IscS, ferrous iron, GSH, and cysteine, time dependent fluorescence quenching was observed (Figure 3-2). This is consistent with Fe-S cluster formation on $IscU_{Rho}$ as has been demonstrated with

unlabeled IscU (59). The reactions were then repeated, but in the presence of an apo-acceptor protein. The acceptors that were utilized were the proposed intermediate cluster carrier Grx4, the terminal target protein Fdx, and a Rieske-type protein (HcaC) that ligates a cluster with a 2-His/2-Cys ligation. Grx4 showed the greatest ability to inhibit IscU quenching and additionally showed the most rapid rescue of the quenching, consistent with its proposed role as an intermediate cluster carrier. Inclusion of either Fdx or HcaC resulted in the surprising result of increased quenching relative to the reaction containing $IscU_{Rho}$ alone. In both cases the fluorescence was rescued at later time points, but at a much slower rate than was observed for Grx4. In all of the cases containing a target protein, the apparent formation and decay of [2Fe-2S]-$IscU_{Rho}$ is consistent with its role as a scaffold protein, since its intermediate-like behavior indicates that cluster transiently binds and is transferred to other apo-target proteins.

Fluorescence of $Grx4_{Rho}$ is sensitive to enzymatically produced Fe-S clusters. For this study, *E. coli* Grx4 (a monothiol glutaredoxin) was purified as an intein fusion protein and fluorescently labeled with sulforhodamine B ($Grx4_{Rho}$). $Grx4_{Rho}$ has previously been shown to be sensitive to cluster binding, with little response in the presence of cysteine, ferrous iron, glutathione (GSH), or sulfide alone. Initially $Grx4_{Rho}$ was added to an Fe-S cluster assembly/transfer reaction containing IscS, IscU, GSH, and ferrous iron. Cysteine was added to initiate the reactions. The reference well contained all components except IscS and cysteine (the IscS was omitted due to an apparent cysteine contamination in the GSH; data not shown). Fluorescence quenching was observed over time, with the final quenching leveling off at 34% (Figure 3-3). This

value is significantly more quenched than measured with chemically reconstituted [2Fe-2S]-Grx4$_{Rho}$. A sample of unlabeled Grx4 was placed in an identical reaction, except this reaction was monitored with CD spectroscopy. The rate of the CD signal increase at

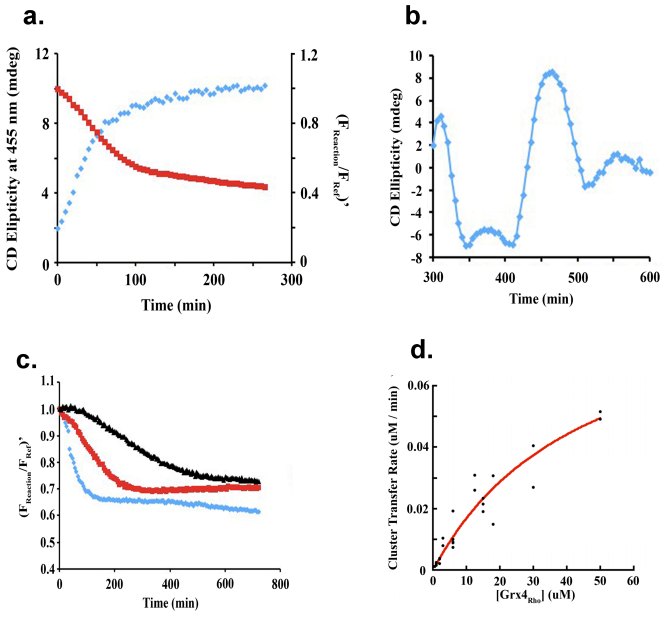

Figure 3-3. Grx4Rho quenching reports on cluster transfer and effect on rate with varying acceptor and GSH concentrations. (a) The rate of IscS:IscU mediated cluster transfer was monitored to Grx4$_{Rho}$ using fluorescence (red) or CD spectroscopy at 455 nm (blue). Reactions contained 10 mM GSH, 100 µM Fe^{2+}, 2 µM IscS, 10 µM IscU, 20 µM Grx4 (labeled or unlabeled), and 100 µM cysteine. (b) The CD spectrum at 265 minutes was subtracted from the spectrum at 0 minutes. (c) Fluorescence quenching was monitored for Grx4$_{Rho}$. GSH concentration used was 10 mM (cyan), 3 mM (red), or 1 mM (black). Reactions contained 100 µM Fe^{2+}, 0.5 µM IscS, 5 µM IscU , 2 uM Grx4$_{Rho}$, and 100 µM cysteine. (d) Cluster transfer rates were plotted as a function of apo-acceptor concentration for Grx4$_{Rho}$. The reactions contained 10 mM GSH, 100 uM Fe^{2+}, 100 nM IscS, 5 µM IscU, 100 µM cysteine and varying concentrations of apo-acceptor. The data was fit to a Michaelis-Menton equation (red).

455nm matches the rate of fluorescence decay observed with labeled protein (Figure 3-3a). Additionally, the difference CD spectrum at the conclusion of the reaction resembles that of a [2Fe-2S]-glutaredoxin (Figure 3-3b).

In order to confirm that the observed quenching was due to enzymatic cluster assembly and not solution Fe-S chemistry, the reactions were repeated either in the presence of DTT or in the absence of IscU. The presence of DTT greatly reduced the observed quenching (Figure 3-4). Likewise, assays lacking IscU resulted in decreased, unstable quenching (Figure 3-5). In order to further establish that the protein was not

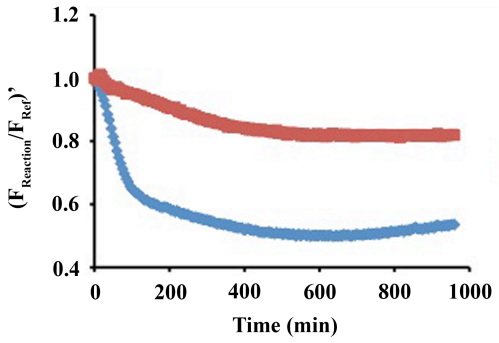

Figure 3-4. Effect of DTT on cluster transfer to $Grx4_{Rho}$. Reactions contained 100 µM Fe^{2+}, 10mM GSH, 0.5 µM IscS, 5 µM IscU, 5 µM $Grx4_{Rho}$, and 100 µM cysteine (blue). Additional reactions were run with all of the previous components but also with 20 mM D,L-DTT (red). The plotted data are the average of three runs. The maximum error was 0.04.

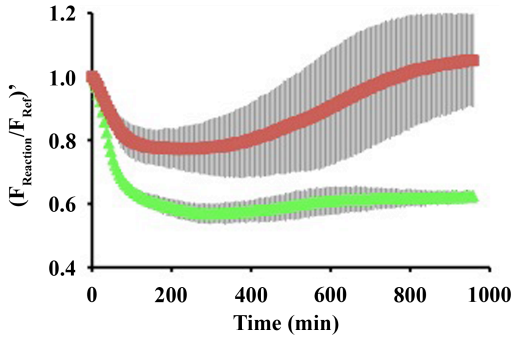

Figure 3-5. Effect of IscU on cluster transfer to $Grx4_{Rho}$. Reactions contained 10 mM GSH, 100 µM Fe^{2+}, 0.5µM IscS, 5 µM $Grx4_{Rho}$, and 100 µM cysteine. Some samples (green) contained 5 µM IscU as well, while others (red) did not. Grey bars represent one standard deviation (n=5).

associating with Fe-S mineral species that have been observed in other Fe-S assembly assays, a size exclusion column was run on a cluster transfer reaction to $Grx4_{Rho}$ after the fluorescence was fully quenched. The results show clear conversion of monomeric $Grx4_{Rho}$ to dimeric $Grx4_{Rho}$ with almost no detectable aggregated material (Figure 3-6). In another experiment the dependence of fluorescence quenching on dimerization was assessed by varying the ratio of labeled to unlabeled Grx4, thereby perturbing the probability of homoFRET quenching (Figure 3-7). Since no difference in quenching extent was observed at decreased ratios of fluorescent Grx4, the contribution due to homoFRET is likely minimal.

Rate-limiting step of reaction is glutathione dependent cluster transfer. We next sought to determine conditions where cluster transfer was rate limiting. In order to do this, we varied the concentrations of GSH and apo-$Grx4_{Rho}$. The quenching rate of $Grx4_{Rho}$ was shown to depend on the concentration of GSH (Figure 3-3). Decreasing the

concentration of GSH decreased the rate of fluorescence quenching. GSH could function in cluster biosynthesis as an electron donor or in cluster transfer as a cluster ligand. To address the functional role of GSH, the dependence of cluster transfer rate on the concentration of apo-acceptor protein was determined (Figure 3-3). The cluster transfer rate appears to increase with increasing acceptor concentration. A fit to

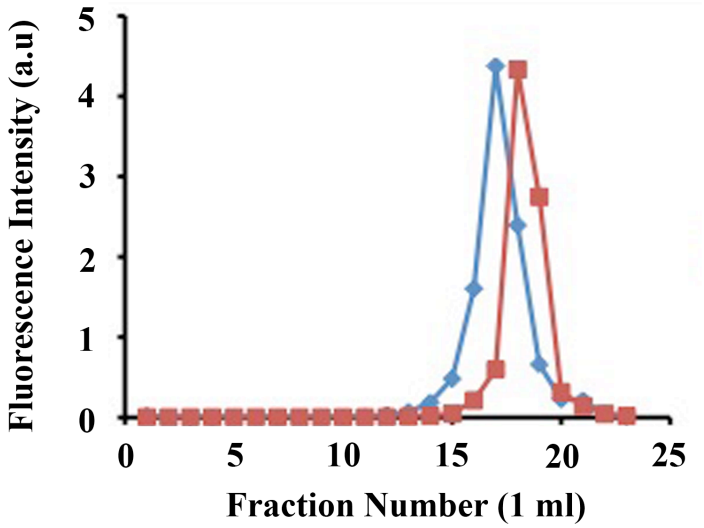

Figure 3-6. Size exclusion chromatography of $Grx4_{Rho}$ before and after cluster transfer. Size exclusion chromatography was run before (red) or after (blue) a cluster transfer reaction for $Grx4_{Rho}$.

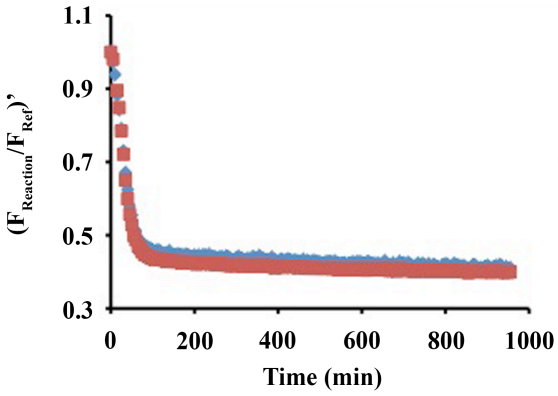

Figure 3-7. Fluorescence of Grx4Rho is sensitive to cluster and not dimerization. A cluster transfer reaction was carried out with $Grx4_{Rho}$ similar to others where the $Grx4_{Rho}$ was 100% fluorescently labeled (red) or 10 % fluorescently labeled (blue).

Michaelis-Menton kinetics gave an apparent K_m of 50±10 μM and an apparent V_{max} of 0.19±0.03 μM cluster/min. Interestingly, holo-Grx4 appears unstable at concentrations of 2 μM or less (Figure 3-8). This may reflect the physiological dimerization/cluster binding constant. Based on these results, and since no function of an apo-acceptor protein in cluster biosynthesis is immediately obvious, we concluded that cluster transfer was the rate-limiting step and that GSH likely plays a functional role in this process.

$Grx4_{Rho}$ directly transfers clusters to apo-Fdx and apo-HcaC. We next investigated the ability of Grx4 to transfer clusters to Fdx and HcaC. In order to determine the mechanism of cluster transfer from $Grx4_{Rho}$ to apo target proteins, the dependence of the transfer rate on the concentration of GSH and terminal acceptor

protein was determined. Holo-Grx4$_{Rho}$ was first produced by an overnight cluster transfer assay using IscS and IscU. The quenched Grx4$_{Rho}$ reaction mixture was then diluted into wells containing varying concentrations of GSH, apo-Fdx, or apo-HcaC (Figure 3-9). In the cases where no apo-acceptor protein was included, only very slow fluorescence recovery was observed, indicating that holo-Grx4$_{Rho}$ is stable upon dilution.

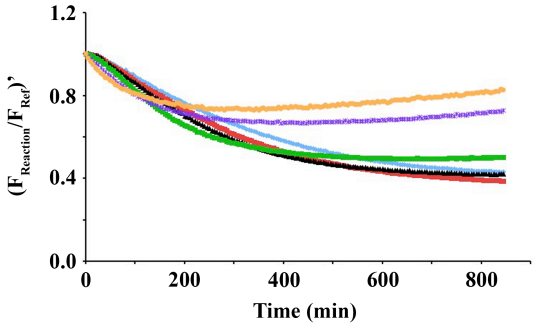

Figure 3-8. Quenching of Grx4$_{Rho}$ as a function of Grx4$_{Rho}$ concentration. Fluorescence quenching was monitored for a cluster transfer reaction from IscS:IscU to Grx4$_{Rho}$. The reactions contained 10 mM GSH, 100 µM Fe^{2+}, 100 nM IscS, 5 µM IscU, 100 µM cysteine and varying concentrations of apo-acceptor. Concentrations of Grx4$_{Rho}$ were 1 µM (orange), 2 µM (purple), 6 µM (green), 15 µM (black), 30 µM (red), and 50 µM (cyan).

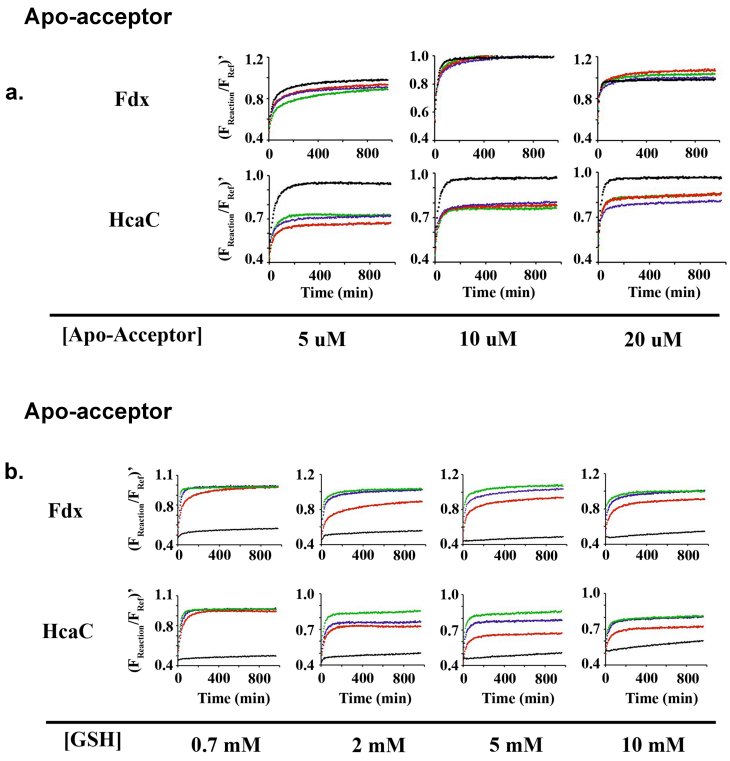

Figure 3-9. Cluster transfer from Grx4 to apo-acceptors is direct and not mediated by GSH. Holo-Grx4$_{Rho}$ was produced and diluted into reactions containing various concentrations of GSH and varying concentrations of apo-Fdx or apo-HcaC. (A) Different GSH concentrations are compared in each panel; concentrations were 0.7 mM (black), 2 mM (green), 5 mM (red), and 10 mM (purple). (B) Different apo protein concentrations were compared in each panel; concentrations used were 0 μM (black), 5 μM (red), 10 μM (purple), and 20 μM (green).

However, upon addition of apo-acceptor protein, the fluorescence began to increase, eventually approaching the fluorescence of apo-Grx4. The rate of the increase in fluorescence was shown to depend heavily on the concentration of apo-acceptor protein.

On the other hand, increasing concentrations of GSH appear to slow cluster transfer from Grx4.

It is worth noting that the fluorescence of [2Fe-2S]-$Grx4_{Rho}$ didn't fully recover in many cases. The inability of lower concentrations of apo-acceptors to fully rescue the fluorescence indicates that an equilibrium may exist between Fdx/HcaC and Grx4 for binding clusters. To test this, the four curves from the 10 mM GSH sample were fit to models for irreversible and reversible cluster transfer from Grx4 to either Fdx or HcaC. In both cases, the reversible model fit better, with $K_{transfer}$ values of 3.3 and 0.14 respectively at 10 mM GSH (Table 3-1 and Figure 3-10).

Apo-target proteins perturb cluster transfer to $Grx4_{Rho}$. In order to investigate whether Grx4 serves as an intermediate cluster carrier between IscU and apo-target proteins, $Grx4_{Rho}$ was placed in a cluster assembly/transfer reaction along with

Table 3-1. Kinetic analysis of cluster transfer from [2Fe-2S]-Grx4Rho to apo-acceptors.

	$k_{degrade}$ (min-1)	k_2 ($uM^{-1}min^{-1}$)	k_{-2} ($uM^{-1}min^{-1}$)	RMS Error
Fdx[a]	0.000156(9)	0.00166(3)	n.d.	0.22
Fdx[b]	0.000161(5)	0.00318(6)	0.00097(3)	0.13
HcaC	0.000306(5)	0.00159(5)	0.0114(4)	0.11

[a]Modeled as an irreversible reaction. [b]Modeled as a reversible reaction.

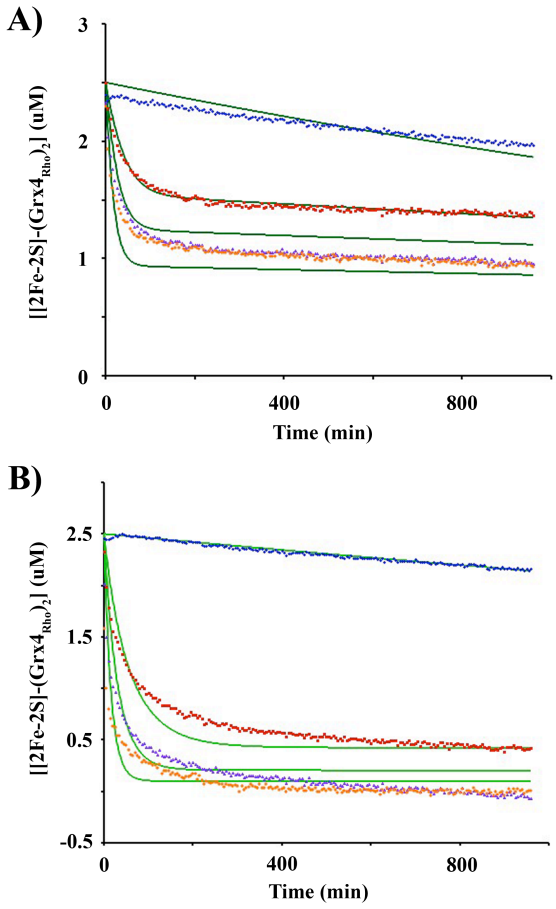

Figure 3-10. Global fit analysis of $Grx4_{Rho}$ cluster transfer to apo-Fdx and apo-HcaC. The data from Figure 3-11 was converted into concentration of holo-$Grx4_{Rho}$ vs. time. The data corresponds to samples containing varying concentrations of apo-HcaC (A) or apo-Fdx (B). Concentrations of apo-target protein used were 0 µM (blue), 5 µM (red), 10 µM (purple), and 20 µM (orange). Green lines are simulations of the best kinetic fits from Table 3-1.

varying concentrations of the apo-terminal acceptor proteins Fdx or HcaC. The fluorescence quenching behavior of $Grx4_{Rho}$ should be sensitive to both the cluster transfer rate from IscU to Grx4 as well as the transfer rate from Grx4 to terminal

acceptor proteins, allowing us to evaluate the rates for all of these processes. When apo-Fdx was added into a reaction mixture with $Grx4_{Rho}$, the time dependence of the fluorescence quenching was greatly perturbed (Figure 3-11). At higher concentrations of apo-Fdx, an initial formation of [2Fe-2S]-$Grx4_{Rho}$ was observed, followed by a steady-state leveling that lessened as the apo-Fdx was depleted. In the case of HcaC, rapid formation of [2Fe-2S]-$Grx4_{Rho}$ was observed followed by leveling off at different values that were dependent on the concentration of apo-HcaC (Figure 3-11). This behavior further supports the observation that Grx4 and HcaC exhibit equilibrium cluster binding. It is also worth noting that in the majority of cases for reactions containing either Fdx or HcaC, the initial kinetics of [2Fe-2S]-$Grx4_{Rho}$ formation were unperturbed

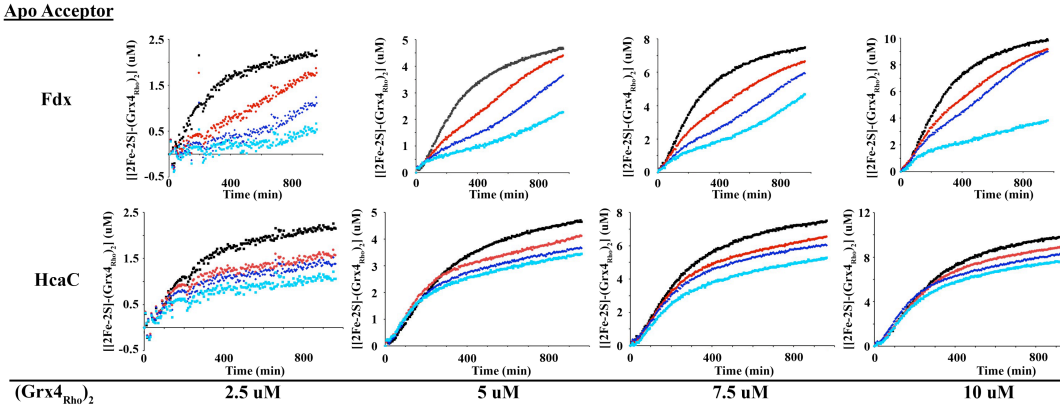

Figure 3-11. Cluster transfer to $Grx4_{Rho}$ in the presence of apo-acceptor proteins. Cluster transfer reactions contained 10 mM GSH, 100 uM Fe^{2+}, 0.1 µM IscS, 5 µM IscU, varying concentrations of $Grx4_{Rho}$, 100 µM cysteine, and either 0 µM (black), 5 µM (red), 10 µM (blue), or 20 µM (cyan) apo-Fdx or apo-HcaC.

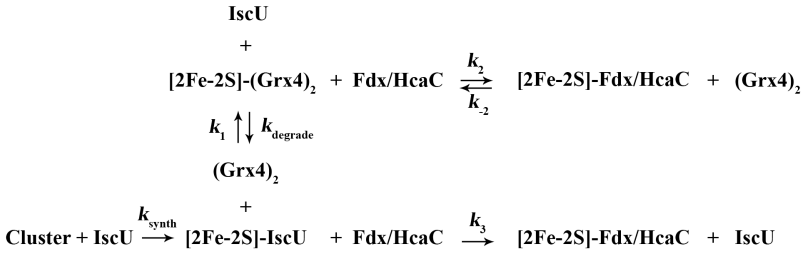

Figure 3-12. Reaction scheme for kinetic modeling. The rate constants listed here correspond to the rate constants in Table 3-1 and Table 3-2.

by the apo acceptor, suggesting that $Grx4_{Rho}$ is an early cluster transfer intermediate and hence successfully outcompetes apo-targets for IscU-bound cluster.

Modeling Grx4 cluster transfer pathways. The kinetic traces for cluster transfer to $Grx4_{Rho}$ in the presence of apo-Fdx or HcaC were used to model the cluster transfer pathway. The observation that the rate-limiting step of the reactions was cluster transfer rather than cluster synthesis allowed us to model the reactions starting with a fixed concentration of [2Fe-2S]-IscU, in most cases. Additionally, fluorescence quenching data and results from other groups suggest that cluster transfer from IscU to either Grx4 or Fdx is irreversible, so all transfer steps from [2Fe-2S]-IscU were modeled as irreversible processes with only a forward rate constant(90, 92). Furthermore, efforts to include Michaelis complexes for transfer reactions from [2Fe-2S]-IscU did not substantially improve the fitting and are not included (data not shown).

Initial models contained only the linear transfer pathway from IscU to Grx4 to a terminal acceptor protein. Additional models were also used that incorporated the ability

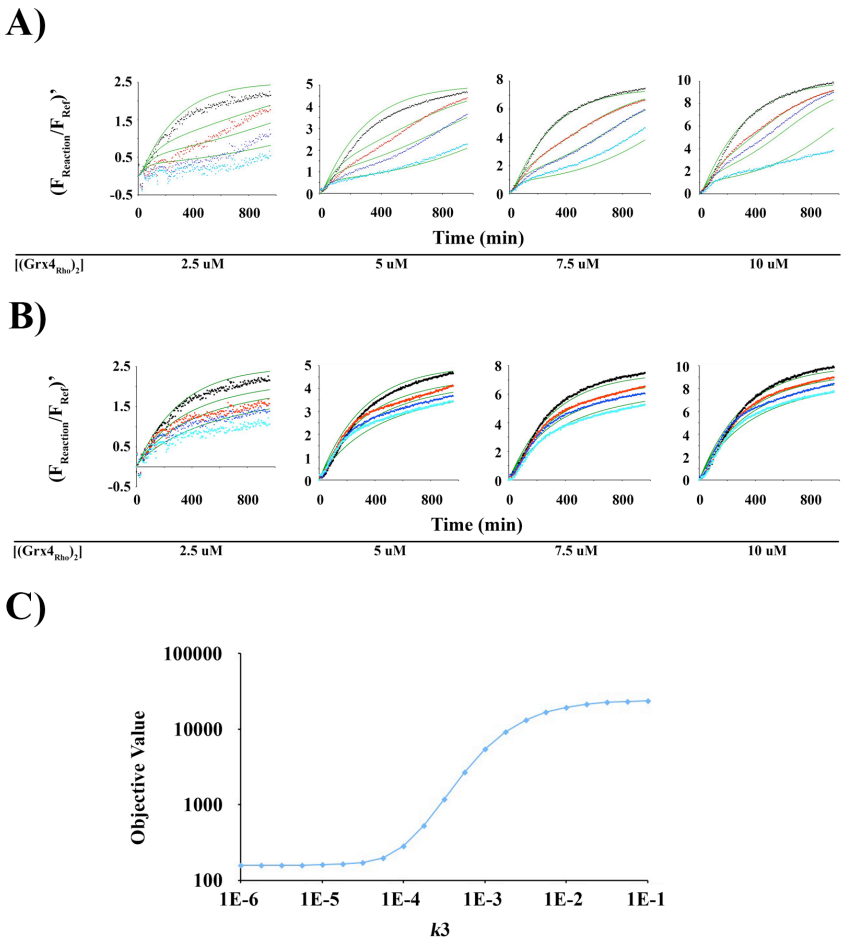

Figure 3-13. Global fit analysis of IscS:IscU cluster transfer to $Grx4_{Rho}$ in the presence of apo-Fdx or HcaC. Data from Figure 3-13 was plotted again for reactions containing apo-Fdx (A) or apo-HcaC (B). Green lines correspond to the best fit from Table 3-2. (C) Objective value (sum of squares) is plotted vs. *k*3 for the reactions containing HcaC and Grx4Rho.

of IscU to donate a cluster directly to the terminal target protein (Figure 3-12). In the case of Fdx, inclusion of a direct transfer pathway for cluster from IscU to Fdx improved the overall fit (Table 3-2). Furthermore, limiting the amount of cluster in the model by including a cluster biosynthesis reaction further improved the fit (Table 3-2, Figure 3-13). Notably, inclusion of k_3 and k_{synth} had only minor effects on k_1 and k_2. The observation that k_3 is ~2-4 fold less than k_1 or k_2 implies that cluster transfer to Fdx proceeds through a [2Fe-2S]-Grx4 intermediate.

In the case of HcaC, the inclusion of a reversible transfer from [2Fe-2S]-Grx4 to HcaC produced a model that very closely approaches the observed data (Table 3-2 and Figure 3-13). In this fit, k_2 and k_{-2} were constrained to values from Table 3-1 since that

Table 3-2. Global fit parameters for $Grx4_{Rho}$:Apo-Acceptor cluster transfer reactions.

	k_{synth} ($uM^{-1}min^{-1}$)	k_1 ($uM^{-1}min^{-1}$)	k_2 ($uM^{-1}min^{-1}$)	k_{-2} ($uM^{-1}min^{-1}$)	k_3 ($uM^{-1}min^{-1}$)	RMS Error
Fdx[a]	n.d.	0.001286(5)	0.00115(1)	n.d.	0.000238(7)	0.39
Fdx[b]	n.d.	0.001431(4)	0.00108(1)	n.d.	n.d.	0.43
Fdx[c]	0.00130(4)	0.00154(1)	0.00108(1)	n.d.	0.00037(1)	0.35
Fdx[d]	n.d.	n.d.	0.000920(2)	n.d.	n.d.	n.d.
HcaC	n.d.	0.001260(3)	0.0017(3)[e]	0.011(2)[e]	n.d.	0.23

[a]Reaction was modeled with IscU to Fdx direct transfer pathway. [b]Reaction was modeled without IscU to Fdx direct transfer pathway. [c]Reaction included a cluster synthesis step and limited amounts of cluster. [d]Rate was determined from CD assay. [e]Parameters were restrained near values derived from Table 3-1.

experiment was more sensitive to those rate constants and attempts to relieve the constraints resulted in unstable values. Attempts at including a pathway from [2Fe-2S]-IscU directly to HcaC, produced k_3 values that converged on 0 and did not improve the fit (data not shown). A scan of curve fit error vs. k_3 shows that k_3 is likely < 0.0001, which is an order of magnitude lower than k_1 or k_2 (Figure 3-13). Thus cluster transfer to HcaC also appears to proceed via a [2Fe-2S]-Grx4 intermediate.

CD data confirms Grx4 enhances cluster incorporation on Fdx. The results from our fluorescence studies suggest that Grx4 acts as an intermediate cluster carrier by

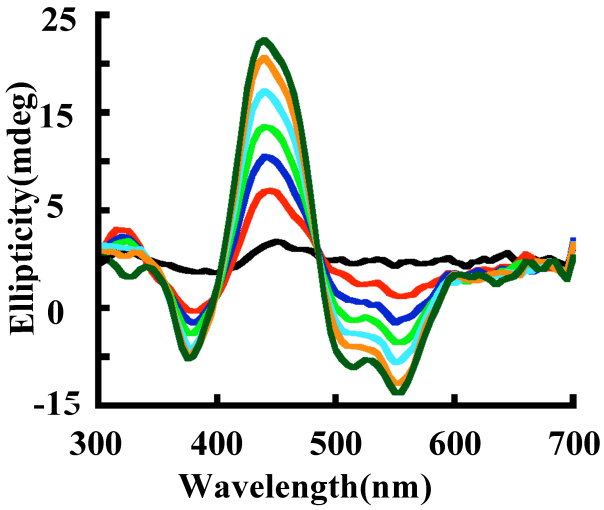

Figure 3-14. Time course of cluster transfer from cluster transfer from holo-IscU to apo-Fdx via Grx4. Reaction includes 10µM IscU, 20µM Grx4, 40 µM apo-Fdx, 400µM Fe^{2+} and 100 µM cysteine and were initiated by the addition of 10mM GSH. Spectra after 0 (black), 60 (red), 120 (blue), 180 (light green), 240 (cyan), 300 (orange) and 360 minutes (dark green) are shown.

kinetically enhancing cluster transfer to apo-target proteins. We then sought to confirm this result with CD spectroscopy. In order to overcome the difficulty of deconvoluting 3-component spectra, the concentration of IscU and Grx4 were kept much lower than that of Fdx. Thus, the majority of the signal change is due to cluster transfer to Fdx. The results clearly show that Grx4 enhances cluster accumulation on Fdx (Figure 3-14, 3-15 and 3-16). The final CD spectra most resemble that of holo-Fdx, consistent with our expected model (Figure 3-14 and 3-15).

Discussion

Iron-sulfur cluster biosynthesis and transfer are complex processes involving a network of numerous competing apo-target proteins and intermediate cluster carriers.

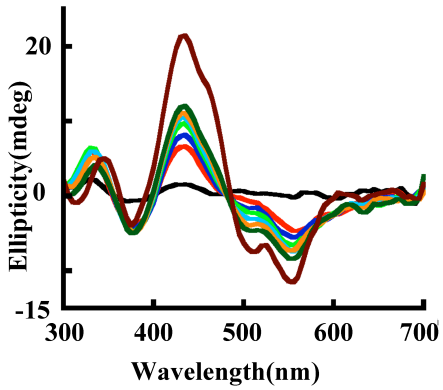

Figure 3-15. Time course of cluster transfer from holo-IscU to apo-Fdx in absence of Grx4. Reaction includes 10µM IscU, 40µM apo-Fdx, 400 µM Fe^{2+} and 100 µM cysteine and were initiated by 10 mM GSH. Spectra after 0 (black), 60 (red), 120 (blue), 180 (light green), 240 (cyan), 300 (orange) and 360 minutes (dark green) are shown. The spectra taken after overnight incubation shows fully reconstituted ferredoxin (brown).

Previous studies include DTT, a reagent that has been shown to artificially enhance cluster transfer reactions, thus calling into question conclusions based on kinetic measurements. Here we demonstrate the ability of DTT to accelerate the physiological cluster transfer reaction between IscU and Fdx in the presence of Grx4. These studies also suggested Grx4 may be enhancing cluster transfer to terminal targets even in the absence of DTT. However, the CD spectra at intermediate time points were difficult to resolve, so we turned to our newly developed fluorescence assay.

Fluorescent cluster binding proteins have been shown to report on cluster binding of a single protein in a reaction mixture, and should allow for the deconvolution of complex kinetic processes involving multiple cluster binding proteins. The fluorescence of $Grx4_{Rho}$, Fdx_{Rho}, and $HcaC_{Rho}$ have all previously been shown to be sensitive to

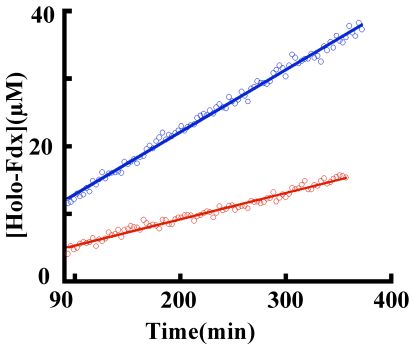

Figure 3-16. Fitting of kinetic traces for cluster transfer to apo-Fdx monitored via CD. The linear region of cluster transfer from IscU to apo-Fdx in the presence (blue) and absence (red) of Grx4 is fitted for the calculation of relative rates.

cluster binding, suggesting that the method is generally applicable. In order to demonstrate the ability of this assay to detect transiently bound iron-sulfur clusters, we first investigated Fe-S cluster assembly on $IscU_{Rho}$. The loss in fluorescence upon cysteine addition is consistent with cluster formation on IscU. In the presence of apo-target proteins, the quenching of $IscU_{Rho}$ was eventually fully rescued, indicating the targets were accepting cluster from [2Fe-2S]-$IscU_{Rho}$. This effect was greatest with Grx4 as the acceptor, with the data indicating rapid loss of cluster from IscU. The observation that Grx4 more readily accepts clusters provides further evidence that it functions as a transfer intermediate. The observation of greater quenching at intermediate time points for the reactions containing Fdx or HcaC may point formation of a transfer complex between the targets and IscU. In all cases, the observation of transient cluster on IscU in a complete cluster assembly and transfer reaction further cements the function of IscU as an Fe-S cluster scaffold.

In this paper, the fluorescence of $Grx4_{Rho}$ was shown to be sensitive to cluster derived from the native IscS:IscU complex with the aid of a native electron donor, GSH. Increased quenching was observed relative to previous chemical reconstitutions, suggesting that enzymatic cluster formation is more efficient and able to more fully reconstitute apo-target proteins. Furthermore, the time course for cluster formation as measured by CD matches well with the fluorescence quenching curve, implying that Grx4 bound cluster is resulting in the signal change. It is also worth noting that the observed spectra most clearly resembles that of [2Fe-2S]-Grx rather than the linear [3Fe-4S] or [4Fe-4S] forms. If either of those alternate forms of holo-Grx is physiologically

relevant, they must require additional factors to form. Importantly, the quenching of $Grx4_{Rho}$ was not due to aggregation, which has been shown to be problematic, particularly in reactions containing DTT. Additionally, the sensitivity of the quenching to IscU and DTT suggests that the observed transfer rate is not due to solution chemistry and that Grx4 is unable to act as an alternate scaffold. The signal instead reports on cluster transfer from IscU and/or the IscS:IscU complex.

We next determined the mechanism of cluster transfer from IscU to $Grx4_{Rho}$. The rate of cluster transfer was shown to depend on the concentration of GSH as well as that of the apo-target protein, implying that cluster transfer is rate-limiting in these combined cluster biosynthesis/transfer reactions. The dependence on GSH could either indicate that cluster biosynthesis is partially rate limiting as well or could suggest a possible GSH chelated cluster intermediate species, as has been hypothesized to exist *in vivo*. The Grx4 concentration dependence suggested Michalis-Menten behavior, though we were unable to reach saturation. Interestingly, if we extrapolate the Grx4 curve to higher concentrations that have been used previously in the literature (45 μM cluster = 90 μM Grx4), we get a rate of 0.13 μM cluster/min, which would correspond to a second order rate constant of 1.1 x 10^3 M^{-1} min^{-1}. This is in good agreement with the rate of cluster formation on Fdx in the presence of Grx4 that we derived from CD spectroscopy (Figure 3-16 and Table 3-2) of 920 M^{-1} min^{-1} (note: the rate-limiting step should be IscU cluster transfer to Grx4 at these concentrations) and the rate of 1.3-1.5 x 10^3 M^{-1} min^{-1} derived from our kinetic modeling (Table 3-2). Notably this is much higher than values that have previously been determined in the absence of chaperones (30 M^{-1} min^{-1})

and even approaches the rate measured with chaperones (2 x 10^4 M^{-1} min^{-1}). This may indicate that the [2Fe-2S]-IscU dimer is not a relevant transfer species in a complete transfer reaction. Alternatively, the differences may reflect differences in homologous proteins from different species, reaction conditions, or saturation of assays. More studies will be needed to fully address this discrepancy.

The ability of Grx4 to transfer clusters to apo-target proteins was then investigated. The fluorescence signal of [2Fe-2S]-Grx_{Rho} increased rapidly in the presence of the apo-acceptor proteins Fdx and HcaC. This indicates that Grx4 is capable of transferring clusters to these target proteins. Importantly, this transfer reaction was shown to depend on the concentration of the acceptor protein and appears to be slowed by GSH. This implies that the cluster transfer reaction from Grx4 involves nucleophilic attack by a residue from the apo-acceptor rather than proceeding through a GSH-cluster intermediate. Additionally, it was revealed that Grx4 and HcaC appear to compete for clusters with Grx4 having a higher affinity for cluster. This may suggest that Rieske proteins can act as a reservoir of iron-sulfur clusters in cases where iron-sulfur clusters become depleted.

Finally, combined cluster biosynthesis and transfer reactions were carried out with Grx4 and terminal apo acceptor proteins. For the Grx4-Fdx reactions, $Grx4_{Rho}$ exhibited clear intermediate-like behavior. The transfer reaction with Grx4 and HcaC, on the other hand, didn't show very clear evidence for intermediate behavior of Grx4, but it again revealed the competition between Grx4 and HcaC for cluster. Fitting of the kinetic traces showed that even when competing pathways for cluster transfer from IscU

directly to Fdx/HcaC were included in the model, these rate constants were significantly slower than transfer through Grx4. This is in contrast to previous results that suggest that Grxs only act as intermediate carriers in the presence of chaperones. Additionally, these results suggest that monothiol Grxs may be universal intermediate carriers by demonstrating their ability to carry clusters to multiple classes of iron-sulfur cluster targets.

These results demonstrate the utility of fluorescent probes in monitoring enzymatic cluster transfer reactions. These tools provide direct evidence for the role of IscU as a scaffold protein and the monothiol glutaredoxin Grx4 as a universal intermediate cluster carrier. We've also revealed the GSH dependence of cluster transfer from IscU and elucidated a direct cluster transfer mechanism from Grx4 to terminal target proteins. By incorporating additional components such as Fdx/FdxR, HscA/HscB, and IscA, this assay will shed further light on the interplay of the complex web of cluster transfer reactions the roles of the numerous proteins in the pathway.

Materials and methods

Preparation of proteins and fluorescent labeling. $Grx4_{Rho}$ and Fdx_{Rho} were purified and fluorescently labeled as described previously (173). IscURho was cloned into an intein fusion vector, purified, and fluorescently labeled the exact same way as $Grx4_{Rho}$ (Chapter 2). IscS and IscU were purified as described previously. Fdx was also purified as described previously (Chapter 2). Grx4 and HcaC were cloned into a GFP expression vector and purified in a manner identical to Fdx (173). Apo-proteins were

prepared by treatment with DTT and TCA, followed by washing with water and dissolving as described previously (Chapter 2).

Cluster transfer assays from IscS:IscU. Kinetic assays contained IscS, IscU, ferrous ammonium sulfate, GSH, fluorescent target protein, and L-cysteine. Reactions were run in 50 mM HEPES, 150 mM KCl pH 7.2 at 25C(Buffer A). Fluorescence intensity was monitored in a fluorescent plate reader containing in an anaerobic glovebox as described and corrected for the inner-filter effect (Chapter 2). Fluorescence data was plotted as a ratio with a reference well that did not contain IscS or cysteine.

CD spectroscopy. CD spectra were recorded using a 1cm pathlength cuvette on an Applied Photophysics Chirascan CD spectrometer. Cuvettes were sealed with a rubber septa and electrical tape in a glove box.

CD cluster transfer assays from IscU to Fdx. The assays were run in 50 mM HEPES, 150 mM KCl, 10mM $MgCl_2$ pH 7.5 (Buffer B) and contained IscU, Grx4, IscS, apo-Fdx, cysteine, ferrous sulfate and GSH.

Size-exclusion chromatography. Reactions contained 10 mM GSH, 100 μM Fe^{2+}, 5 μM IscS, 10 μM IscU, 10 μM Fdx_{Rho} or $Grx4_{Rho}$, and 100 μM cysteine. A reference well contained all of the components except IscS and cysteine. The reactions were run in 50 mM Tris, 150 mM KCl pH 7.2 at 25C until the fluorescence stopped quenching. At that time, the sample was loaded on a Superdex 200 column (10 x 300 mm) that had been equilibrated with 50 mM Tris, 150 mM KCl pH 7.2. Fractions (1 ml) were collected and analyzed by fluorescence with an excitation wavelength of 550 nm and an emission wavelength of 600 nm.

Measuring dependence of cluster transfer rate on apo-target protein concentration. Fluorescence quenching data was collected and data between 30 min and 75 min was isolated and fit to a linear equation. The slope was converted to a rate of cluster transfer by assuming that the minimum observed fluorescence corresponded to 100% cluster transfer and then scaling the fluorescence percentage based on the concentration of apo-fluorescent protein used.

Cluster transfer assays from holo-Grx4Rho. Holo-$Grx4_{Rho}$ was produced by mixing 100 μM Fe^{2+}, 100 nM IscS, 5 μM IscU, 40 μM $Grx4_{Rho}$, 10 mM GSH, and 100 μM L-cysteine overnight. The fluorescence quenching was monitored during this time. A reference sample lacking IscS and cysteine was also prepared at this time.

The following day, the reaction mixtures containing holo-$Grx4_{Rho}$ were diluted into mixtures containing varying concentrations of GSH and apo-Fdx or apo-HcaC (final concentration of $Grx4_{Rho}$ was 5 μM). The fluorescence was recorded as done previously and plotted relative to a sample of diluted reference well containing an identical concentration of GSH.

Kinetic modeling. Copasi kinetic modeling software was used to fit the data using evolutionary programming with a population size of >100 and >300 generations. Initially, fluorescence data had to be converted into [[2Fe-2S]-$(Grx4_{Rho})_2$]. This was done by assuming that the minimum fluorescence for the data set corresponded to 100% cluster transfer. The fluorescence ratio was corrected by the following formula to give [[2Fe-2S]-$(Grx4_{Rho})_2$].

$$[[2Fe\text{-}2S]\text{-}(Grx4_{Rho})_2]_t=(1-(F_{Reaction}/F_{Ref})'_t)/((1-\min(F_{Reaction}/F_{Ref})')/[(Grx4_{Rho})_2])$$

Kinetic data was modeled assuming a constant concentration of [2Fe-2S]-(IscU)2 except when otherwise stated. Additionally, cluster transfer to glutaredoxin was modeled as being first order in glutaredoxin concentration. The restraints for variables were adjusted as needed to give optimal fits, but in general were kept at least an order of magnitude away from the observed final rate constants. Parameter scans were also carried out using Copasi, where one variable was systematically varied and the others were optimized using evolutionary programming. The sum of squares (objective value) was obtained as a function of the variable that was varied.

CHAPTER IV

INVESTIGATING THE ROLE OF THE DITHIOL GLUTAREDOXINS IN FE-S CLUSTER TRANSFER USING FLUORESCENT PROBES

Introduction

Iron-sulfur clusters are protein cofactors that play critical roles in electron transfer and redox processes in organisms throughout the kingdoms of life (1, 12-16). These clusters must be synthesized and inserted into apo proteins in a controlled manner in order to avoid production of toxic by-products or insoluble minerals (3, 41). Numerous proteins are involved in cluster biosynthesis and transfer, with four separate, but often intertwined, systems functioning in different organisms (47-50). In numerous bacteria as well as in the mitochondria of eukaryotes, the ISC system is responsible for cluster biosynthesis (6, 159). This system uses a cysteine desulfurase (IscS), a scaffold protein (IscU), and a ferredoxin to synthesize iron sulfur clusters (6, 59, 174). These clusters are then transferred to apo target proteins with the aid of numerous other protein factors. One of the key players in cluster transfer is the monothiol glutaredoxins (160, 161). A separate subfamily of the glutaredoxins, the dithiol glutaredoxins appears to be important for cellular resistance to toxins and ROS, but may be involved in cluster transfer as well (175-183).

Glutaredoxins are mysterious proteins with a seemingly wide variety of functions. They have been shown to function as electron donors, having the ability to reduce disulfides on proteins such as ribonucleotide reductase or reverse

glutathionylation (162-164). Additionally, many glutaredoxins have been shown to bind to iron-sulfur clusters (Fe-S) in a homo-dimeric complex (107, 165-168). Glutaredoxins (both monothiol and dithiol) have been shown to be able to donate their clusters to a variety of apo target proteins such as IscA and Fdx in *in vitro* experiments (92, 118, 125). Interestingly, cluster binding interferes with the ability of glutaredoxins to reduce disulfides, possibly indicating a regulatory mechanism (106). Finally, the monothiol glutaredoxins can also form Fe-S containing heterodimers with BolA/Fra2, which appears to allow for specific targeting of the bound iron-sulfur cluster to regulatory proteins in the cell (25, 120, 121, 124, 171).

The exact function of the glutaredoxins is further complicated by their diversity. The glutaredoxins can be subdivided into two groups, the type I and type II glutaredoxins (184). Traditionally the type I and type II glutaredoxins were referred to as dithiol and monothiol glutaredoxins respectively. The names refer to the number of cysteine residues in the active site of the protein where disulfides are reduced and where the Fe-S cluster is bound. The monothiol glutaredoxins typically have a CGFS motif whereas the dithiols exhibit a CP(Y/F)C motif (160). Due to the dual cysteines, dithiol glutaredoxins are most efficient at disulfide reduction chemistry, whereas the monothiol glutaredoxins appear to primarily function in the reduction of glutathionylated proteins (67). The first cysteine residue in each motif provides one ligand to the [2Fe-2S] cluster in the proteins' holo states, and is also the redox active cysteine for the glutaredoxin's reduction activity (67, 107, 165-168). The other ligand is provided by a non-covalently bound glutathione (GSH) molecule. Each monomer of the homo-dimeric complex

provides a single cysteine ligand and a GSH ligand, thereby completing the four ligands needed to ligate a [2Fe-2S] cluster.

While the monothiol glutaredoxins appear to function as intermediate cluster carriers for cluster biosynthesis and transfer, the function of the dithiol Grx's remains much more mysterious. When dithiol Grx's are depleted, the observed phenotypes include growth defects and sensitivity towards cell death inducers, particularly ROS (175-183). Additionally, some studies have linked deficiencies in dithiol Grx's to depleted iron-sulfur clusters (179). *In vitro* studies suggest that dithiol Grx's bind clusters more tightly than monothiol Grx's (185). Additionally, it has been demonstrated that oxidized glutathione, dithionite, and ascorbate can induce cluster loss from dithiol Grx's leading to the hypothesis that reversible cluster binding may regulate the protein's disulfide reduction chemistry (106). Finally, a recent study showed that dithiol Grx's can transfer a cluster to ferredoxin in the presence of DTT and revealed that GSH inhibits this transfer reaction (118). It is worth noting that DTT has been shown to dramatically increase cluster transfer rates (Chapter 2). These observations have led to the hypothesis that the dithiol glutaredoxins function as sensor molecules rather than as cluster transfer agents.

Here we utilize a newly developed fluorescence assay to investigate the ability of the ISC system in *E. coli* to build and transfer clusters to the dithiol glutaredoxins Grx1 and Grx3. We then probe the ability of these proteins to transfer their clusters to apo-target proteins. Finally, by carrying out assays using fluorescent dithiol glutaredoxins in the presence of apo monothiol Grx's or other apo target proteins, we demonstrate the

ability both classes of Grx's to function as intermediate cluster carriers and thereby develop a model for the function of the dithiol glutaredoxins in cells.

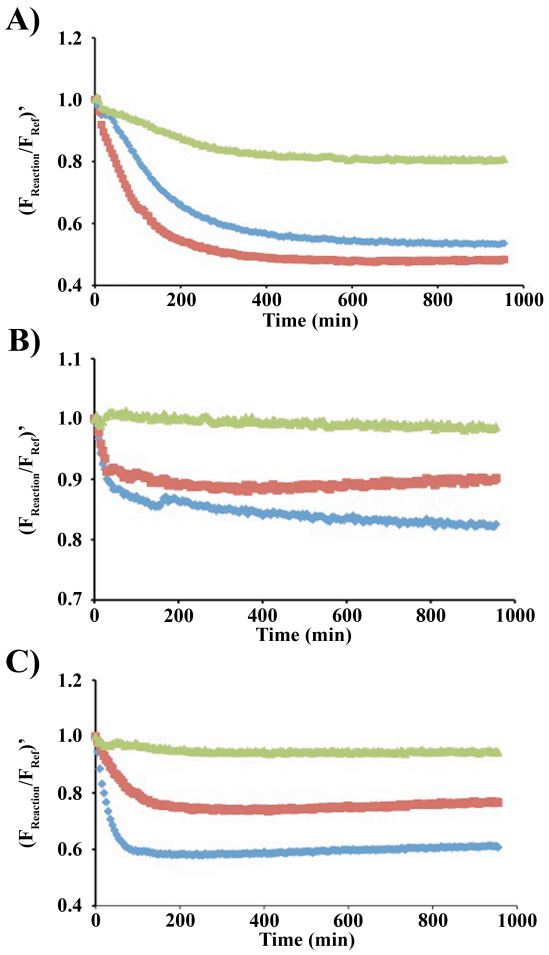

Figure 4-1. GSH dependence of cluster transfer to monothiol and dithiol glutaredoxins. Reactions were carried out with $Grx4_{Rho}$ (A), $Grx1_{Rho}$ (B), or $Grx3_{Rho}$ (C) as the apo acceptors. Reactions contained 20 mM (blue), 10 mM (red), or 2 mM (green) glutathione.

Results

Dithiol glutaredoxins are sensitive to GSH concentration. Iron-sulfur cluster biosynthesis and transfer reactions were carried out with IscS, IscU, ferrous iron, cysteine, and varying concentrations of glutathione. The synthesized clusters were transferred to fluorescently labeled glutaredoxins that were labeled with a C-terminal sulforhodamine B. The fluorescence was recorded and plotted as a ratio with a sample that did not contain IscS or cysteine. The results are shown in Figure 4-1. The *E. coli* monothiol glutaredoxin Grx4 showed an increasing rate of cluster transfer at increasing glutathione concentrations (Figure 4-1A). Additionally, the extent of the fluorescence quenching varied with glutathione concentration. When the glutathione concentration decreased from 20mM to 10mM, very little change was observed with slightly increased quenching being observed. In contrast, the dithiol glutaredoxins, Grx1 and Grx3, showed substantially less quenching when the glutathione concentration decreased to 10mM (Figure 4-1B and 4-1C). Additionally, when the glutathione concentration decreased to 2mM, no significant quenching was observed. In contrast, Grx4 still exhibited ~40% of the maximal quenching at 2mM GSH. Finally, the rate of cluster transfer to the dithiol glutaredoxins was appears to be faster than transfer to Grx4 at 20mM GSH.

Dithiol glutaredoxins compete with monothiol glutaredoxins for cluster. It is currently not known how the dithiol Grx's get their clusters. Many models present in the literature would suggest that they are dependent on the monothiol Grx's for their cluster. Alternatively, they may lie on separate pathways and both accept cluster from IscU. In

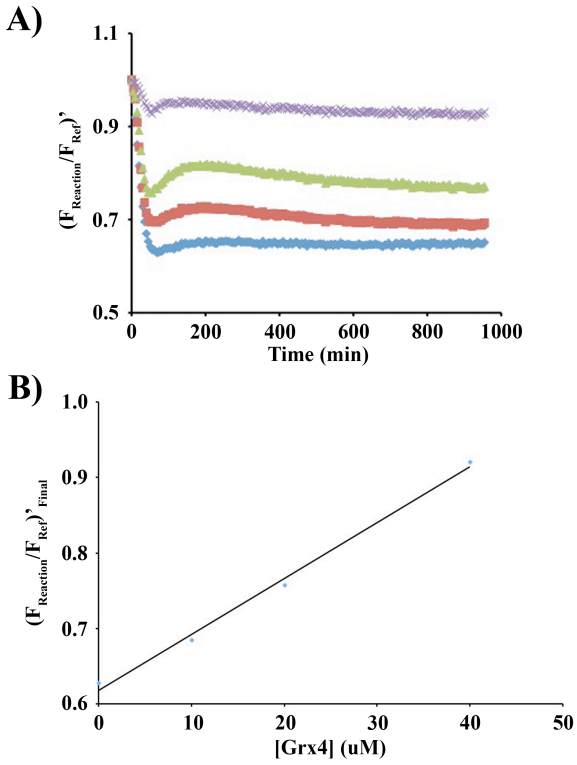

Figure 4-2. Competition between $Grx3_{Rho}$ and Grx4 for newly synthesized Fe-S cluster. (A) Fluorescence of reactions mixtures containing 10 µM apo-$Grx3_{Rho}$ and 0 µM (blue), 10 µM (red), 20 µM (green), or 40 µM (purple) apo-Grx4. Fluorescence ratio at the conclusion of the reactions was plotted as a function of Grx4 concentration and fit to a linear regression line (B). The fit gave a $K_{0.5}$ of 26 uM.

order to determine the interplay of the monothiol and dithiol Grx's, a series of cluster biosynthesis and transfer reactions were carried out that contained both fluorescent $Grx3_{Rho}$ and unlabeled Grx4. Rapid quenching of the fluorescence of $Grx3_{Rho}$ was observed in all cases (Figure 4-2A). The extent of the fluorescence quenching decreased as a function of increasing Grx4. Importantly, the quenching of a related glutaredoxin,

Grx4, was shown to respond to cluster content and not to dimerization (Chapter 3). As a result, we can interpret the decreased quenching as being a result of an equilibrium competition between Grx4 and $Grx3_{Rho}$ rather than due to loss of homoFRET quenching as a result of forming $Grx3_{Rho}$-Grx4 heterodimers. When the quenching extent is plotted as a function of Grx4 concentration, we find that a concentration of ~25μM decreases the quenching of 10μM $Grx3_{Rho}$ by approximately half (Figure 4-2B). As a result, we can conclude that $Grx3_{Rho}$ has a higher affinity for cluster than Grx4, at least at 20mM GSH.

Additionally, the quenching behavior is consistent with cluster delivery to Grx3 followed by transfer from Grx3 to Grx4. In all but the 40 μM Grx4 sample, the initial quenching rate was unchanged, consistent with Grx3 and Grx4 both having very high K_m's for holo-IscU or with Grx3 functioning as an intermediate carrier to Grx4. At intermediate concentrations of Grx4, initial quenching of $Grx3_{Rho}$ was observed, consistent with it receiving a Fe-S cluster. Importantly, no increase in cluster transfer rate to Grx3 was observed with increasing concentrations of Grx4. At approximately 60 minutes, the fluorescence increases, consistent with cluster loss from $Grx3_{Rho}$. The magnitude of this increase is more dramatic at 10 and 20 μM Grx4 than in the sample that didn't contain Grx4. As a result, it appears that this increase is dependent of Grx4, consistent with cluster transfer from $Grx3_{Rho}$ to Grx4.

Dithiol glutaredoxins can transfer clusters to Fdx and HcaC. At this point, holo labeled dithiol glutaredoxin was produced. This material was then diluted into reaction mixtures containing varying concentrations of apo-Fdx or apo-HcaC. Both

$Grx3_{Rho}$ and $Grx1_{Rho}$ exhibited significant cluster loss, even in the absence of an apo cluster acceptor. However, the presence of an apo-acceptor protein increased the quenching rate (Figure 4-3). Often, the initial kinetics of the fluorescence rescue were

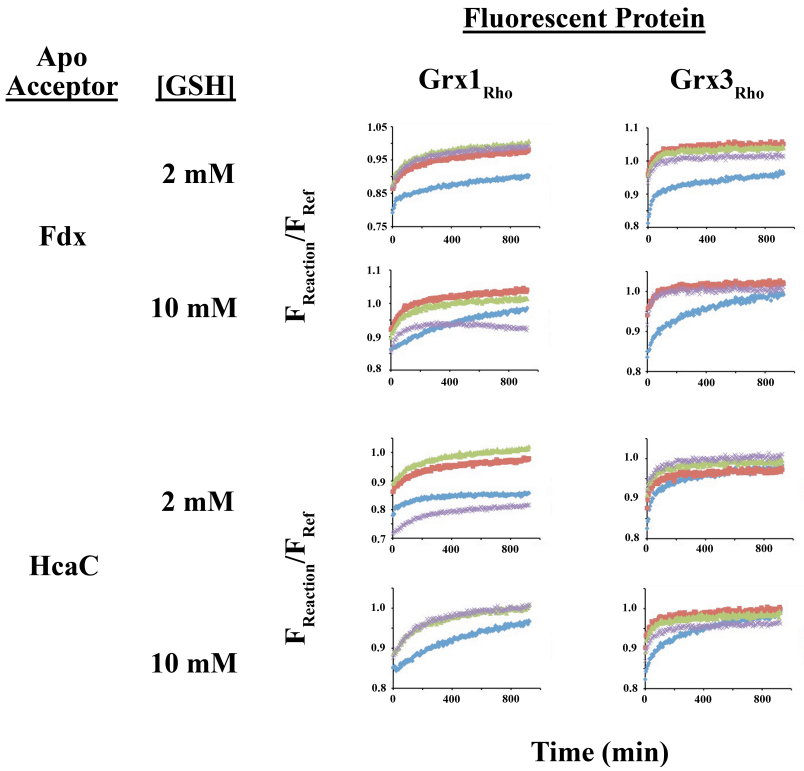

Figure 4-3. Rescue of fluorescence quenching of dithiol glutaredoxins by Fdx and HcaC. Rescue of fluorescence was initiated by addition of 5 μM holo $Grx1_{Rho}$ or $Grx3_{Rho}$ into a reaction mixture containing 0 μM (blue), 5 μM (red), 10 μM (green), or 20 μM (purple) apo-Fdx or HcaC in the presence of 10 mM GSH

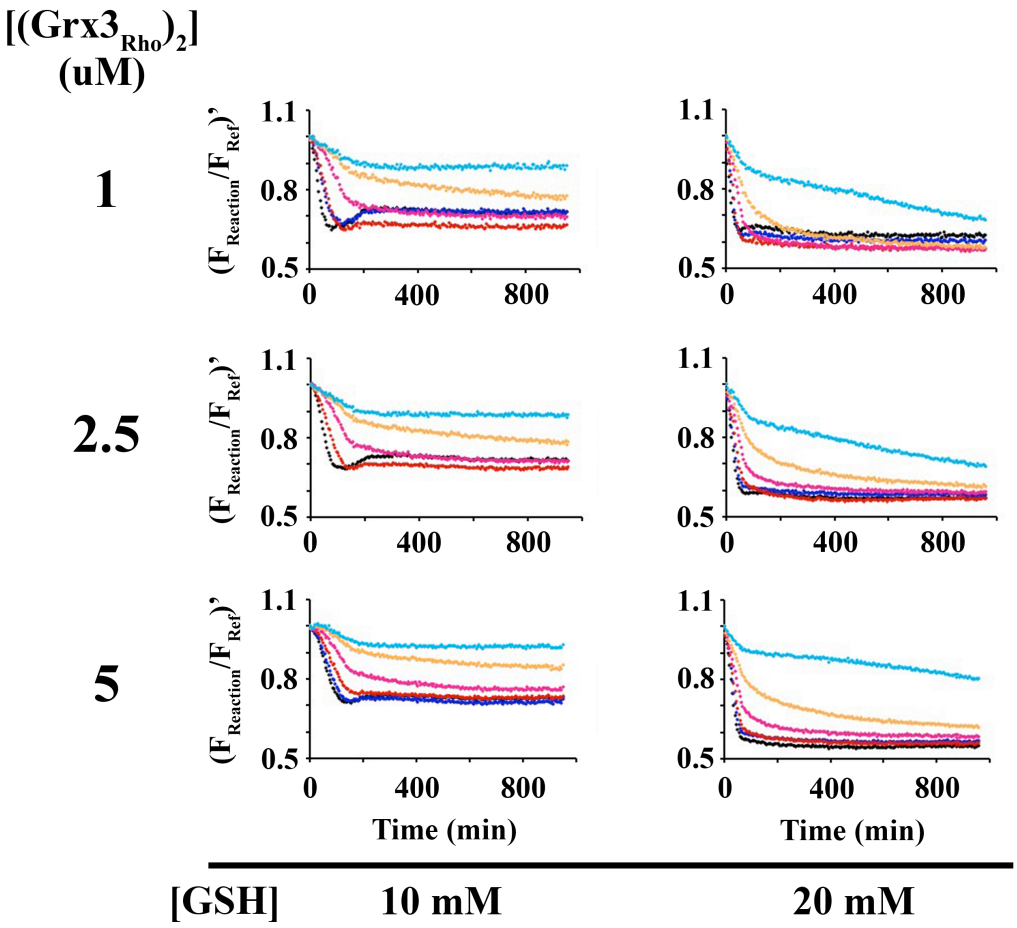

Figure 4-4. Competition between $Grx3_{Rho}$ and Fdx for IscU bound cluster. Curves represent Fdx concentrations of 0 μM (black), 1 μM (blue), 2 μM (red), 5 μM (pink), 10 μM (orange), and 20 μM (cyan).

missing because they appear to have occurred prior to starting data collection. It was also observed that the rescue of the fluorescence for holo-Grx3 appears to be enhanced for Fdx transfer relative to HcaC transfer. Also, unlike the monothiol Grx's, no apparent equilibrium was observed between either Grx1 or Grx3 and HcaC. Intriguingly, the

rescue of the fluorescence did not seem to depend on either GSH concentration or on the concentration of the apo-acceptor protein.

$Grx3_{Rho}$ and apo-target proteins compete for IscS:IscU derived Fe-S clusters. Reactions were then carried out with $Grx3_{Rho}$ and varying concentrations of

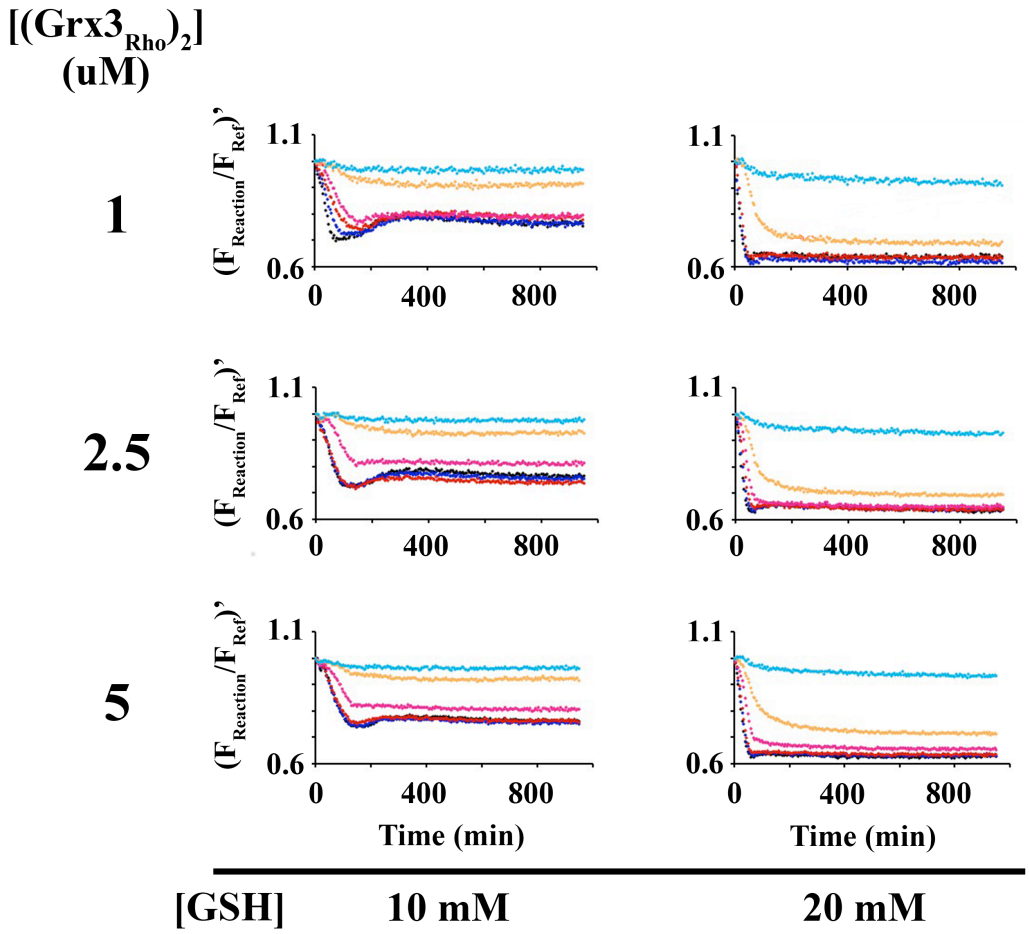

Figure 4-5. Competition between $Grx3_{Rho}$ and HcaC for IscU bound cluster. Curves represent HcaCconcentrations of 0 μM (black), 1 μM (blue), 2 μM (red), 5 μM (pink), 10 μM (orange), and 20 μM (cyan).

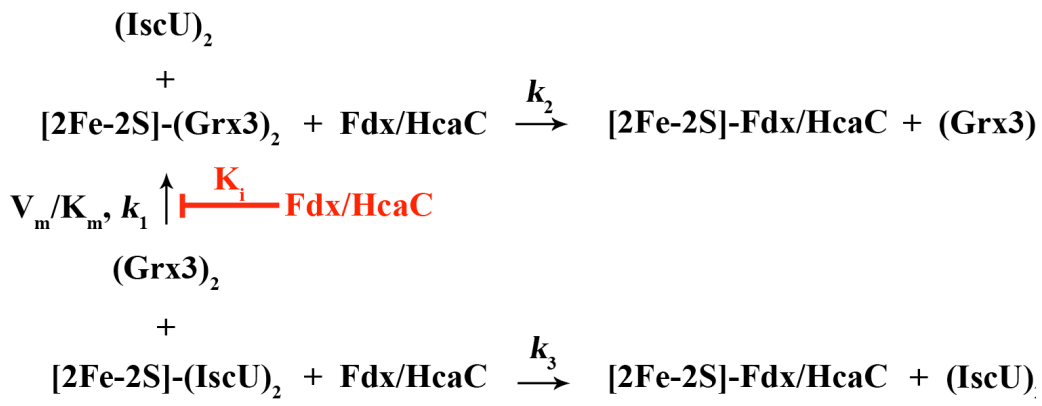

Figure 4-6. Kinetic scheme for cluster transfer with dithiol Grx and Fdx/HcaC. The reaction scheme depicts the different kinetic processes that were modeled in Table 4-1.

either apo-Fdx or apo-HcaC (Figures 4-4 and 4-5). The kinetic data were then fit using a variety of global models (Figure 4-6), the results of which are shown (Figure 4-7, Table 4-1). In contrast to similar assays carried out for the monothiol Grxs, the initial kinetics of cluster transfer to Grx3Rho were dramatically perturbed by the presence of either apo-Fdx or apo-HcaC. This is most easily explained by competition between $Grx3_{Rho}$ and apo-acceptor proteins for IscU-bound cluster.

In the cases where high concentrations of Fdx and GSH were used, the kinetic trace suggests that Grx3Rho may be able to act as an intermediate carrier. The data shows an initial decrease in fluorescence that levels out for a time before again dropping. This is consistent with the formation of a nearly steady-state level of holo-Grx3Rho as the protein is both accepting and donating clusters in the assay. At 10 mM GSH, however, this behavior was not observed. In the case of HcaC, intermediate-type

behavior was not observed; instead the presence of apo-target protein appears to simply inhibit cluster transfer to Grx3Rho.

To further investigate the possible models, kinetic modeling was used. In the case of reactions containing Fdx, the kinetics fit poorly to a model in which $Grx3_{Rho}$ serves as an intermediate carrier to Fdx. Inclusion of direct cluster transfer from IscU to Fdx failed to improve the fit, and the rate constant k3 converged on 0. Next the data was fit to a model that allowed for Fdx to act as a competitive inhibitor of a Michaelis-Menton-type transfer of cluster from IscU to $Grx3_{Rho}$. In this case V_{max} and K_m did not converge, suggesting that we have not reached saturation with Grx3. However, this

Table 4-1. Fitting kinetic traces for Grx3Rho competition experiments with Fdx/HcaC

	K_m	V_m	K_i (μM)	k_1 (μM^{-1} min^{-1})	k_2 (μM^{-1} min^{-1})	k_3 (μM^{-1} min^{-1})	RMS Error
Fdx[a]	n.d.	n.d.	n.d.	0.00385(4)	0.00081(2)	0.00000(2)	0.45
Fdx[b]	N/A[c]	N/A[c]	1.93(6)	n.d.	0.000292(8)	0.00000(1)	0.23

[a]Traces were fit to competing 2nd order processes and allowed for transfer from holo-$Grx3_{Rho}$ to apo-target proteins. [b]Traces were modeled as competitive inhibition of cluster transfer from IscU to Grx3 by apo-target protein that also allowed for transfer from holo-$Grx3_{Rho}$ to apo-target protein. [c]Data did not converge (error was greater than 100%).

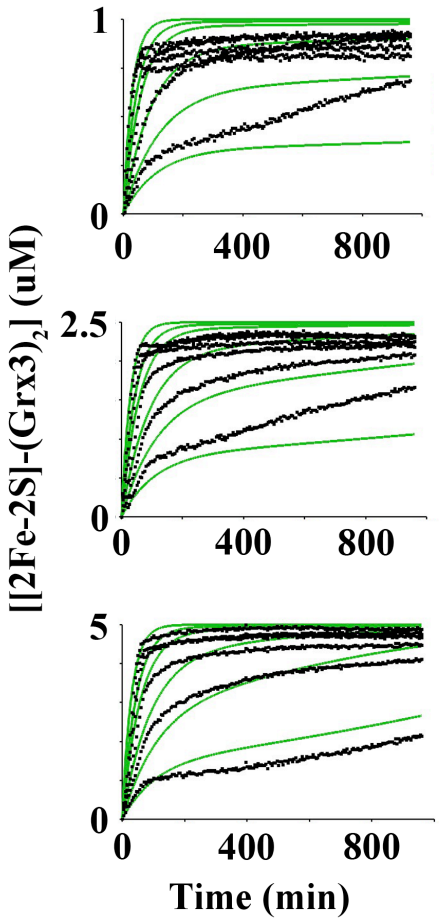

Figure 4-7. Global fit of Fdx:Grx3$_{Rho}$ competition data. Black data points are calculated from measured fluorescence data. Green lines are the best fit to a competitive inhibition model (Table 4-1)

model best fit the data and gave a K_i of 1.9 μM. When k3 was included the rate constant again converged on 0. However, k2 was non-zero, indicating that Grx3 can act as an intermediate carrier, although it must compete with Fdx for cluster. The data for the samples containing HcaC showed similar changes in the initial rate of cluster transfer with increasing concentrations of apo-acceptor. Our attempts at modeling the data failed

to adequately reproduce the observed curves. However, based on the similarities to the Fdx-containing data, it is likely that competition between HcaC and Grx3 for IscU-bound cluster is a necessary component of the model.

Discussion

The function of monothiol glutaredoxins vs. dithiol glutaredoxins is a matter of intense investigation in the iron-sulfur cluster biosynthesis field. The observation that both types of glutaredoxins are capable of binding Fe-S clusters links both classes to cluster biosynthesis. Whether the clusters bound to glutaredoxins function as transfer intermediates, cluster storage, sensors, or regulatory elements is a matter of debate. To begin to address these different possibilities, kinetic analyses were carried out using fluorescently labeled dithiol glutaredoxins.

Initially, the dithiol glutaredoxins' (Grx1 and Grx3) ability to accept an Fe-S cluster was compared to that of the monothiol glutaredoxin (Grx4) as a function of GSH concentration. It was shown that the dithiol glutaredoxins appear to accept clusters quicker than Grx4, but the thermodynamics of their cluster binding was very dependent on GSH concentration. This is consistent with the observed GSH inhibition of cluster transfer that has previously been observed for dithiol Grx's. Notably at 2mM GSH, almost no detectable binding of cluster was observed for either Grx1 or Grx3. It is worth noting that cellular GSH concentrations are known to vary over a wide range, from 0.5-14mM (186, 187). Thus the apparent sensitivity of the dithiol glutaredoxins to low GSH concentration may be a part of a cellular redox sensing mechanism.

Previous studies have implicated the monothiol glutaredoxins as being intimately involved in cluster biosynthesis, as they appear to function as intermediate cluster carriers to apo target proteins. We next wanted to carry out cluster competition studies with $Grx3_{Rho}$ and Grx4 to determine if they are capable of transferring clusters between themselves, or if they simply compete for a common cluster source. The kinetic traces showed that the initial rate of cluster transfer was not significantly different for $Grx3_{Rho}$ except in the case of 40 μM Grx4. Additionally, an increase in fluorescence was observed at intermediate Grx4 concentrations, consistent with $Grx3_{Rho}$ transferring its cluster to Grx4. Finally, the fluorescence leveled off at varying values that depended on the concentration of Grx4. This is consistent with equilibrium cluster transfer between Grx3 and Grx4. This equilibrium tends to favor binding to Grx3 at least at 20mM GSH. The dependence of this equilibrium on GSH concentration is a matter of future interest, since our GSH dependence studies suggest that Grx3 should loose cluster affinity more rapidly than Grx4. Importantly, this result suggests that the dithiol glutaredoxins, under conditions of high GSH, may be able to act upstream of the monothiol glutaredoxins in cluster transfer.

The ability of Grx1 and Grx3 to transfer their clusters to other apo targets was also investigated. Clusters on both Grx1 and Grx3 appear to be relatively unstable compared to Grx4 in the absence of any apo-acceptor. However, the presence of the apo acceptor proteins HcaC and Fdx, dramatically increased the rate of cluster loss from the dithiol glutaredoxins. Interestingly, this cluster loss didn't appear to depend on acceptor concentration as was the case for Grx4. Similarly, changes in GSH concentration had no

discernable effect. This leads us to favor a model in which clusters bound to dithiol glutaredoxins are continuously being released and rebound. Thus the mechanism of cluster transfer from dithiol glutaredoxins would resemble an SN1-like reaction. It is worth noting that these results conflict with previous studies that showed significant inhibition of cluster transfer by GSH from dithiol glutaredoxins in the presence of DTT. We hypothesize that the DTT may have artificially accelerated the transfer reaction and that the apparent slowing by GSH was simply due to a competition between the two ligands, which masked the underlying transfer in the presence of GSH alone.

Finally, cluster transfer experiments were carried out with fluorescent Grx3 and varying concentrations of apo acceptors. The most notable difference between Grx3 and Grx4 was that the presence of apo acceptors affects the initial rate of cluster transfer to Grx3. This is consistent with competition between Grx3 and the apo acceptor proteins for IscU-bound cluster. Kinetic modeling of the data containing Fdx revealed strong competitive inhibition. However, the model also showed that Grx3 was able to act as an intermediate carrier protein in the presence of Fdx and 20 mM GSH. Lower concentrations of GSH produced curves that lacked obvious intermediate behavior. Similarly, the samples containing HcaC also lacked obvious intermediate behavior, but still showed evidence for competition between the terminal acceptor and Grx3.

The observed data suggests that the dithiol glutaredoxins likely serve as sensor molecules and cluster storage proteins. Low GSH concentrations favor apo-Grx1 and Grx3, and these proteins appear to be capable of transferring their Fe-S clusters at least at 2 mM and 10 mM GSH. Grx3 only showed the ability to act as an intermediate

carrier at very high GSH concentrations, and was even then forced to compete with other proteins for IscU-bound cluster. We hypothesize that only under very high GSH concentrations is cluster formation on Grx3 is favored relative to Grx4, allowing Grx3 to act as an intermediate carrier. Under normal cellular conditions, the dithiol Grxs likely function as terminal acceptor proteins.

Materials and methods

Protein purification and fluorescent labeling. IscS and IscU were purified as done before. $Grx4_{Rho}$, Grx4, Fdx, and HcaC were purified as described in Chapter 3. $Grx1_{Rho}$ and $Grx3_{Rho}$ were cloned into the intein vector, purified, and fluorescently labeled as done in Chapter 2 for $Grx4_{Rho}$. Apo protein was generated by DTT treatment followed by TCA precipitation, washing of the protein, and dissolving it as described in Chapter 2.

Fluorescent kinetic assays. Assays were carried out in a Tecan fluorescent plate reader contained in an anaerobic glovebox as described previously. All reactions were run in 50 mM HEPES, 150 mM KCl pH 7.2 at 25C.

GSH dependence of cluster transfer. Clusters were transferred to 10 μM $Grx1_{Rho}$, $Grx3_{Rho}$, or $Grx4_{Rho}$ in reaction mixtures that contained varying concentrations of GSH, 100 μM Fe^{2+}, 0.5 μM IscS, 5 μM IscU, and 100 μM L-cysteine. The reactions were carried out in 50 mM HEPES, 150 mM KCl pH 7.2 at 25C. Fluorescence was recorded as done previously and plotted as a ratio to a reference well that contained all of the reaction components except IscS and cysteine.

Competition between $Grx3_{Rho}$ and Grx4 for cluster. Reactions were carried out with 10 μM $Grx3_{Rho}$, 20 mM GSH, 100 μM Fe^{2+}, 0.5 μM IscS, 0.5 μM IscU, and varying concentrations of apo-Grx4. Reactions were initiated by the addition of 100 μM L-cysteine. The fluorescence was compared to a reference well lacking IscS and cysteine.

Transfer of cluster from $Grx1_{Rho}$ and $Grx3_{Rho}$ to apo-acceptor proteins. Holo $Grx1_{Rho}$ and $Grx3_{Rho}$ were produced by mixing 100 μM Fe^{2+}, 10 mM GSH, 0.1 μM IscS, 5 μM IscU, 40 μM $Grx1_{Rho}$ or $Grx3_{Rho}$, and 100 μM L-cysteine. The following day, the reaction mixture was diluted (to 5 μM [Fluorescent Grx]) into a mixture containing a final concentration of either 2mM or 10 mM GSH with varying concentrations of either apo-Fdx or apo-HcaC. As a reference, 40 μM $Grx1_{Rho}$ or Grx3 rho were similarly treated in a mixture that didn't contain IscS or cysteine. The following day, these samples were diluted to 5 μM in a mixture containing either 2 mM or 10 mM GSH.

Competition between $Grx3_{Rho}$ and apo-Fdx/apo-HcaC. Varying concentrations of apo-target protein were incubated in assay mixtures containing 100 μM Fe^{2+}, 10 mM GSH, 1 μM IscS, 5 μM IscU, 5 μM $Grx3_{Rho}$, and 100 μM cysteine. Reference wells didn't contain IscS or cysteine.

Kinetic modeling. The y-axis of the kinetic traces was first converted from a fluorescence ratio to a concentration of holo-$Grx3_{Rho}$. This was done by assuming that the minimum fluorescence observed for $Grx3_{Rho}$ in Figure 1 represented 100% cluster transfer. The magnitude of the fluorescence decrease was scaled to reflect the total

concentration of $Grx3_{Rho}$ in the reaction mixture. Thus the magnitude of fluorescence decrease for the kinetic runs in Figure 4 could be converted to a concentration of holo-$Grx3_{Rho}$ formed.

The kinetics were analyzed using Copasi software and fit to a variety of models as was done in Chapter 3.

CHAPTER V

CONCLUSIONS

The studies presented here are aimed at developing new tools to probe the kinetics of Fe-S cluster assembly and transfer reactions. We developed fluorescent labeling strategies that proved to be sensitive to Fe-S cluster binding. By fusing either a BFP or a rhodamine label to a Fe-S cluster binding protein, the fluorescence was shown to quench upon cluster binding in all but one case. Additionally, the sensors were shown to be relatively insensitive to other reagents or by products of Fe-S cluster assembly and transfer reactions. Interestingly these same probes appear to also be sensitive to the binding of other metal ions such as Ni^{2+} and Cu^{2+}. It is tempting to hypothesize that fluorescently labeled proteins could be used for the *in vitro* study of other metallotrafficking processes. Future directions could include incorporating rhodamine labels into the SCO proteins that are involved in copper trafficking in order to elucidate the kinetic and thermodynamic details of those transfer pathways.

Using a fluorescently labeled ferredoxin and mass spectrometry, we showed that iron-sulfur clusters can be swapped between ferredoxin proteins, but the process requires exogenous thiols. DTT was particularly effective at catalyzing this reaction. This observation is quite important to the study of metallocofactor trafficking and casts much of the results in the field in a new light. Ferredoxin's Fe-S cluster is both thermodynamically and kinetically stable. However, the presence of DTT is able to greatly destabilize the cluster, causing formation of a putative DTT ligated [2Fe-2S]

intermediate that can be transferred between proteins. Since the majority of cluster transfer reactions in the literature include DTT, the rates and conclusions of these papers need to be reinvestigated.

In the third chapter, we use this new assay to investigate the function of monothiol glutaredoxins in cluster transfer reactions. Using a combination of fluorescence and CD spectroscopy, the ability of IscS and IscU to build and transfer Fe-S clusters to ferredoxin and Grx4 was demonstrated in the absence of DTT. Additionally, holo-Grx4 was shown to transfer its clusters to HcaC or ferredoxin in a mechanism that depends on the concentration of apo acceptor and not on GSH. This implies that cluster transfer from Grx4 is direct, without any intermediate solution GSH ligated cluster. Additionally, it was demonstrated that HcaC and Grx4 are able to compete for cluster with Grx4 actually having a higher affinity, at least at 10 mM GSH. A potential future study would look at the dependence of the HcaC:Grx4 cluster equilibrium on GSH concentration.

Next, experiments were carried out in which newly synthesized clusters were allowed to transfer to either Grx4 or HcaC/Fdx. These are the first studies to investigate the competition between Grx4 and other apo acceptor proteins for Fe-S clusters from IscU. The results confirm that Grx4 has the ability to act as an intermediate cluster carrier with the rate constants for transfer to the apo-target protein that proceed through Grx4 being comparable or larger than the rate contants from IscU to the apo-target directly. It is worth noting that the observed cluster transfer rates are greater than those that have been reported in the literature previously for cluster transfer from [2Fe-2S]-

IscU to monothiol Grx. This leads us to hypothesize that the holo-IscU dimer may not a functionally relevant transfer species in a complete reaction. Comparative studies using the holo-IscU dimer carried out under identical reaction conditions will be required to fully resolve this question.

In the fourth chapter, we repeated many of the studies from chapter 3, using the *E. coli* dithiol glutaredoxins Grx1 and Grx3. Cluster biosynthesis and transfer studies revealed that the ability of dithiol Grxs to accept cluster is much more sensitive to GSH concentration than the monothiol glutaredoxin, Grx4. Both the kinetics and thermodynamics of cluster transfer were affected, with transfer being abolished at a GSH concentration of 2mM. In another study, cluster transfer was carried out in a mixture of Grx3 and Grx4 at 20mM GSH. Under these conditions, Grx3 accept a cluster faster than Grx4 and appears to outcompete Grx4 for clusters from IscU. Intriguingly, an increase in fluorescence at intermediate time points is consistent with cluster transfer from Grx3 to Grx4. Furthermore, the apparent equilibrium of cluster binding between Grx3 and Grx4 suggests that Grx3 has a higher affinity for iron-sulfur cluster. This is surprising since monothiol Grxs are thought to have more labile Fe-S clusters. However this belief may be based more on differences in oxygen succeptibility rather than actual binding affinity.

Since Grx3 appears to be able to act upstream of Grx4, we hypothesized that it may also serve as an intermediate cluster carrier. Cluster transfer from Grx3 to Fdx and HcaC was demonstrated using fluorescence. Curiously, cluster bound to the dithiol Grx appears to be less stable, kinetically, than cluster on Grx4. This could be due to a

number of factors including differences in GSH cluster stabilization or dimerization equillibria. Finally, the dithiol Grx3 was incorporated into a transfer assay containing alternate apo-acceptor proteins, Fdx and HcaC. These results that Fdx and HcaC compete with Grx3 for IscU-bound cluster. However, at high GSH concentrations, intermediate-type behavior was observed for reactions containing Grx3 and Fdx. Combined these results suggest that the dithiol Grx's assemble clusters only under conditions when GSH concentrations are high. They likely function primarily as cluster storage proteins rather than as intermediate carriers due to significant competition with Fdx and HcaC for IscU bound cluster.

These studies demonstrate the utility of fluorescence to probe the kinetics of cluster transfer processes. This technique enables the investigation of these processes in a high-throughput manner at concentrations that were previously unattainable. By combining the ability of fluorescence to monitor the kinetics of cluster transfer with the ability of CD spectroscopy to confirm the details of cluster species, we hope to greatly broaden the understanding of Fe-S cluster metabolism. Future studies that incorporate the electron donor Fdx/FdxR will allow for the investigation of the effect of cluster reduction on transfer. Adding the chaperone proteins HscA and HscB will allow us to ascertain their function and determine which subsets of proteins require them for effective cluster transfer. Also, by adding in components such as frataxin or IscA, we hope to determine whether they are capable of accelerating cluster transfer or leading to the formation of [4Fe-4S] clusters respectively. Finally, by incorporating fluorophores

into these molecules and utilizing FRET and/or fluorescence anisotropy, the dynamics of complex assembly and disassembly will be resolved and understood.

REFERENCES

1. Johnson DC, Dean DR, Smith AD, & Johnson M (2005) Structure, function, and formation of biological iron-sulfur clusters. *Annu Rev Biochem,* 74:247-281.
2. Russell MJ (2007) The alkaline solution to the emergence of life: energy, entropy and early evolution. *Acta Biotheor,* 55(2):133-179.
3. Kabil O, Vitvitsky V, & Banerjee R (2014) Sulfur as a signaling nutrient through hydrogen sulfide. *Annu Rev Nutr,* 34:171-205.
4. Takahashi Y & Tokumoto U (2002) A third bacterial system for the assembly of iron-sulfur clusters with homologs in archaea and plastids. *J Biol Chem,* 277(32):28380-28383.
5. Jacobson MR, Brigle KE, Bennett LT, Setterquist RA, Wilson MS*, et al.* (1989) Physical and genetic map of the major nif gene cluster from Azotobacter vinelandii. *J Bacteriol,* 171(2):1017-1027.
6. Zheng L, Cash VL, Flint DH, & Dean DR (1998) Assembly of iron-sulfur clusters. Identification of an iscSUA-hscBA-fdx gene cluster from Azotobacter vinelandii. *J Biol Chem,* 273(21):13264-13272.
7. Balk J, Aguilar Netz DJ, Tepper K, Pierik AJ, & Lill R (2005) The essential WD40 protein Cia1 is involved in a late step of cytosolic and nuclear iron-sulfur protein assembly. *Mol Cell Biol,* 25(24):10833-10841.

8. Balk J, Pierik AJ, Netz DJ, Muhlenhoff U, & Lill R (2004) The hydrogenase-like Nar1p is essential for maturation of cytosolic and nuclear iron-sulphur proteins. *Embo J,* 23(10):2105-2115.

9. Hausmann A, Aguilar Netz DJ, Balk J, Pierik AJ, Muhlenhoff U*, et al.* (2005) The eukaryotic P loop NTPase Nbp35: an essential component of the cytosolic and nuclear iron-sulfur protein assembly machinery. *Proc Natl Acad Sci U S A,* 102(9):3266-3271.

10. Netz DJ, Pierik AJ, Stumpfig M, Muhlenhoff U, & Lill R (2007) The Cfd1-Nbp35 complex acts as a scaffold for iron-sulfur protein assembly in the yeast cytosol. *Nat Chem Biol,* 3(5):278-286.

11. Bak DW & Elliott SJ (2014) Alternative FeS cluster ligands: tuning redox potentials and chemistry. *Curr Opin Chem Biol,* 19:50-58.

12. Baradaran R, Berrisford JM, Minhas GS, & Sazanov LA (2013) Crystal structure of the entire respiratory complex I. *Nature,* 494(7438):443-448.

13. Sun F, Huo X, Zhai Y, Wang A, Xu J*, et al.* (2005) Crystal structure of mitochondrial respiratory membrane protein complex II. *Cell,* 121(7):1043-1057.

14. Zhang Z, Huang L, Shulmeister VM, Chi YI, Kim KK*, et al.* (1998) Electron transfer by domain movement in cytochrome bc1. *Nature,* 392(6677):677-684.

15. Bruschi M & Guerlesquin F (1988) Structure, function and evolution of bacterial ferredoxins. *FEMS Microbiol Rev,* 4(2):155-175.

16. Shisler KA & Broderick JB (2012) Emerging themes in radical SAM chemistry. *Curr Opin Struct Biol,* 22(6):701-710.

17. Cicchillo RM, Baker MA, Schnitzer EJ, Newman EB, Krebs C*, et al.* (2004) Escherichia coli L-serine deaminase requires a [4Fe-4S] cluster in catalysis. *J Biol Chem,* 279(31):32418-32425.

18. Lauble H, Kennedy MC, Beinert H, & Stout CD (1992) Crystal structures of aconitase with isocitrate and nitroisocitrate bound. *Biochemistry,* 31(10):2735-2748.

19. Mulder DW, Shepard EM, Meuser JE, Joshi N, King PW*, et al.* (2011) Insights into [FeFe]-hydrogenase structure, mechanism, and maturation. *Structure,* 19(8):1038-1052.

20. Peters JW, Lanzilotta WN, Lemon BJ, & Seefeldt LC (1998) X-ray crystal structure of the Fe-only hydrogenase (CpI) from Clostridium pasteurianum to 1.8 angstrom resolution. *Science,* 282(5395):1853-1858.

21. Einsle O, Tezcan FA, Andrade SL, Schmid B, Yoshida M*, et al.* (2002) Nitrogenase MoFe-protein at 1.16 A resolution: a central ligand in the FeMo-cofactor. *Science,* 297(5587):1696-1700.

22. Doukov TI, Iverson TM, Seravalli J, Ragsdale SW, & Drennan CL (2002) A Ni-Fe-Cu center in a bifunctional carbon monoxide dehydrogenase/acetyl-CoA synthase. *Science,* 298(5593):567-572.

23. Darnault C, Volbeda A, Kim EJ, Legrand P, Vernede X*, et al.* (2003) Ni-Zn-[Fe4-S4] and Ni-Ni-[Fe4-S4] clusters in closed and open subunits of acetyl-CoA synthase/carbon monoxide dehydrogenase. *Nat Struct Biol,* 10(4):271-279.

24. Crack JC, Green J, Hutchings MI, Thomson AJ, & Le Brun NE (2012) Bacterial iron-sulfur regulatory proteins as biological sensor-switches. *Antioxid Redox Signal,* 17(9):1215-1231.

25. Poor CB, Wegner SV, Li H, Dlouhy AC, Schuermann JP*, et al.* (2014) Molecular mechanism and structure of the Saccharomyces cerevisiae iron regulator Aft2. *Proc Natl Acad Sci U S A,* 111(11):4043-4048.

26. Mettert EL & Kiley PJ (2014) Coordinate regulation of the Suf and Isc Fe-S cluster biogenesis pathways by IscR is essential for viability of Escherichia coli. *J Bacteriol,* 196(24):4315-4323.

27. Rudolf J, Makrantoni V, Ingledew WJ, Stark MJ, & White MF (2006) The DNA repair helicases XPD and FancJ have essential iron-sulfur domains. *Mol Cell,* 23(6):801-808.

28. Sontz PA, Mui TP, Fuss JO, Tainer JA, & Barton JK (2012) DNA charge transport as a first step in coordinating the detection of lesions by repair proteins. *Proc Natl Acad Sci U S A,* 109(6):1856-1861.

29. Netz DJ, Stith CM, Stumpfig M, Kopf G, Vogel D*, et al.* (2012) Eukaryotic DNA polymerases require an iron-sulfur cluster for the formation of active complexes. *Nat Chem Biol,* 8(1):125-132.

30. Lessner FH, Jennings ME, Hirata A, Duin EC, & Lessner DJ (2012) Subunit D of RNA polymerase from Methanosarcina acetivorans contains two oxygen-labile [4Fe-4S] clusters: implications for oxidant-dependent regulation of transcription. *J Biol Chem,* 287(22):18510-18523.

31. Hudder BN, Morales JG, Stubna A, Munck E, Hendrich MP*, et al.* (2007) Electron paramagnetic resonance and Mossbauer spectroscopy of intact mitochondria from respiring Saccharomyces cerevisiae. *J Biol Inorg Chem,* 12(7):1029-1053.

32. Albers A, Demeshko S, Propper K, Dechert S, Bill E*, et al.* (2013) A super-reduced diferrous [2Fe-2S] cluster. *J Am Chem Soc,* 135(5):1704-1707.

33. Meyer J (2008) Iron-sulfur protein folds, iron-sulfur chemistry, and evolution. *J Biol Inorg Chem,* 13(2):157-170.

34. Xia D, Yu CA, Kim H, Xia JZ, Kachurin AM*, et al.* (1997) Crystal structure of the cytochrome bc1 complex from bovine heart mitochondria. *Science,* 277(5322):60-66.

35. Kauppi B, Lee K, Carredano E, Parales RE, Gibson DT*, et al.* (1998) Structure of an aromatic-ring-hydroxylating dioxygenase-naphthalene 1,2-dioxygenase. *Structure,* 6(5):571-586.

36. Zu Y, Fee JA, & Hirst J (2001) Complete thermodynamic characterization of reduction and protonation of the bc(1)-type Rieske [2Fe-2S] center of Thermus thermophilus. *J Am Chem Soc,* 123(40):9906-9907.

37. Watt GD & Reddy KRN (1994) Formation of an all ferrous Fe4s4 cluster in the iron protein-component of Azotobacter-vinelandii nitrogenase. *J Inorg Biochem,* 53(4):281-294.

38. Shomura Y, Yoon KS, Nishihara H, & Higuchi Y (2011) Structural basis for a [4Fe-3S] cluster in the oxygen-tolerant membrane-bound [NiFe]-hydrogenase. *Nature,* 479(7372):253-256.

39. Boer JL, Mulrooney SB, & Hausinger RP (2014) Nickel-dependent metalloenzymes. *Arch Biochem Biophys,* 544:142-152.

40. Spatzal T, Aksoyoglu M, Zhang L, Andrade SL, Schleicher E*, et al.* (2011) Evidence for interstitial carbon in nitrogenase FeMo cofactor. *Science,* 334(6058):940.

41. Rickard D & Luther GW (2007) Chemistry of iron sulfides. *Chem Rev,* 107(2):514-562.

42. Beinert H, Holm RH, & Munck E (1997) Iron-sulfur clusters: nature's modular, multipurpose structures. *Science,* 277(5326):653-659.

43. Que L, Jr., Holm RH, & Mortenson LE (1975) Letter: Extrusion of Fe2S2 and Fe4S4 cores from the active sites of ferredoxin proteins. *J Am Chem Soc,* 97(2):463-464.

44. Bruice TC, Maskiewicz R, & Job R (1975) The acid-base properties, hydrolytic mechanism, and susceptibility to O(2) oxidation of Fe(4)S(4)(SR)(4) clusters. *Proc Natl Acad Sci U S A,* 72(1):231-234.

45. Job RC & Bruice TC (1975) Iron-sulfur clusters II: Kinetics of ligand exchange studied on a water-soluble Fe(4)S(4)(SR)(4) cluster. *Proc Natl Acad Sci U S A,* 72(7):2478-2482.

46. Lo W, Scott TA, Zhang P, Ling CC, & Holm RH (2011) Stabilities of cubane type [Fe(4)S(4)(SR)(4)](2-) clusters in partially aqueous media. *J Inorg Biochem,* 105(4):497-508.

47. Kennedy C & Dean D (1992) The nifU, nifS and nifV gene products are required for activity of all three nitrogenases of Azotobacter vinelandii. *Mol Gen Genet,* 231(3):494-498.

48. Dai Y & Outten FW (2012) The E. coli SufS-SufE sulfur transfer system is more resistant to oxidative stress than IscS-IscU. *FEBS Lett,* 586(22):4016-4022.

49. Lill R & Mühlenhoff U (2008) Maturation of iron-sulfur proteins in eukaryotes: mechanisms, connected processes, and diseases. *Annu Rev Biochem,* 77:22.21-22.32.

50. Kispal G, Csere P, Prohl C, & Lill R (1999) The mitochondrial proteins Atm1p and Nfs1p are essential for biogenesis of cytosolic Fe/S proteins. *EMBO J,* 18(14):3981-3989.

51. Bandyopadhyay S, Chandramouli K, & Johnson MK (2008) Iron-sulfur cluster biosynthesis. *Biochem Soc Trans,* 36(Pt 6):1112-1119.

52. Albrecht AG, Netz DJ, Miethke M, Pierik AJ, Burghaus O*, et al.* (2010) SufU is an essential iron-sulfur cluster scaffold protein in Bacillus subtilis. *J Bacteriol,* 192(6):1643-1651.

53. Olson JW, Agar JN, Johnson MK, & Maier RJ (2000) Characterization of the NifU and NifS Fe-S cluster formation proteins essential for viability in Helicobacter pylori. *Biochemistry,* 39(51):16213-16219.

54. Takahashi Y & Nakamura M (1999) Functional assignment of the ORF2-iscS-iscU-iscA-hscB-hscA-fdx-ORF3 gene cluster involved in the assembly of Fe-S clusters in Escherichia coli. *J Biochem,* 126(5):917-926.

55. Tokumoto U & Takahashi Y (2001) Genetic analysis of the isc operon in Escherichia coli involved in the biogenesis of cellular iron-sulfur proteins. *J Biochem,* 130(1):63-71.

56. Rouault TA & Tong W-H (2008) Iron-sulfur cluster biogenesis and human disease. *Trends Genet,* 24:398-407.

57. Sheftel A, Stehling O, & Lill R (2010) Iron-sulfur proteins in health and disease. *Trends Endocrinol Metab,* 21(5):302-314.

58. Vickery LE, Silberg JJ, & Ta DT (1997) Hsc66 and Hsc20, a new heat shock cognate molecular chaperone system from Escherichia coli. *Protein Sci,* 6(5):1047-1056.

59. Agar J, Krebs C, Frazzon J, Huynh BH, Dean DR*, et al.* (2000) IscU as a scaffold for iron-sulfur cluster biosynthesis: sequential assembly of [2Fe-2S] and [4Fe-4S] clusters in IscU. *Biochemistry,* 39(27):7856-7862.

60. Krebs C, Agar J, Smith AD, Frazzon J, Dean DR*, et al.* (2001) IscA, an alternate scaffold for Fe-S cluster biosynthesis. *Biochemistry,* 40(46):14069-14080.

61. Wollenberg M, Berndt C, Bill E, Schwenn JD, & Seidler A (2003) A dimer of the FeS cluster biosynthesis protein IscA from cyanobacteria binds a [2Fe2S] cluster between two protomers and transfers it to [2Fe2S] and [4Fe4S] apo proteins. *Eur J Biochem,* 270(8):1662-1671.

62. Ding H, Clark RJ, & Ding B (2004) IscA mediates iron delivery for assembly of iron-sulfur clusters in IscU under the limited accessible free iron conditions. *J Biol Chem,* 279(36):37499-37504.

63. Ollagnier-de-Choudens S, Sanakis Y, & Fontecave M (2004) SufA/IscA: reactivity studies of a class of scaffold proteins involved in [Fe-S] cluster assembly. *J Biol Inorg Chem,* 9(7):828-838.

64. Kim JH, Frederick RO, Reinen NM, Troupis AT, & Markley JL (2013) [2Fe-2S]-ferredoxin binds directly to cysteine desulfurase and supplies an electron for iron-sulfur cluster assembly but is displaced by the scaffold protein or bacterial frataxin. *J Am Chem Soc,* 135(22):8117-8120.

65. Kim JH, Bothe JR, Frederick RO, Holder JC, & Markley JL (2014) Role of IscX in iron-sulfur cluster biogenesis in Escherichia coli. *J Am Chem Soc,* 136(22):7933-7942.

66. Pastore C, Adinolfi S, Huynen MA, Rybin V, Martin S*, et al.* (2006) YfhJ, a molecular adaptor in iron-sulfur cluster formation or a frataxin-like protein? *Structure,* 14(5):857-867.

67. Couturier J, Przybyla-Toscano J, Roret T, Didierjean C, & Rouhier N (2015) The roles of glutaredoxins ligating Fe-S clusters: Sensing, transfer or repair functions? *Biochim Biophys Acta,* 1853(6):1513-1527.

68. Py B, Gerez C, Angelini S, Planel R, Vinella D*, et al.* (2012) Molecular organization, biochemical function, cellular role and evolution of NfuA, an atypical Fe-S carrier. *Mol Microbiol,* 86(1):155-171.

69. Cossee M, Puccio H, Gansmuller A, Koutnikova H, Dierich A*, et al.* (2000) Inactivation of the Friedreich ataxia mouse gene leads to early embryonic lethality without iron accumulation. *Hum Mol Genet,* 9(8):1219-1226.

70. Vazzola V, Losa A, Soave C, & Murgia I (2007) Knockout of frataxin gene causes embryo lethality in Arabidopsis. *FEBS Lett,* 581(4):667-672.

71. Tsai CL & Barondeau DP (2010) Human frataxin is an allosteric switch that activates the Fe-S cluster biosynthetic complex. *Biochemistry,* 49(43):9132-9139.

72. Bou-Abdallah F, Adinolfi S, Pastore A, Laue TM, & Dennis Chasteen N (2004) Iron binding and oxidation kinetics in frataxin CyaY of Escherichia coli. *J Mol Biol,* 341(2):605-615.

73. Correia AR, Pastore C, Adinolfi S, Pastore A, & Gomes CM (2008) Dynamics, stability and iron-binding activity of frataxin clinical mutants. *FEBS J,* 275(14):3680-3690.

74. Urbina HD, Silberg JJ, Hoff KG, & Vickery LE (2001) Transfer of sulfur from IscS to IscU during Fe/S cluster assembly. *J Biol Chem,* 276(48):44521-44526.

75. Prischi F, Konarev PV, Iannuzzi C, Pastore C, Adinolfi S*, et al.* (2010) Structural bases for the interaction of frataxin with the central components of iron-sulphur cluster assembly. *Nat Commun,* 1:95.

76. Shi R, Proteau A, Villarroya M, Moukadiri I, Zhang L*, et al.* (2010) Structural basis for Fe-S cluster assembly and tRNA thiolation mediated by IscS protein-protein interactions. *PLoS Biol,* 8(4):e1000354.

77. Majewska J, Ciesielski SJ, Schilke B, Kominek J, Blenska A*, et al.* (2013) Binding of the chaperone Jac1 protein and cysteine desulfurase Nfs1 to the iron-sulfur cluster scaffold Isu protein is mutually exclusive. *J Biol Chem,* 288(40):29134-29142.

78. Leimkuhler S & Rajagopalan KV (2001) A sulfurtransferase is required in the transfer of cysteine sulfur in the in vitro synthesis of molybdopterin from precursor Z in Escherichia coli. *J Biol Chem,* 276(25):22024-22031.

79. Kambampati R & Lauhon CT (2000) Evidence for the transfer of sulfane sulfur from IscS to ThiI during the in vitro biosynthesis of 4-thiouridine in Escherichia coli tRNA. *J Biol Chem,* 275(15):10727-10730.

80. Marinoni EN, de Oliveira JS, Nicolet Y, Raulfs EC, Amara P*, et al.* (2012) (IscS-IscU)2 complex structures provide insights into Fe2S2 biogenesis and transfer. *Angew Chem Int Ed Engl,* 51(22):5439-5442.

81. Kato S, Mihara H, Kurihara T, Takahashi Y, Tokumoto U*, et al.* (2002) Cys-328 of IscS and Cys-63 of IscU are the sites of disulfide bridge formation in a covalently bound IscS/IscU complex: implications for the mechanism of iron-sulfur cluster assembly. *Proc Natl Acad Sci U S A,* 99(9):5948-5952.

82. Mihara H, Kurihara T, Yoshimura T, & Esaki N (2000) Kinetic and mutational studies of three NifS homologs from Escherichia coli: mechanistic difference between L-cysteine desulfurase and L-selenocysteine lyase reactions. *J Biochem,* 127(4):559-567.

83. Bonomi F, Iametti S, Ta D, & Vickery LE (2005) Multiple turnover transfer of [2Fe2S] clusters by the iron-sulfur cluster assembly scaffold proteins IscU and IscA. *J Biol Chem,* 280(33):29513-29518.

84. Bridwell-Rabb J, Fox NG, Tsai CL, Winn AM, & Barondeau DP (2014) Human frataxin activates Fe-S cluster biosynthesis by facilitating sulfur transfer chemistry. *Biochemistry,* 53(30):4904-4913.

85. Bonomi F, Iametti S, Morleo A, Ta D, & Vickery LE (2011) Facilitated transfer of IscU-[2Fe2S] clusters by chaperone-mediated ligand exchange. *Biochemistry,* 50(44):9641-9650.

86. Shimomura Y, Wada K, Fukuyama K, & Takahashi Y (2008) The asymmetric trimeric architecture of [2Fe-2S] IscU: implications for its scaffolding during iron-sulfur cluster biosynthesis. *J Mol Biol,* 383(1):133-143.

87. Ramelot TA, Cort JR, Goldsmith-Fischman S, Kornhaber GJ, Xiao R*, et al.* (2004) Solution NMR structure of the iron-sulfur cluster assembly protein U (IscU) with zinc bound at the active site. *J Mol Biol,* 344(2):567-583.

88. Nuth M, Yoon T, & Cowan JA (2002) Iron-sulfur cluster biosynthesis: characterization of iron nucleation sites for assembly of the [2Fe-2S]2+ cluster core in IscU proteins. *J Am Chem Soc,* 124(30):8774-8775.

89. Colin F, Martelli A, Clemancey M, Latour JM, Gambarelli S*, et al.* (2013) Mammalian frataxin controls sulfur production and iron entry during de novo Fe4S4 cluster assembly. *J Am Chem Soc,* 135(2):733-740.

90. Chandramouli K & Johnson M (2006) HscA and HscB stimulate [2Fe-2S] cluster transfer from IscU to apoferredoxin in an ATP-dependent reaction. *Biochemistry,* 45(37):11087-11095.

91. Chandramouli K, Unciuleac MC, Naik S, Dean DR, Huynh BH*, et al.* (2007) Formation and properties of [4Fe-4S] clusters on the IscU scaffold protein. *Biochemistry,* 46(23):6804-6811.

92. Shakamuri P, Zhang B, & Johnson MK (2012) Monothiol glutaredoxins function in storing and transporting [Fe(2)S(2)] clusters assembled on IscU scaffold proteins. *J Am Chem Soc,* 134(37):15213-15216.

93. Cupp-Vickery JR, Peterson JC, Ta DT, & Vickery LE (2004) Crystal structure of the molecular chaperone HscA substrate binding domain complexed with the IscU recognition peptide ELPPVKIHC. *J Mol Biol,* 342(4):1265-1278.

94. Hoff KG, Ta DT, Tapley TL, Silberg JJ, & Vickery LE (2002) Hsc66 substrate specificity is directed toward a discrete region of the iron-sulfur cluster template protein IscU. *J Biol Chem,* 277(30):27353-27359.

95. Tokumoto U, Nomura S, Minami Y, Mihara H, Kato S*, et al.* (2002) Network of protein-protein interactions among iron-sulfur cluster assembly proteins in Escherichia coli. *J Biochem,* 131(5):713-719.

96. Nuth M & Cowan JA (2009) Iron-sulfur cluster biosynthesis: characterization of IscU-IscS complex formation and a structural model for sulfide delivery to the [2Fe-2S] assembly site. *J Biol Inorg Chem,* 14(6):829-839.

97. Yan R, Kelly G, & Pastore A (2014) The scaffold protein IscU retains a structured conformation in the Fe-S cluster assembly complex. *Chembiochem,* 15(11):1682-1686.

98. Campuzano V, Montermini L, Molto MD, Pianese L, Cossee M*, et al.* (1996) Friedreich's ataxia: autosomal recessive disease caused by an intronic GAA triplet repeat expansion. *Science,* 271(5254):1423-1427.

99. Whitnall M, Suryo Rahmanto Y, Huang ML, Saletta F, Lok HC*, et al.* (2012) Identification of nonferritin mitochondrial iron deposits in a mouse model of Friedreich ataxia. *Proc Natl Acad Sci U S A,* 109(50):20590-20595.

100. Bridwell-Rabb J, Iannuzzi C, Pastore A, & Barondeau DP (2012) Effector role reversal during evolution: the case of frataxin in Fe-S cluster biosynthesis. *Biochemistry,* 51(12):2506-2514.

101. Layer G, Ollagnier-de Choudens S, Sanakis Y, & Fontecave M (2006) Iron-sulfur cluster biosynthesis: characterization of Escherichia coli CyaY as an iron donor for the assembly of [2Fe-2S] clusters in the scaffold IscU. *J Biol Chem,* 281(24):16256-16263.

102. Fox NG (2014) A biophysical approach to investigate the human Fe-S cluster assembly pathway. PhD Dissertation (Texas A&M Univeristy, College Station, TX).

103. Bridwell-Rabb J, Winn AM, & Barondeau DP (2011) Structure-function analysis of Friedreich's ataxia mutants reveals determinants of frataxin binding and activation of the Fe-S assembly complex. *Biochemistry,* 50(33):7265-7274.

104. Yan R, Konarev PV, Iannuzzi C, Adinolfi S, Roche B*, et al.* (2013) Ferredoxin competes with bacterial frataxin in binding to the desulfurase IscS. *J Biol Chem,* 288(34):24777-24787.

105. Huynen MA, Snel B, Bork P, & Gibson TJ (2001) The phylogenetic distribution of frataxin indicates a role in iron-sulfur cluster protein assembly. *Hum Mol Genet,* 10(21):2463-2468.

106. Lillig CH, Berndt C, Vergnolle O, Lonn ME, Hudemann C*, et al.* (2005) Characterization of human glutaredoxin 2 as iron-sulfur protein: a possible role as redox sensor. *Proc Natl Acad Sci U S A,* 102(23):8168-8173.

107. Iwema T, Picciocchi A, Traore DA, Ferrer JL, Chauvat F*, et al.* (2009) Structural basis for delivery of the intact [Fe2S2] cluster by monothiol glutaredoxin. *Biochemistry,* 48(26):6041-6043.

108. Rouhier N, Couturier J, Johnson MK, & Jacquot JP (2010) Glutaredoxins: roles in iron homeostasis. *Trends Biochem Sci,* 35(1):43-52.

109. Tan G, Lu J, Bitoun J, Huang H, & Ding H (2009) IscA/SufA paralogs are required for the [4Fe-4S] cluster assembly in enzymes of multiple physiological pathways in Escherichia coli under aerobic growth conditions. *Biochem J*.

110. Muhlenhoff U, Richter N, Pines O, Pierik AJ, & Lill R (2011) Specialized function of yeast Isa1 and Isa2 proteins in the maturation of mitochondrial [4Fe-4S] proteins. *J Biol Chem,* 286(48):41205-41216.

111. Angelini S, Gerez C, Ollagnier-de Choudens S, Sanakis Y, Fontecave M*, et al.* (2008) NfuA, a new factor required for maturing Fe/S proteins in Escherichia

coli under oxidative stress and iron starvation conditions. *J Biol Chem,* 283(20):14084-14091.

112. Mapolelo DT, Zhang B, Naik SG, Huynh BH, & Johnson MK (2012) Spectroscopic and functional characterization of iron-sulfur cluster-bound forms of Azotobacter vinelandii (Nif)IscA. *Biochemistry,* 51(41):8071-8084.

113. Landry AP, Cheng Z, & Ding H (2013) Iron binding activity is essential for the function of IscA in iron-sulphur cluster biogenesis. *Dalton Trans,* 42(9):3100-3106.

114. Zhang B, Crack JC, Subramanian S, Green J, Thomson AJ*, et al.* (2012) Reversible cycling between cysteine persulfide-ligated [2Fe-2S] and cysteine-ligated [4Fe-4S] clusters in the FNR regulatory protein. *Proc Natl Acad Sci U S A,* 109(39):15734-15739.

115. Hoff KG, Silberg JJ, & Vickery LE (2000) Interaction of the iron-sulfur cluster assembly protein IscU with the Hsc66/Hsc20 molecular chaperone system of Escherichia coli. *Proc Natl Acad Sci U S A,* 97(14):7790-7795.

116. Maio N, Singh A, Uhrigshardt H, Saxena N, Tong W-H*, et al.* (2014) Cochaperone binding to LYR motifs confers specificity of iron sulfur cluster delivery. *Cell Metab,* 19(3):445-457.

117. Unciuleac M-C, Chandramouli K, Naik S, Mayer S, Huynh BH*, et al.* (2007) In vitro activation of apo-aconitase using a [4Fe-4S] cluster-loaded form of the IscU [Fe-S] cluster scaffolding protein. *Biochemistry,* 46(23):6812-6821.

118. Wang L, Ouyang B, Li Y, Feng Y, Jacquot JP*, et al.* (2012) Glutathione regulates the transfer of iron-sulfur cluster from monothiol and dithiol glutaredoxins to apo ferredoxin. *Protein Cell,* 3(9):714-721.

119. Comini MA, Krauth-Siegel RL, & Bellanda M (2012) Mono- and dithiol glutaredoxins in the trypanothione-based redox metabolism of pathogenic Trypanosomes. *Antioxid Redox Signal,* 16(7):636-638.

120. Li H, Mapolelo DT, Randeniya S, Johnson MK, & Outten CE (2012) Human glutaredoxin 3 forms [2Fe-2S]-bridged complexes with human BolA2. *Biochemistry,* 51(8):1687-1696.

121. Yeung N, Gold B, Liu NL, Prathapam R, Sterling HJ*, et al.* (2011) The E. coli monothiol glutaredoxin GrxD forms homodimeric and heterodimeric FeS cluster containing complexes. *Biochemistry,* 50(41):8957-8969.

122. Willems P, Wanschers BFJ, Esseling J, Szklarczyk R, Kudla U*, et al.* (2013) BOLA1 is an aerobic protein that prevents mitochondrial morphology changes induced by glutathione depletion. *Antioxid Redox Signal,* 18(2):129-138.

123. Roret T, Tsan P, Couturier J, Zhang B, Johnson MK*, et al.* (2014) Structural and spectroscopic insights into BolA-glutaredoxin complexes. *J Biol Chem,* 289(35):24588-24598.

124. Li H, Mapolelo DT, Dingra NN, Naik SG, Lees NS*, et al.* (2009) The yeast iron regulatory proteins Grx3/4 and Fra2 form heterodimeric complexes containing a [2Fe-2S] cluster with cysteinyl and histidyl ligation. *Biochemistry,* 48(40):9569-9581.

125. Mapolelo DT, Zhang B, Randeniya S, Albetel A-N, Li H*, et al.* (2013) Monothiol glutaredoxins and A-type proteins: partners in Fe-S cluster trafficking. *Dalton Trans,* 42(9):3107-3115.

126. Sheftel AD, Stehling O, Pierik AJ, Netz DJ, Kerscher S*, et al.* (2009) Human ind1, an iron-sulfur cluster assembly factor for respiratory complex I. *Mol Cell Biol,* 29(22):6059-6073.

127. Gillum WO, Mortenson LE, Chen JS, & Holm RH (1977) Quantitative extrusions of the Fe4S4 cores of the active sites of ferredoxins and the hydrogenase of Clostridium pasteurianum. *J Am Chem Soc,* 99(2):584-595.

128. Qi W, Li J, Chain CY, Pasquevich GA, Pasquevich AF*, et al.* (2012) Glutathione complexed Fe-S centers. *J Am Chem Soc,* 134(26):10745-10748.

129. Ryle MJ, Lanzilotta WN, Seefeldt LC, Scarrow RC, & Jensen GM (1996) Circular dichroism and x-ray spectroscopies of Azotobacter vinelandii nitrogenase iron protein. MgATP and MgADP induced protein conformational changes affecting the [4Fe-4S] cluster and characterization of a [2Fe-2S] form. *J Biol Chem,* 271(3):1551-1557.

130. Qi W & Cowan JA (2011) Mechanism of glutaredoxin-ISU [2Fe-2S] cluster exchange. *Chem Commun (Camb),* 47(17):4989-4991.

131. Ba LA, Doering M, Burkholz T, & Jacob C (2009) Metal trafficking: from maintaining the metal homeostasis to future drug design. *Metallomics,* 1(4):292-311.

132. Nevitt T, Ohrvik H, & Thiele DJ (2012) Charting the travels of copper in eukaryotes from yeast to mammals. *Biochim Biophys Acta,* 1823(9):1580-1593.

133. Lill R, Hoffmann B, Molik S, Pierik AJ, Rietzschel N*, et al.* (2012) The role of mitochondria in cellular iron-sulfur protein biogenesis and iron metabolism. *Biochim Biophys Acta,* 1823(9):1491-1508.

134. Kaler SG (2013) Inborn errors of copper metabolism. *Handb Clin Neurol,* 113:1745-1754.

135. Py B & Barras F (2010) Building Fe-S proteins: bacterial strategies. *Nat Rev Microbiol,* 8(6):436-446.

136. Takahashi Y & Tokumoto U (2002) A third bacterial system for the assembly of iron-sulfur clusters with homologs in archaea and plastids. *The Journal of biological chemistry,* 277(32):28380-28383.

137. Tong W-H, Jameson GNL, Huynh BH, & Rouault TA (2003) Subcellular compartmentalization of human Nfu, an iron-sulfur cluster scaffold protein, and its ability to assemble a [4Fe-4S] cluster. *Proc Natl Acad Sci USA,* 100(17):9762-9767.

138. Bandyopadhyay S, Naik S, O'Carroll I, Huynh BH, Dean DR*, et al.* (2008) A proposed role for the Azotobacter vinelandii NfuA protein as an intermediate iron-sulfur cluster carrier. *J Biol Chem,* 283(20):14092-14099.

139. Gupta V, Sendra M, Naik SG, Chahal HK, Huynh BH*, et al.* (2009) Native Escherichia coli SufA, coexpressed with SufBCDSE, purifies as a [2Fe-2S]

protein and acts as an Fe-S transporter to Fe-S target enzymes. *J Am Chem Soc,* 131(17):6149-6153.

140. Bonomi F, Iametti S, Morleo A, Ta D, & Vickery L (2008) Studies on the mechanism of catalysis of iron-sulfur cluster transfer from IscU[2Fe2S] by HscA/HscB chaperones. *Biochemistry,* 47:12795-12801.

141. Drsata J, Bousova I, & Malon P (2005) Determination of quality of pyridoxal-5'-phosphate enzyme preparations by spectroscopic methods. *J Pharm Biomed Anal,* 37(5):1173-1177.

142. Hoff KG, Goodlitt R, Li R, Smolke CD, & Silberg JJ (2009) Fluorescence detection of a protein-bound 2Fe2S cluster. *Chembiochem,* 10(4):667-670.

143. Miyawaki A, Llopis J, Heim R, McCaffery JM, Adams JA*, et al.* (1997) Fluorescent indicators for Ca2+ based on green fluorescent proteins and calmodulin. *Nature,* 388(6645):882-887.

144. Domaille DW, Que EL, & Chang CJ (2008) Synthetic fluorescent sensors for studying the cell biology of metals. *Nat Chem Biol,* 4(3):168-175.

145. Honda M, Park J, Pugh RA, Ha T, & Spies M (2009) Single-molecule analysis reveals differential effect of ssDNA-binding proteins on DNA translocation by XPD helicase. *Mol Cell,* 35(5):694-703.

146. Balint EE, Petres J, Szabo M, Orban CK, Szilagyi L*, et al.* (2013) Fluorescence of a histidine-modified enhanced green fluorescent protein (EGFP) effectively quenched by copper(II) ions. *J Fluoresc,* 23(2):273-281.

147. Krishnamoorthy K & Begley TP (2010) Reagent for the detection of protein thiocarboxylates in the bacterial proteome: lissamine rhodamine B sulfonyl azide. *J Am Chem Soc,* 132(33):11608-11612.

148. Landry AP & Ding H (2014) Redox control of human mitochondrial outer membrane protein MitoNEET [2Fe-2S] clusters by biological thiols and hydrogen peroxide. *J Biol Chem,* 289(7):4307-4315.

149. Lepore BW, Ruzicka FJ, Frey PA, & Ringe D (2005) The x-ray crystal structure of lysine-2,3-aminomutase from Clostridium subterminale. *Proc Natl Acad Sci U S A,* 102(39):13819-13824.

150. MacDonald RI (1990) Characteristics of self-quenching of the fluorescence of lipid-conjugated rhodamine in membranes. *J Biol Chem,* 265(23):13533-13539.

151. Kakuta Y, Horio T, Takahashi Y, & Fukuyama K (2001) Crystal structure of Escherichia coli Fdx, an adrenodoxin-type ferredoxin involved in the assembly of iron-sulfur clusters. *Biochemistry,* 40(37):11007-11012.

152. Senda M, Kishigami S, Kimura S, Fukuda M, Ishida T*, et al.* (2007) Molecular mechanism of the redox-dependent interaction between NADH-dependent ferredoxin reductase and Rieske-type [2Fe-2S] ferredoxin. *J Mol Biol,* 373(2):382-400.

153. Kurra Y, Odoi KA, Lee YJ, Yang Y, Lu T*, et al.* (2014) Two rapid catalyst-free click reactions for in vivo protein labeling of genetically encoded strained alkene/alkyne functionalities. *Bioconjug Chem,* 25(9):1730-1738.

154. Barondeau DP, Putnam CD, Kassmann CJ, Tainer JA, & Getzoff ED (2003) Mechanism and energetics of green fluorescent protein chromophore synthesis revealed by trapped intermediate structures. *Proc Natl Acad Sci U S A,* 100(21):12111-12116.

155. Miyazaki K (2011) MEGAWHOP cloning: a method of creating random mutagenesis libraries via megaprimer PCR of whole plasmids. *Methods Enzymol,* 498:399-406.

156. Haugland R (1996) *Handbook of fluorescent probes and research chemicals* (Molecular Probes, Eugene, OR) 6th Ed.

157. Stookey LL (1970) Ferrozine---a new spectrophotometric reagent for iron. *Anal Chem,* 42(7):779-781.

158. Suhara K, Takemori S, Katagiri M, Wada K, & Kobayashi H (1975) Estimation of labile sulfide in iron-sulfur proteins. *Anal Biochem,* 68(2):632-636.

159. Muhlenhoff U & Lill R (2000) Biogenesis of iron-sulfur proteins in eukaryotes: a novel task of mitochondria that is inherited from bacteria. *Biochim Biophys Acta,* 1459(2-3):370-382.

160. Rodriguez-Manzaneque MT, Ros J, Cabiscol E, Sorribas A, & Herrero E (1999) Grx5 glutaredoxin plays a central role in protection against protein oxidative damage in Saccharomyces cerevisiae. *Mol Cell Biol,* 19(12):8180-8190.

161. Rodriguez-Manzaneque MT, Tamarit J, Belli G, Ros J, & Herrero E (2002) Grx5 is a mitochondrial glutaredoxin required for the activity of iron/sulfur enzymes. *Mol Biol Cell,* 13(4):1109-1121.

162. Holmgren A (1976) Hydrogen donor system for Escherichia coli ribonucleoside-diphosphate reductase dependent upon glutathione. *Proc Natl Acad Sci U S A,* 73(7):2275-2279.

163. Chrestensen CA, Starke DW, & Mieyal JJ (2000) Acute cadmium exposure inactivates thioltransferase (Glutaredoxin), inhibits intracellular reduction of protein-glutathionyl-mixed disulfides, and initiates apoptosis. *J Biol Chem,* 275(34):26556-26565.

164. Davis DA, Newcomb FM, Starke DW, Ott DE, Mieyal JJ*, et al.* (1997) Thioltransferase (glutaredoxin) is detected within HIV-1 and can regulate the activity of glutathionylated HIV-1 protease in vitro. *J Biol Chem,* 272(41):25935-25940.

165. Couturier J, Stroher E, Albetel AN, Roret T, Muthuramalingam M*, et al.* (2011) Arabidopsis chloroplastic glutaredoxin C5 as a model to explore molecular determinants for iron-sulfur cluster binding into glutaredoxins. *J Biol Chem,* 286(31):27515-27527.

166. Johansson C, Kavanagh KL, Gileadi O, & Oppermann U (2007) Reversible sequestration of active site cysteines in a 2Fe-2S-bridged dimer provides a mechanism for glutaredoxin 2 regulation in human mitochondria. *J Biol Chem,* 282(5):3077-3082.

167. Johansson C, Roos AK, Montano SJ, Sengupta R, Filippakopoulos P*, et al.* (2011) The crystal structure of human GLRX5: iron-sulfur cluster co-ordination, tetrameric assembly and monomer activity. *Biochem J,* 433(2):303-311.

168. Rouhier N, Unno H, Bandyopadhyay S, Masip L, Kim SK*, et al.* (2007) Functional, structural, and spectroscopic characterization of a glutathione-ligated [2Fe-2S] cluster in poplar glutaredoxin C1. *Proc Natl Acad Sci U S A,* 104(18):7379-7384.

169. Feng Y, Zhong N, Rouhier N, Hase T, Kusunoki M*, et al.* (2006) Structural insight into poplar glutaredoxin C1 with a bridging iron-sulfur cluster at the active site. *Biochemistry,* 45(26):7998-8008.

170. Zhang B, Bandyopadhyay S, Shakamuri P, Naik SG, Huynh BH*, et al.* (2013) Monothiol glutaredoxins can bind linear [Fe3S4]+ and [Fe4S4]2+ clusters in addition to [Fe2S2]2+ clusters: spectroscopic characterization and functional implications. *J Am Chem Soc,* 135(40):15153-15164.

171. Dhalleine T, Rouhier N, & Couturier J (2014) Putative roles of glutaredoxin-BolA holo-heterodimers in plants. *Plant Signal Behav,* 9(3):e28564.

172. Muhlenhoff U, Gerber J, Richhardt N, & Lill R (2003) Components involved in assembly and dislocation of iron-sulfur clusters on the scaffold protein Isu1p. *EMBO J,* 22(18):4815-4825.

173. Vranish JN, Russell WK, Yu LE, Cox RM, Russell DH*, et al.* (2015) Fluorescent probes for tracking the transfer of iron-sulfur cluster and other metal cofactors in biosynthetic reaction pathways. *J Am Chem Soc,* 137(1):390-398.

174. Webert H, Freibert SA, Gallo A, Heidenreich T, Linne U*, et al.* (2014) Functional reconstitution of mitochondrial Fe/S cluster synthesis on Isu1 reveals the involvement of ferredoxin. *Nat Commun,* 5:5013.

175. Benyamina SM, Baldacci-Cresp F, Couturier J, Chibani K, Hopkins J*, et al.* (2013) Two Sinorhizobium meliloti glutaredoxins regulate iron metabolism and symbiotic bacteroid differentiation. *Environ Microbiol,* 15(3):795-810.

176. Berndt C, Poschmann G, Stuhler K, Holmgren A, & Brautigam L (2014) Zebrafish heart development is regulated via glutaredoxin 2 dependent migration and survival of neural crest cells. *Redox Biol,* 2:673-678.

177. Brautigam L, Jensen LD, Poschmann G, Nystrom S, Bannenberg S*, et al.* (2013) Glutaredoxin regulates vascular development by reversible glutathionylation of sirtuin 1. *Proc Natl Acad Sci U S A,* 110(50):20057-20062.

178. Izquierdo A, Casas C, Muhlenhoff U, Lillig CH, & Herrero E (2008) Saccharomyces cerevisiae Grx6 and Grx7 are monothiol glutaredoxins associated with the early secretory pathway. *Eukaryot Cell,* 7(8):1415-1426.

179. Lee DW, Kaur D, Chinta SJ, Rajagopalan S, & Andersen JK (2009) A disruption in iron-sulfur center biogenesis via inhibition of mitochondrial dithiol glutaredoxin 2 may contribute to mitochondrial and cellular iron dysregulation in mammalian glutathione-depleted dopaminergic cells: implications for Parkinson's disease. *Antioxid Redox Signal,* 11(9):2083-2094.

180. Lillig CH, Lonn ME, Enoksson M, Fernandes AP, & Holmgren A (2004) Short interfering RNA-mediated silencing of glutaredoxin 2 increases the sensitivity of HeLa cells toward doxorubicin and phenylarsine oxide. *Proc Natl Acad Sci U S A,* 101(36):13227-13232.

181. Mesecke N, Spang A, Deponte M, & Herrmann JM (2008) A novel group of glutaredoxins in the cis-Golgi critical for oxidative stress resistance. *Mol Biol Cell,* 19(6):2673-2680.

182. Wu H, Lin L, Giblin F, Ho YS, & Lou MF (2011) Glutaredoxin 2 knockout increases sensitivity to oxidative stress in mouse lens epithelial cells. *Free Radic Biol Med,* 51(11):2108-2117.

183. Brautigam L, Schutte LD, Godoy JR, Prozorovski T, Gellert M*, et al.* (2011) Vertebrate-specific glutaredoxin is essential for brain development. *Proc Natl Acad Sci U S A,* 108(51):20532-20537.

184. Couturier J, Jacquot JP, & Rouhier N (2009) Evolution and diversity of glutaredoxins in photosynthetic organisms. *Cell Mol Life Sci,* 66(15):2539-2557.

185. Bandyopadhyay S, Gama F, Molina-Navarro MM, Gualberto JM, Claxton R*, et al.* (2008) Chloroplast monothiol glutaredoxins as scaffold proteins for the assembly and delivery of [2Fe-2S] clusters. *EMBO J,* 27(7):1122-1133.

186. Lushchak VI (2012) Glutathione homeostasis and functions: potential targets for medical interventions. *J Amino Acids,* 2012:736837.

187. Mari M, Morales A, Colell A, Garcia-Ruiz C, Kaplowitz N*, et al.* (2013) Mitochondrial glutathione: features, regulation and role in disease. *Biochim Biophys Acta,* 1830(5):3317-3328.